BNL-NUREG- 27544
INFORMAL REPORT

THERMAL-HYDRAULIC EFFECTS ON CENTER ROD DROP ACCIDENTS IN A BOILING WATER REACTOR

HSIANG-SHOU CHENG AND DAVID J. DIAMOND

THERMAL REACTOR SAFETY DIVISION

DATE PUBLISHED

JULY 1980

DEPARTMENT OF NUCLEAR ENERGY BROOKHAVEN NATIONAL LABORATORY
UPTON, NEW YORK 11973

PREPARED FOR THE U.S. NUCLEAR REGULATORY COMMISSION
OFFICE OF NUCLEAR REACTOR REGULATION
UNDER INTERAGENCY AGREEMENT DE-AC-2-76CH00016

BNL-NUREG - 2754
INFORMAL REPORT
LIMITED DISTRIBU

THERMAL-HYDRAULIC EFFECTS ON CENTER ROD DROP ACCIDENTS IN A BOILING WATER REACTOR

Hsiang-Shou Cheng and David J. Diamond
Reactor Safety Analysis Group
Department of Nuclear Energy
BROOKHAVEN NATIONAL LABORATORY
Upton, New York 11973

July 1980

Prepared for
U. S. Nuclear Regulatory Commission
Washington, D.C. 20555
Under Interagency Agreement DE-AC 2-76CH00016
NRC Fin No. A-3323

TABLE OF CONTENTS

ABSTRACT

The center rod drop accident was calculated for a boiling water reactor using the two-dimensional (R,Z) core dynamics code BNL-TWIGL. This code accounts for both Doppler (fuel) and moderator feedback. Analysts frequently neglect moderator feedback under the assumption that it leads to conservative results. The present study shows that the peak of the power burst and peak fuel enthalpy can be reduced by a factor of two or more by including this effect. The magnitude of the effect depends on reactor conditions. Moderator feedback is particularly important when there are voids in the core initially (i.e. at power conditions) or when the core is near saturation condition. When the reactor is initially at zero power and considerably subcooled, moderator feedback will influence the power peak by less than 10% but will have a much larger effect on the peak fuel enthalpy which occurs later in time.

The moderator feedback is the result of heat conducted from the fuel rod and direct energy deposition. Calculations show that at power conditions the time constant for heat conduction is small and this is the primary mechanism for changing the steam void content during the accident. At zero power the initial thermal time constant is very large and hence any generation of voids at short times is due to direct energy deposition in the moderator.

This study also calculates the effect of changing power level, flow rate, inlet subcooling, delayed neutron fraction, rod drop speed, and accident rod worth. In all cases with moderator feedback accounted for the maximum fuel enthalpy during the accident is well below presently established limits. Results are insensitive to the delayed neutron fraction and rod drop velocity. The parameters of most significance are inlet subcooling and accident rod worth.

SUMMARY

The rod drop accident is a design basis accident for boiling water reactors. In the past, the unavailability of rigorous calculational methods and the great expense that those methods would incur if available, have led to the use of approximate, conservative methods. Typically, a simple feedback model is used, which neglects moderator feedback due to steam voids and coolant temperature. The present work quantifies the conservatism of this approach and studies the effect of different reactor conditions.

The BNL-TWIGL code used in the study is an R-Z geometry reactor dynamics code which accounts for feedback due to changes in fuel temperature, moderator conditions, and control rod movement. The two group, time dependent neutron diffusion equations are coupled to a time dependent two-phase thermal hydraulic model. Because of the R-Z geometry, a center rod drop was considered. The code could calculate the accident with and without the moderator feedback during the transient. This feedback depends on the amount of heat conducted from the fuel rod as well as on the energy deposited directly in the coolant. The direct energy deposition fraction could be varied to determine the relative magnitude of these effects.

Several reactor conditions were considered; power levels of 10% and 10^{-4}% ("zero" rated power, two flow rates, two rod speeds, several rod worths, power shapes, three inlet subcooling values, and two delayed neutron fractions corresponding to beginning-of-life and end-of-cycle conditions).

The resulting calculations are summarized in Table S-1 for the 10% power cases and in Table S-2 for the hot zero power cases. Each set of results for peak power and peak fuel enthalpy must be compared with the appropriate base case in order to understand the effect of a particular change.

The results (cf. Cases 1,3,5,11) show the dramatic effect on peak fuel enthalpy and peak power of incorporating moderator feedback in the calculational model. This is especially true when there are voids in the core (i.e. at power conditions) or at zero power when the coolant is close to saturation so that voids can be easily formed and is a consequence of the large void reactivity coefficient inherent in BWRs. The effect is less strong when the reactor is initially at zero power and considerably subcooled (cf. Cases 4, 12, 13). In these cases moderator feedback only slightly influences the transient power peak but does have a large effect on the peak fuel enthalpy which occurs later in time. In all cases with moderator feedback accounted for, the peak fuel enthalpy is significantly below the current limiting criterion of 280 cal/gm.

Calculations show that at power conditions the thermal time constant for heat conduction in the fuel is small to begin with and becomes even smaller as the accident progresses due to the change in temperature gradient across the rod. This is the primary mechanism for changing the void content (cf. Case 2) during the accident. At zero power the initial time constant is very large (corresponding to no temperature gradient), hence any generation of voids at short times is due to direct energy deposition in the moderator (cf. Case 7).

With moderator feedback neglected results are sensitive to rod worth. (The difference between static and dynamic worth is quantified and discussed in the report.) Rod worth depends on several factors; the power distribution being one of the most important (cf. Cases 3, 11, and 12.). Rod speed and hence insertion rate is significant in the early part of the transient (cf. Cases 6 and 8) and influences the peak power but it is not important in determining the maximum fuel enthalpy. The delayed neutron fraction which varies during a fuel cycle also influences the transient (cf. Cases 9 and 10) but again is of little significance relative to the peak fuel enthalpy exceeding limits.

1.0 INTRODUCTION

An important design-basis accident for boiling water reactors (BWRs) is the control rod drop accident (CRDA). This accident is defined[1] to be a rapid reactor transient caused by an accidental drop (out of the core) of the highest-worth control rod at various conditions ranging from cold start-up to about 10% of rated power. Despite the fact that the chance of a CRDA is extremely unlikely,[2] the consequence of the CRDA is of concern because of the potential for damage to fuel rods and the reactor.

TABLE S-1

CENTER ROD DROP ACCIDENT AT 10% POWER[a]

Case No.	Compare to Case	Principal Change	Transient Moderator Feedback	Time to Peak Power, s	Peak Power GW	Scram Initiated[b]	Peak Fuel Enthalpy cal/gm
1a	1a	-	Yes	2.36	1.99	No	41
1b	1a	Moderator Feedback	No	2.36	8.85	Yes	78
2	1a	DMH = 0%	Yes	2.38	2.46	No	44
3a	1a	W_o = 37%	Yes	0.99	1.20	No	42
		ρ_A = 0.0050					
3b	3a	F_Z = 1.53	No	1.00	4.74	Yes	86
8	1b	v = 3.1 ft/s	No	3.77	5.27	Yes	76
9	1b	β = 0.00546	No	2.66	14.10	Yes	89

a) Reactor conditions except where changed
Rod initially fully inserted
Inlet subcooling 20°F
W_o = 18.5% rated flow
DMH = 2% direct moderator heating
F_Z = 1.48, axial peaking
F_r = 1.73, radial peaking
ρ_A = 0.0089, static rod worth
β = 0.00738, delayed neutron fraction
v = 5 ft/s, rod drop velocity

b) Determined by power exceeding 120% of rated

TABLE S -2

CENTER ROD DROP ACCIDENT AT HOT ZERO POWER[a]

Case Number	Compare to Case	Principal Change	Transient Moderator Feedback	Static Rod Worth (Δk/k)	Inlet Subcooling °F	Time to Power Peak, s	Peak Power (GW)	Peak Fuel Enthalpy (cal/gm)
4a	4a	-	Yes	.0118[b]	20	.49	12.10	86
4b	4a	Moderator Feedback	No	.0118[b]	20	.49	13.00	120
5a	4a	Inlet Subcooling (No Scram)	Yes	.0121	0	.46	3.01	35
5b	5a	Moderator Feedback	No	.0121	0	.48	13.60	136
6	5b	v = 3.1 ft/s	No	.0121	0	.67	8.96	125
7	5a	DMH = 0%	Yes	.0121	0	.48	13.20	85
10	5b	β = 0.00546	No	.0121	0	.37	21.1	141
11a	5a	Rod fully in F_Z=2.6, F_R=5.6	Yes	.0208	0	.50	16.5	50
11b	11a	Rod Worth, Moderator Feedback	No	.0208	0	.51	80.5	326
12a	11a	Inlet subcooling F_Z=2.5, F_R=5.1	Yes	.0211	100	.50	73.0	179
12b	12a	Moderator Feedback	No	.0211	100	.50	79.3	312
13a	5a	Inlet subcooling	Yes	.0119	100	.49	13.4	109
13b	13a	Moderator Feedback	No	.0119	100	.49	14.5	147

a) Reactor Conditions except where changed
W_o = 18.5% rated flow
DMH = 2%, direct moderator heating
β = 0.00738, delayed neutron fraction
F_Z = 3.6 axial peaking
F_R = 11.8 radial peaking
v = 5 ft/s rod drop velocity
Scram always initiated
Rod initially 10 ft inserted

Historically, the unavailability of a realistic multi-dimensional reactor dynamic code has necessitated the use of approximate methods with a simple feedback model.[3,4,5] The simple feedback model usually takes into account Doppler feedback and reactor scram but neglects moderator feedback due to steam voids and moderator temperature on the ground that this approach is conservative.

The CRDA has been analyzed by various methods with different degrees of sophistication. General Electric employs an adiabatic prompt excursion model[5] in (R,Z) geometry without consideration of the moderator feedback. Audit calculations of the CRDA were performed by Brookhaven National Laboratory for a BWR/2 using both one-and two-dimensional space-time models.[6,7,8] Emphasis was placed on the sensitivity of the CRDA to scram characteristics and Doppler feedback.[9] The potentially significant effect of the moderator feedback was discussed but not quantitatively evaluated. The Germans[10] have also studied the CRDA. Their interest was in three-dimensional neutronic effects and again moderator feedback was not considered.

The present work attempts to provide some quantitative answer to the moderator feedback effect on a center rod drop accident (CRDA) in a BWR/4 using the improved two-dimensional (R,Z) core dynamics code BNL-TWIGL.[11]

The analysis performed took into account only the reactor core behavior during the accident. The core inlet conditions which link the core to the other parts of the power plant were treated as the boundary conditions invariant in time. As such, the interaction between the core and the plant system is not considered. This is assumed to be a minor effect. The accidents considered consist of a 10% power case and a hot zero power (HZP) case, involving two core flow rates (18.5% and 37%), two direct moderator heating (DMH) fractions (0 and 2%), three inlet subcoolings (0,20 and 100°F), two accidental rod drop velocities (3.1 ft/s and 5.0 ft/s), and two delayed neutron fractions (0.00738 for beginning of life (BOL), and 0.00546 for end of cycle (EOC)). For each case, the calculations were done with and without the moderator feedback so that the moderator feedback effect can be evaluated. The effects of core flow, DMH, inlet subcooling, rod drop velocity, and the delayed neutron fraction were studied and their significance quantified.

The report is organized as follows. Section 2.0 describes the method of analysis, accident conditions, and nuclear data. Section 3.0 presents the results of calculations and discusses their significance and implications. Section 4.0 provides a summary and draws important conclusions.

2.0 ANALYSIS

2.1 Accident Conditions

The CRDA is defined as a rapid core transient initiated by an accidental drop of the highest-worth (center) control rod at various initial core conditions. Here we have assumed that the accident has occurred without consideration of the chance of such an accident. In fact, the chance of a CRDA is extremely unlikely. Reference 2 provides an excellent discussion on the probability of a CRDA exceeding the 280 cal/gm limit.

To define the accident, the initial conditions of the core must be specified. They are the core thermal power (CTP), exposure, flow, pressure, inlet subcooling, power distribution, and control rod pattern. The power profile influences the accident rod worth, and is, therefore, a particularly important initial condition.

We considered 13 accident cases involving two different power levels, two core flow rates, two DMH fractions, three inlet subcoolings, two rod drop velocities, and two delayed neutron fractions (representing BOL and EOC). The two power levels are 10% of rated power (3294 MW) and hot zero power (HZP). HZP is defined as 10^{-6} of the rated power. The two flow rates are 18.5% and 37% of rated flow (320 lb/ft^2-s). The core pressure is the operating pressure (1035 psia). The DMH fractions are 0 and 2% of the total core thermal power. The inlet subcooling is 20°F for the 10% power cases, and zero for most HZP cases except for Case 4 (20°F subcooling), and Cases 12 and 13 (100°F subcooling). The two delayed neutron fractions considered are 0.00738 to simulate BOL conditions and 0.00546 for EOC. Table I summarizes the accident conditions of the 13 cases considered in the present study.

The reactor is assumed to be initially critical at the specified core conditions with the general reactor geometry (defined by GE[5]) as shown in Figures 1 and 2 for the HZP and 10% power cases, respectively. The actual control density profiles used in each radial zone shown in the figures may be different in each case depending on the initial conditions of the core. This will be discussed below.

The accident starts at time zero by dropping the center control rod at a speed of either 1.524 m/s (5 ft/s) or 0.945 m/s (3.1 ft/s). Scram is activated when the core thermal power reaches 120% of rated with 0.2 s delay. The scram speed is assumed to be 0.914 m/s (3 ft/s).

2.2 Calculational Model

The calculational model simulates the accident in (R,Z) geometry as shown in Figure 3. The finite cylinder geometry is a good approximation since the accident control rod is situated at the center of the core and the control rod patterns involved are all symmetric. Table II lists the radial and axial dimensions of the reactor model defined in Figure 3.

There are five radial scram zones within the active core to represent the initial control rod pattern and the subsequent rod drop and scram bank simulation. The central radial zone which represents the four-bundle supercell at the core center is used to simulate the accident rod drop movement. When scram is activated, this central rod does not scram but is assumed to continue to drop out of the core. The rest of the control rods represented by the other four scram zones will scram at a constant speed after some delay. The actual control rod pattern is represented by a piecewise step control density profile in each of the five scram zones. These profiles were determined from the actual rod pattern by volume weighting. Figures 4 through 7 present the piecewise control density profiles for the 13 CRDA cases studied.

TABLE I

INITIAL CONDITIONS OF CENTER ROD DROP ACCIDENTS

CRDA Case	Power % Rated	Flow % Rated	Pressure (psia)	Inlet Subcooling (°F)	Direct Mod. Heating (%)	Ft. Center Rod is In (ft)	Rod Drop Velocity (ft/sec)	Delayed Neutron Fraction (β)
1	10	18.5	1035	20	2	12	5.0	0.00738
2	10	18.5	1035	20	0	12	5.0	0.00738
3	10	37.0	1035	20	2	12	5.0	0.00738
4	10^{-4}	18.5	1035	20	2	10	5.0	0.00738
5	10^{-4}	18.5	1035	0	2	10	5.0	0.00738
6	10^{-4}	18.5	1035	0	2	10	3.1	0.00738
7	10^{-4}	18.5	1035	0	0	10	5.0	0.00738
8	10	18.5	1035	20	2	12	3.1	0.00738
9	10	18.5	1035	20	2	12	5.0	0.00546
10	10^{-4}	18.5	1035	0	2	10	5.0	0.00546
11 *	10^{-4}	18.5	1035	0	2	12	5.0	0.00738
12	10^{-4}	18.5	1035	100	2	12	5.0	0.00738
13	10^{-4}	18.5	1035	100	2	12	5.0	0.00738

* Same as Case 5 except for a different rod pattern to approximately double accident rod worth.

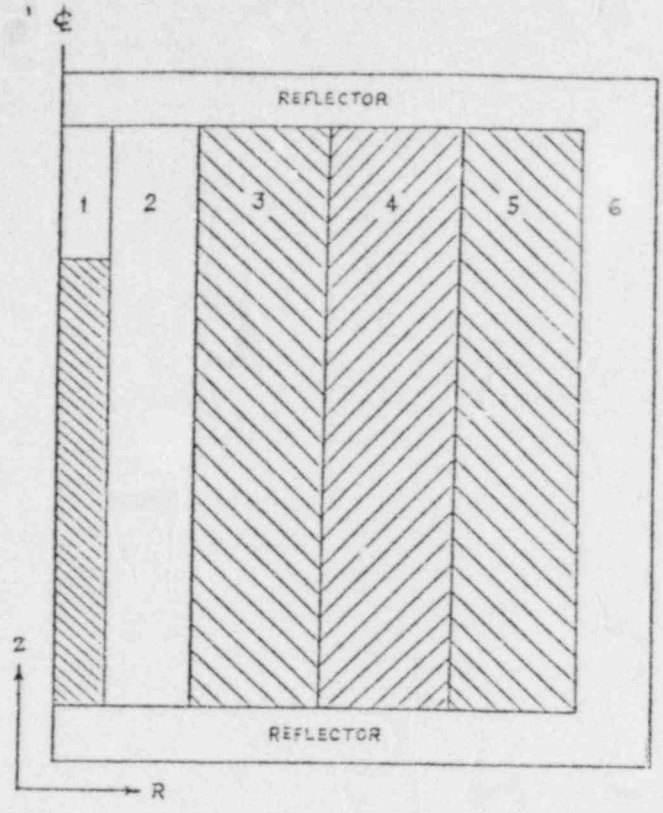

Region	Description
1	Accident control rod region equivalent to 4-bundle supercell.
2	Uncontrolled fuel region equivalent to 8 supercells surrounding the central one.
3	Partially controlled region equivalent to 36 supercells surrounding the second region.
4	Partially controlled region equivalent to 64 supercells surrounding the third region.
5	Partially controlled region equivalent to 72 supercells in the peripheral region.
6	Reflector region (H_2O or H_2O + S.S.)

Figure 1 Reactor geometry for analyzing rod drop accidents at HZP

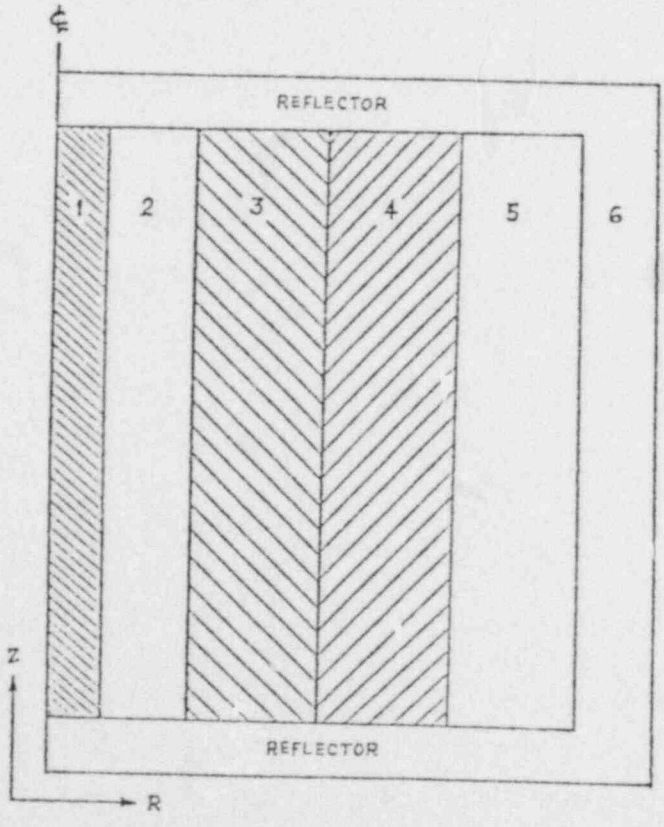

Region	Description
1	Accident control rod region equivalent to 4-bundle supercell.
2	Uncontrolled fuel region equivalent to 8 supercells surrounding the central one.
3	Partially controlled region equivalent to 36 supercells surrounding the second region.
4	Partially controlled region ecuivalent to 64 supercells surrounding the third region.
5	Uncontrolled region equivalent to 72 supercells in the peripheral region of the core.
6	Reflector region (H_2O or H_2O + S.S.).

Figure 2 Reactor geometry for analyzing rod drop accidents at 10% power

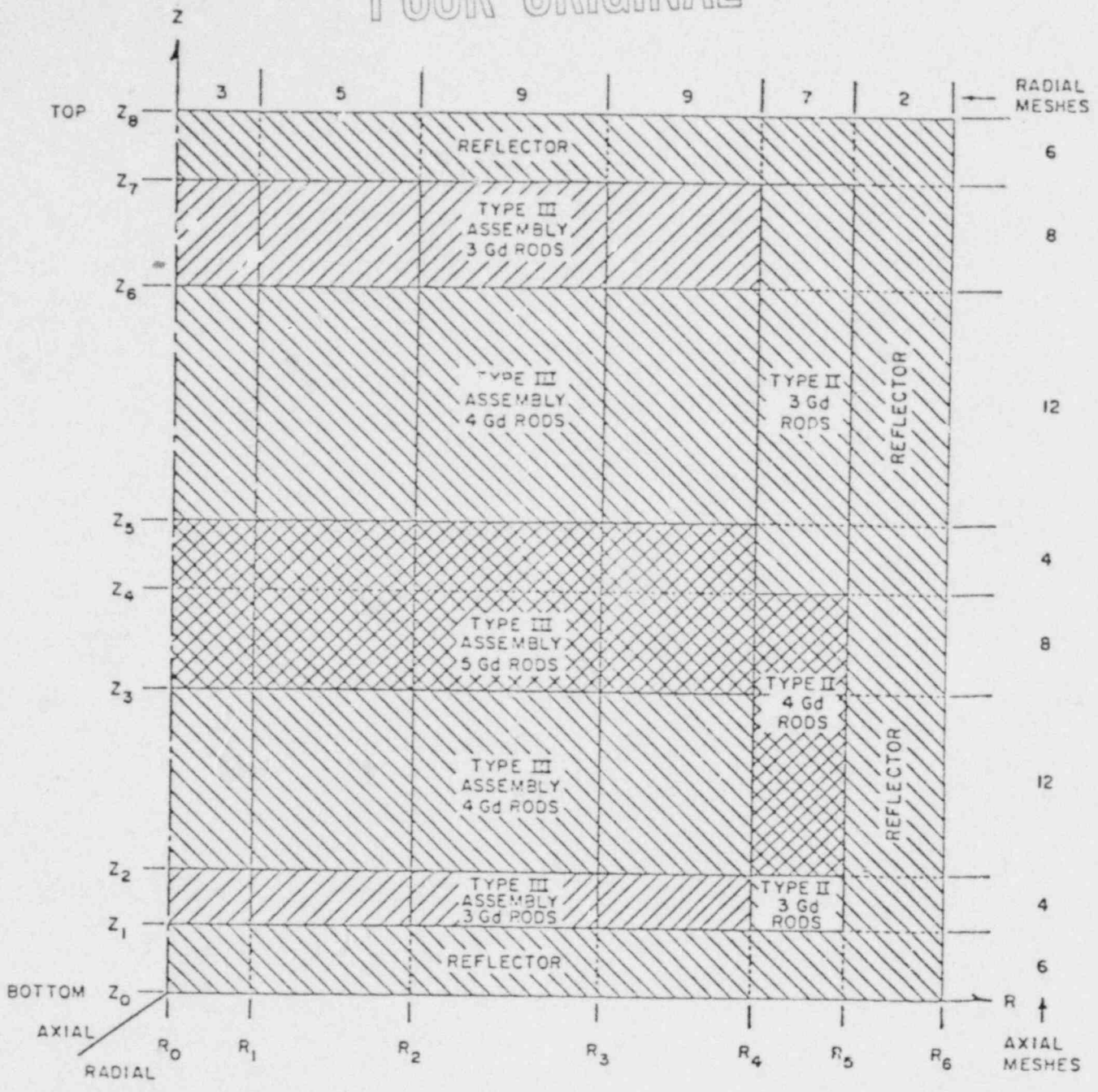

Figure 3 The (R,Z) reactor model for CRDA analysis

TABLE II

RADIAL AND AXIAL DIMENSIONS OF THE REACTOR MODEL

i	R_i (cm)	Z_i (cm)
0	0.0	0.0
1	17.1965	30.48
2	51.5895	60.96
3	115.3576	152.40
4	181.1764	213.36
5	237.6604	243.84
6	268.1404	335.28
7		396.24
8		426.72

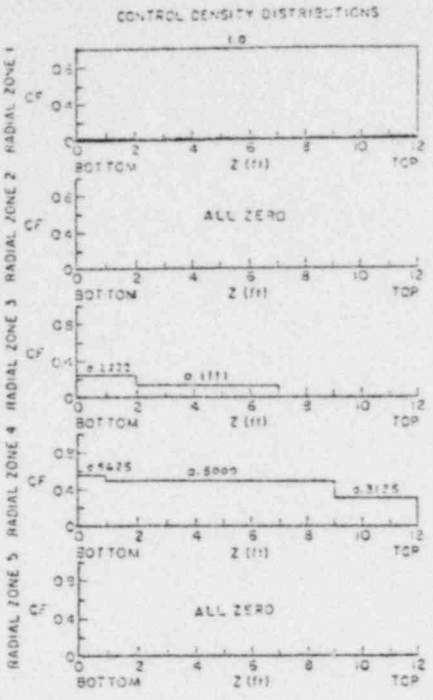

Figure 4 Control density profiles for Cases 1, 2, 8, 9

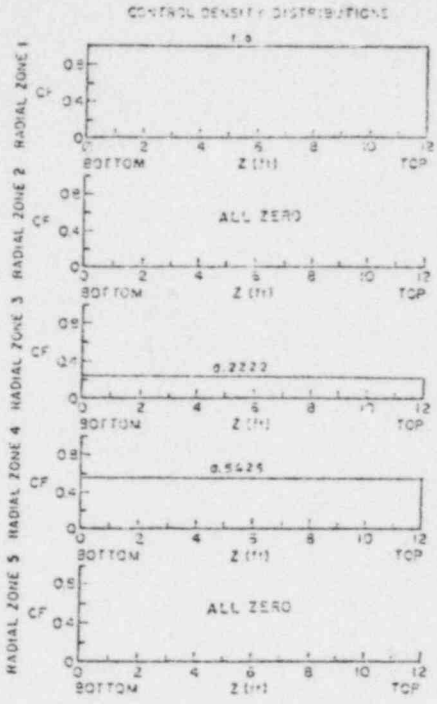

Figure 5 Control density profiles for Case 3

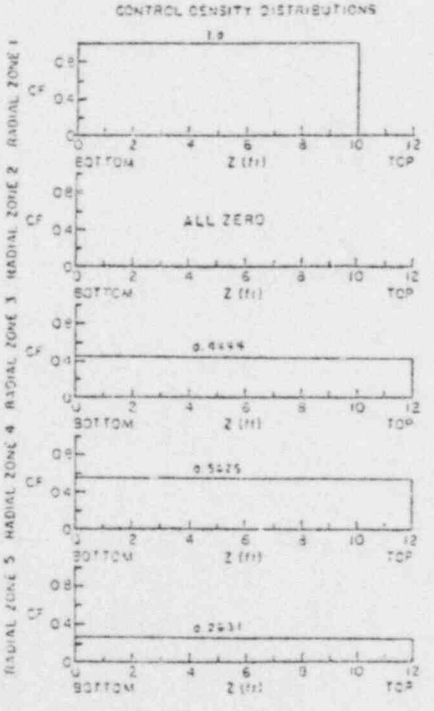

Figure 6 Control density profiles for Case 4, 5, 6, 7, 10, 13

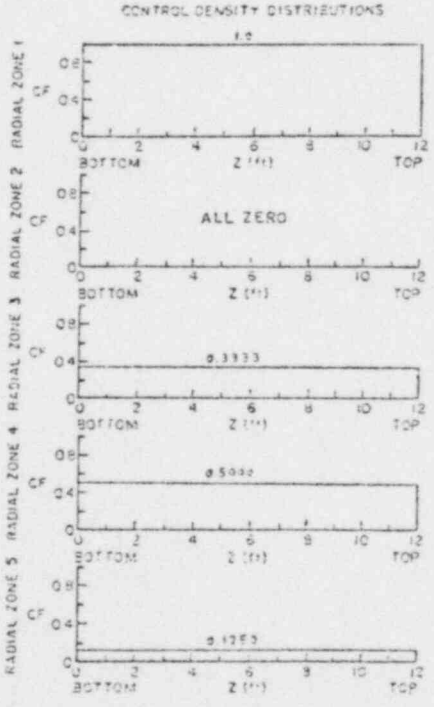

Figure 7 Control density profiles for Case 11, 12

The entire reactor, including the reflectors, is partitioned into 11 radial channels and 26 axial planes for thermal-hydraulic representation, and 36 radial mesh points and 61 axial mesh points for the neutronics.

The axial reflectors are assumed to be a mixture of 60% stainless steel and 40% water. The water of the bottom reflector is at a hot operating condition with no steam voids, while that of the top reflector is assumed to consist of 60% voids. The radial reflector is pure water at hot operating condition without voids.

The calculations were done with the BNL-TWIGL code.[10] It solves the time-dependent neutron diffusion equation in (R,Z) geometry with two energy groups and up to six delayed neutron precursor groups in tandem with time-dependent thermal-hydraulic equations. The neutronics and thermal-hydraulics are coupled through a feedback model that takes into account the effect of fuel temperature (Doppler), steam voids, moderator temperature, and control rods on the two-group cross sections for each material. Cross section data have a quadratic dependence on void fraction, a linear dependence on the square root of fuel temperature, and a linear dependence on the moderator temperature. The coefficients of the quadratic depend on whether or not the region contains control rods. This core dynamics model is similar to that used for the recent scram[12] and void feedback[13,14] studies.

2.3 Nuclear Data

The two-group cross section data were generated by a series of eight-group, two-dimensional, four-bundle supercell calculations with TWOTRAN-II (Reference 15). An S_4 approximation with transport-corrected isotropic scattering and reflecting boundary conditions was used. Within this representation, each fuel cell was homogenized and designated as a distinct material. Control blades (if present), channel boxes, an extra water film next to the channel, and inter assembly gap water were also explicitly represented. The resulting fluxes were used to spatially homogenize and group collapse the data to the required form. The eight-group data were calculated using the HAMMER[16] 84-group integral transport theory code. Libraries for this code are based on ENDF/B-IV data.

Data generation was done for a reference state corresponding to full-power operation; namely, an average fuel temperature of 922K (1200°F), a moderator temperature of 599K (547°F), and an average void fraction of 40%. Data were also generated at perturbed conditions 250K above the reference fuel temperature, 66K below the reference moderator temperature, and at void fractions of 0 and 60%. These perturbed conditions together with the reference condition were used to determine the feedback coefficients of the two-group cross sections.

The accident calculation requires a set of delayed neutron data representative of the reactor condition. Table III lists the delayed neutron data for the six precursor groups used in the present analysis for the BOL and EOC conditions.

TABLE III

DELAYED NEUTRON DATA

Delayed Group i	BOL Yield Fraction β_i	EOC Yield Fraction β_i	Decay Constant $\lambda_i(sec^{-1})$
1	0.000280	0.000207	0.0127
2	0.001572	0.001163	0.0317
3	0.001387	0.001027	0.1150
4	0.003004	0.002222	0.3110
5	0.000945	0.000699	1.4000
6	0.000192	0.000142	3.8700
Total:	0.007380	Total:	0.005460

3.0 RESULTS

The present analysis of center rod drop accidents consists of the steady-state calculations and transient calculations. The steady-state calculations were performed to establish the initial accident conditions as specified in Table I. For each case the reactor was made critical with the control density profiles as shown in Figures 4 through 7. The nuclear-thermal-hydraulic coupling was established through a feedback model as described in Section 2.2 by iterating on the thermal-hydraulic region power until its largest fractional change becomes less than 10^{-4}. The spatial neutron fluxes were converged to within 10^{-6}. After the final converged steady-state solution was obtained, an exact adjoint calculation for each case was performed to provide the weighting function for reactivity edits during the transient.

The transient calculations for the first five cases were performed with and without the moderator feedback. The case without the moderator feedback was done by holding the void distribution and coolant temperature profile fixed at the steady-state values throughout the transient. In both cases, fuel rod temperature calculations were done to provide Doppler feedback on the accident. For all cases, scram was activated with a 0.20 s delay once the core thermal power exceeds 120% of rated power. Table IV summarizes the status of important feedback mechanisms of each CRDA case.

3.1 Accident Rod Worth

Since the consequence of the accident depends strongly on the accident rod worth, the determination of the accident rod worth is an important matter. This has been customarily done by a series of steady-state calculations based on the adiabatic approximation. Here the work "adiabatic" means that the thermal-hydraulic feedback (including Doppler) is entirely neglected. That is, the thermal-hydraulic conditions of the perturbed state remain the same as the original unperturbed state.

The accident rod worth so determined is called the "static rod worth" which is expected to be different from the actual "dynamic rod worth". The dynamic rod worth is defined as the reactivity worth of the accident control rod obtained from the dynamic calculation using BNL-TWIGL where all the important feedback mechanisms are taken into account, including the continuous movement of the accident rod. The dynamic rod worth is considered the actual worth of the accident rod; whereas, the static rod worth is an approximation. Appendix A discusses the mathematical definitions of the accident rod worths.

We have calculated the dynamic and static rod worths for each case using BNL-TWIGL. The dynamic rod worth is obtained from the transient dynamic calculation; whereas, the static rod worth is the result of the adiabatic steady-state calculation. In BNL-TWIGL, the steady-state solution is obtained by solving a pseudo-transient problem with a vanishingly small time derivative. The same solution technique is used to obtain the spatial solution at each pseudo-time step. In the case of the adiabatic steady-state calculation at the perturbed state corresponding to the accident rod being fully withdrawn,

TABLE IV

FEEDBACK MECHANISMS FOR CRDA CASES

CRDA CASE	MODERATOR FEEDBACK	DMH FEEDBACK	DOPPLER FEEDBACK	REACTOR SCRAM
1	Yes, No	Yes, No	Yes	No, Yes
2	Yes	No	Yes	No
3	Yes, No	Yes, No	Yes	No, Yes
4	Yes, No	Yes, No	Yes	Yes, Yes
5	Yes, No	Yes, No	Yes	No, Yes
6	No	No	Yes	Yes
7	Yes	No	Yes	Yes
8	No	No	Yes	Yes
9	No	No	Yes	Yes
10	No	No	Yes	Yes
11	Yes, No	Yes, No	Yes	Yes
12	Yes, No	Yes, No	Yes	Yes, Yes
13	Yes, No	Yes, No	Yes	Yes, Yes

the neutron flux will grow exponentially with a constant period that corresponds to a constant positive reactivity. This positive reactivity will approach its asymptotic value as the number of pseudo-time steps increases. The saturated positive reactivity is the static rod worth defined in Appendix A. Figure 8 illustrates the saturation of the static rod worth for Case 5.

Table V summarizes the results of the accident rod worth calculations for the CRDA cases considered. In general, the static rod worth is greater than the dynamic rod worth. This is due to the fact that the thermal-hydraulic feedback due to a rod drop is negative in a BWR. For a rapid rod insertion we would expect the dynamic rod worth to be greater than the static worth for similar reasons.

3.2 Initial Steady-State Conditions

The initial conditions can be characterized by several steady-state neutronics and thermal-hydraulic parameters. The neutronics is represented by the average axial and radial power profiles, whereas, the thermal-hydraulics is represented by the average void distribution, fuel temperature profile, clad surface heat flux distribution, and the coolant temperature profile.

3.2.1 Steady-State Neutronics

Figures 9 and 10 present the initial core-average axial and radial power profiles of the 10% power cases. The corresponding power profiles of the HZP cases are shown in Figure 11 for the average axial power distribution and in Figure 12 for the radial power profile. While the power profiles of the 10% power cases are more or less as expected of normal operating conditions, the HZP cases exhibit a rather severe power peaking. This is because the center rod is initially two feet withdrawn from the top of the core (see Figure 1) and because more control rods are present in the core expecially in the peripheral region to achieve the zero power condition.

Power peaking factors are of interest because of their impact on the accident rod worth and the peak fuel enthalpy. Let F_Z denote the radially averaged axial power peaking factor, F_R represent the axially averaged radial power peaking factor, and F_L the local power peaking factor. The overall (total) power peaking factor (F_Q) is customarily defined as

$$F_Q = F_Z F_R F_L.$$

Table VI summarizes the power peaking factors of the accident cases studied. Here we have assumed that the local peaking factor is 1.2 for all cases. The 10% power cases have fairly normal peaking factors while the HZP cases possess much higher peaking factors. Note that the total peaking factor defined above is not meant to represent the real peaking factor. Rather, it is just useful in characterizing the power peaking.

3.2.2 Steady-State Thermal-Hydraulics

The initial average axial distributions of void fraction, fuel temperature, surface heat flux, and coolant temperature for the 10% power cases are presented in Figures 13 through 16. The initial axial distributions of fuel

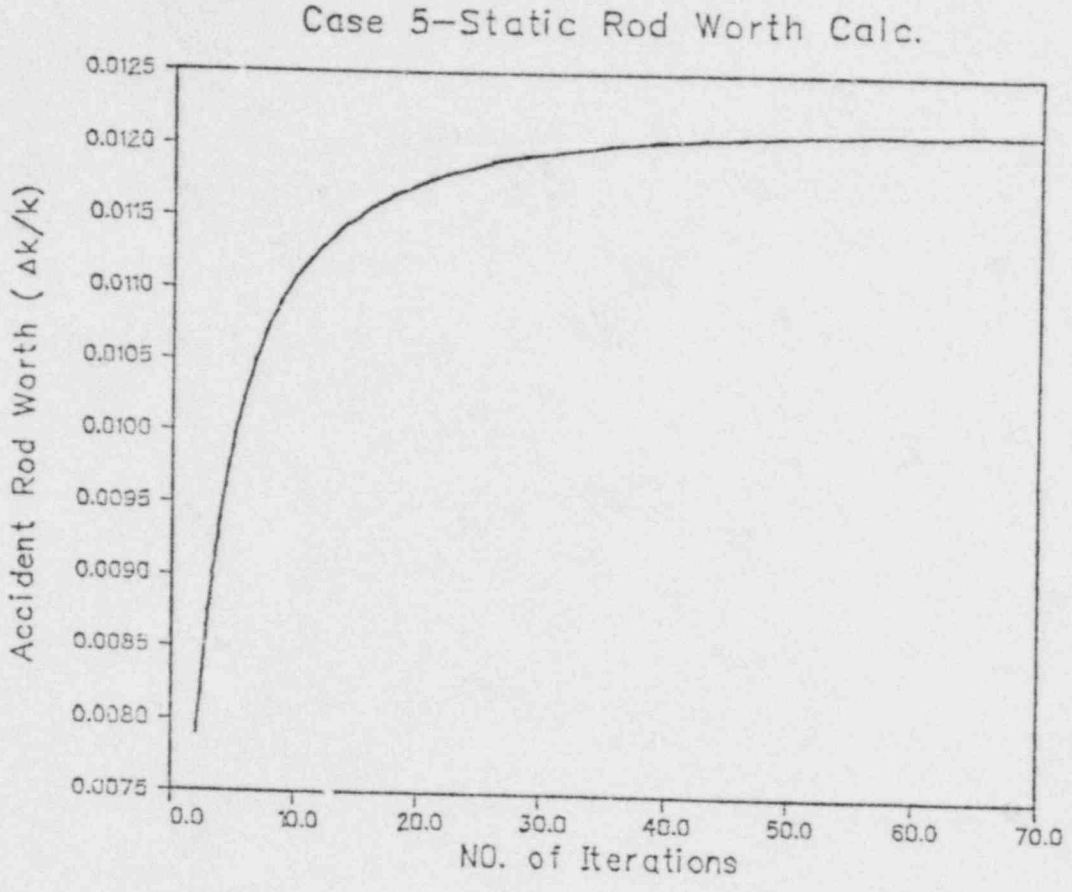

Figure 8 Saturation behavior of the static rod worth of Case 5

TABLE V

ACCIDENT ROD WORTH CALCULATIONS

CRDA CASE	DYNAMIC WORTH (Δk/k)	STATIC WORTH (Δk/k)
1	0.00826	0.00887
2	0.00831	0.00892
3	0.00467	0.00503
4	0.01155	*
5	0.01197	0.01210
6	0.01193	0.01210
7	0.01204	0.01210
8	0.00822	0.00887
9	0.00829	0.00887
10	0.01203	0.01210
11	0.01921	0.02077
12	*	0.02112
13	*	0.01192

* Data not available

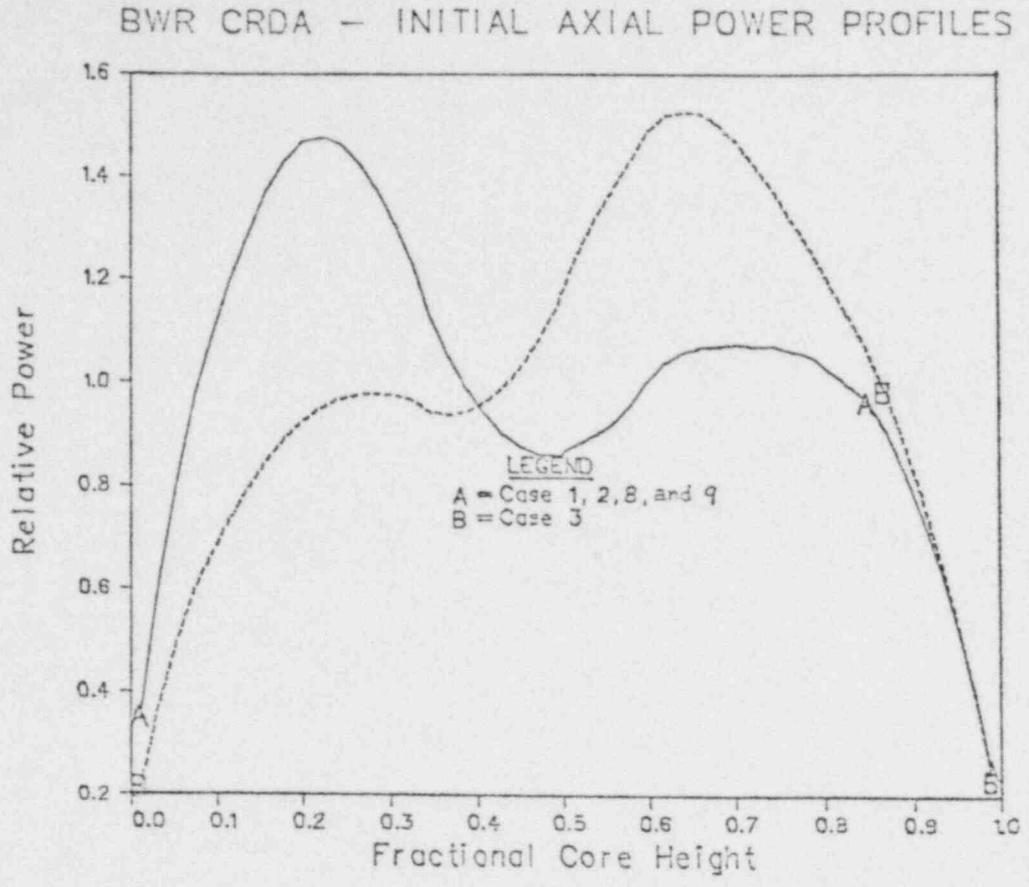

Figure 9 Initial axial power profiles of the 10% power cases

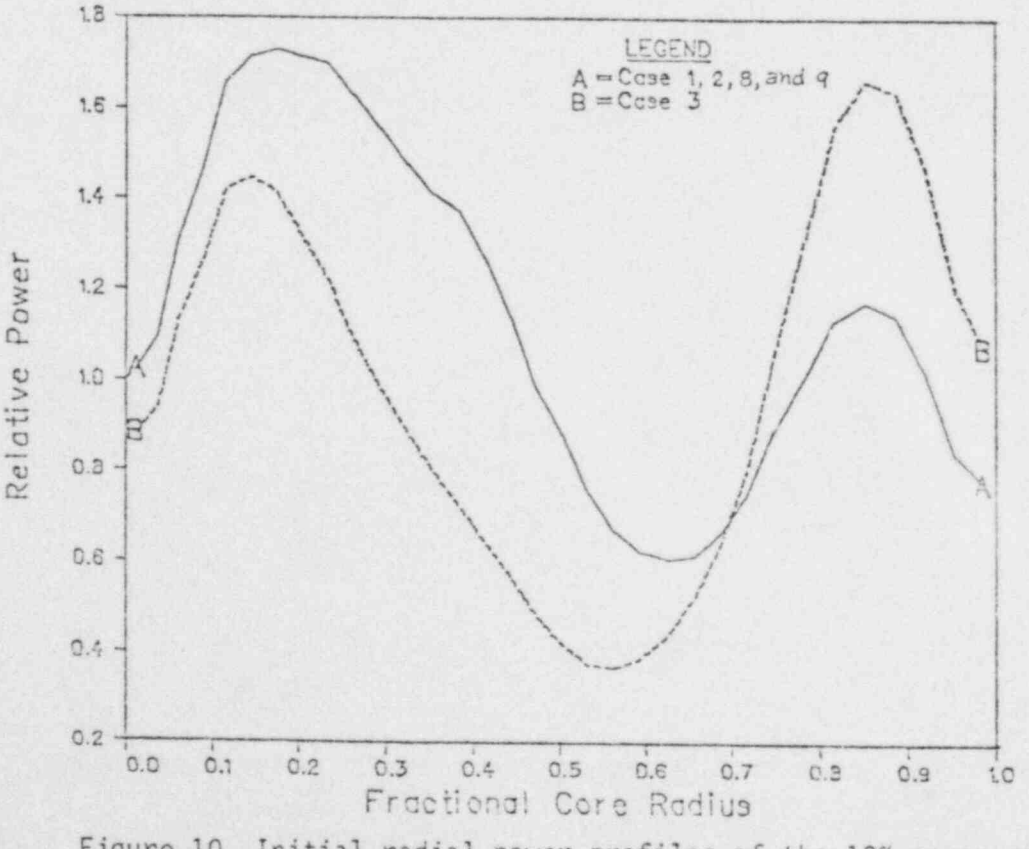

Figure 10 Initial radial power profiles of the 10% power cases

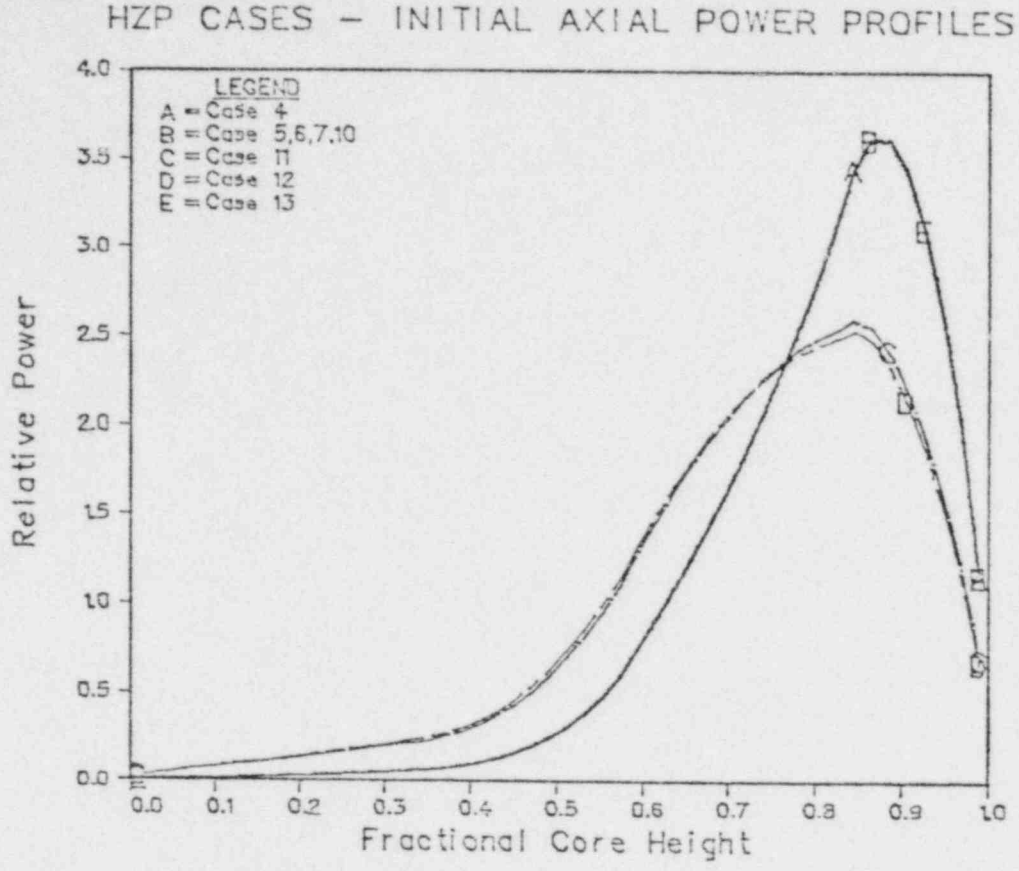

Figure 11 Initial axial power profiles of the HZP cases

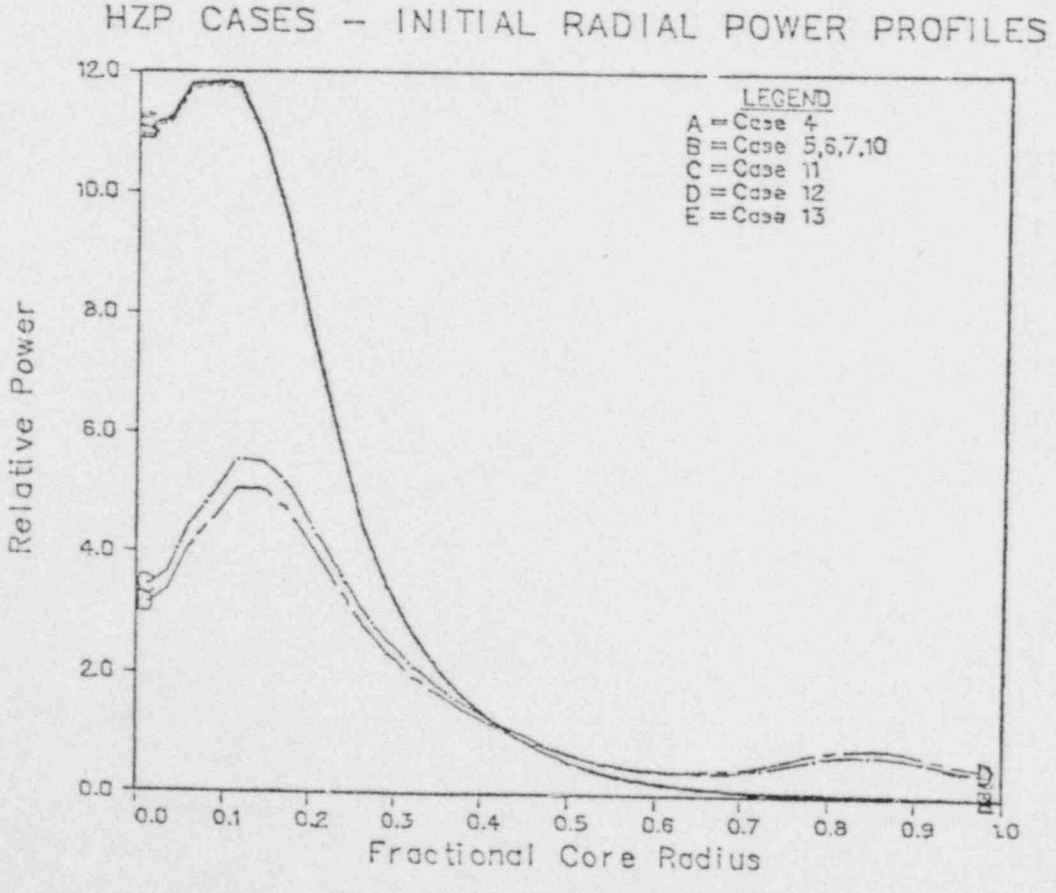

Figure 12 Initial radial power profiles of the HZP cases

TABLE VI

INITIAL POWER PEAKING FACTORS OF THE ROD DROP ACCIDENTS

CRDA CASE	AXIAL F_Z	RADIAL F_R	LOCAL F_L	OVERALL F_Q
1	1.48	1.73	1.20	3.07
2	1.47	1.73	1.20	3.05
3	1.53	1.67	1.20	3.07
4	3.64	11.87	1.20	51.85
5	3.61	11.78	1.20	51.03
6	3.61	11.78	1.20	51.03
7	3.61	11.78	1.20	51.03
8	1.48	1.73	1.20	3.07
9	1.48	1.73	1.20	3.07
10	3.61	11.78	1.20	51.03
11	2.60	5.55	1.20	17.32
12	2.53	5.08	1.20	15.42
13	3.62	11.83	1.20	51.39

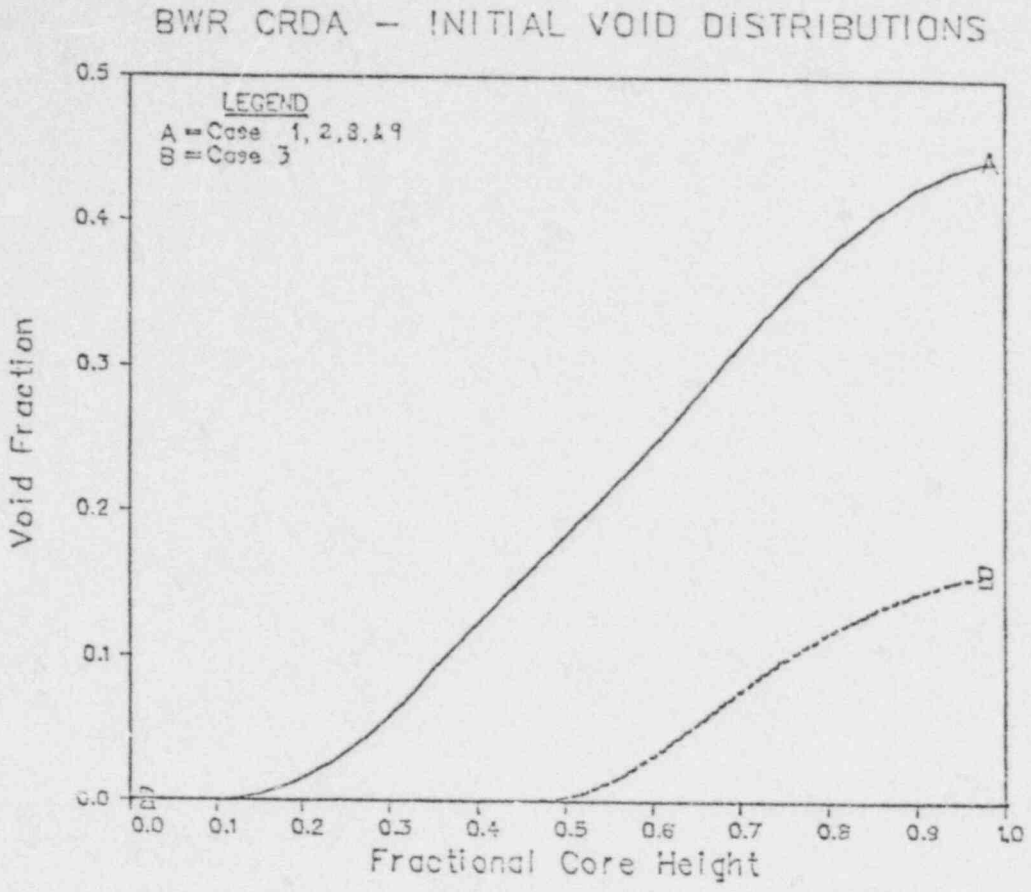

Figure 13 Initial axial void distribution of the 10% power cases

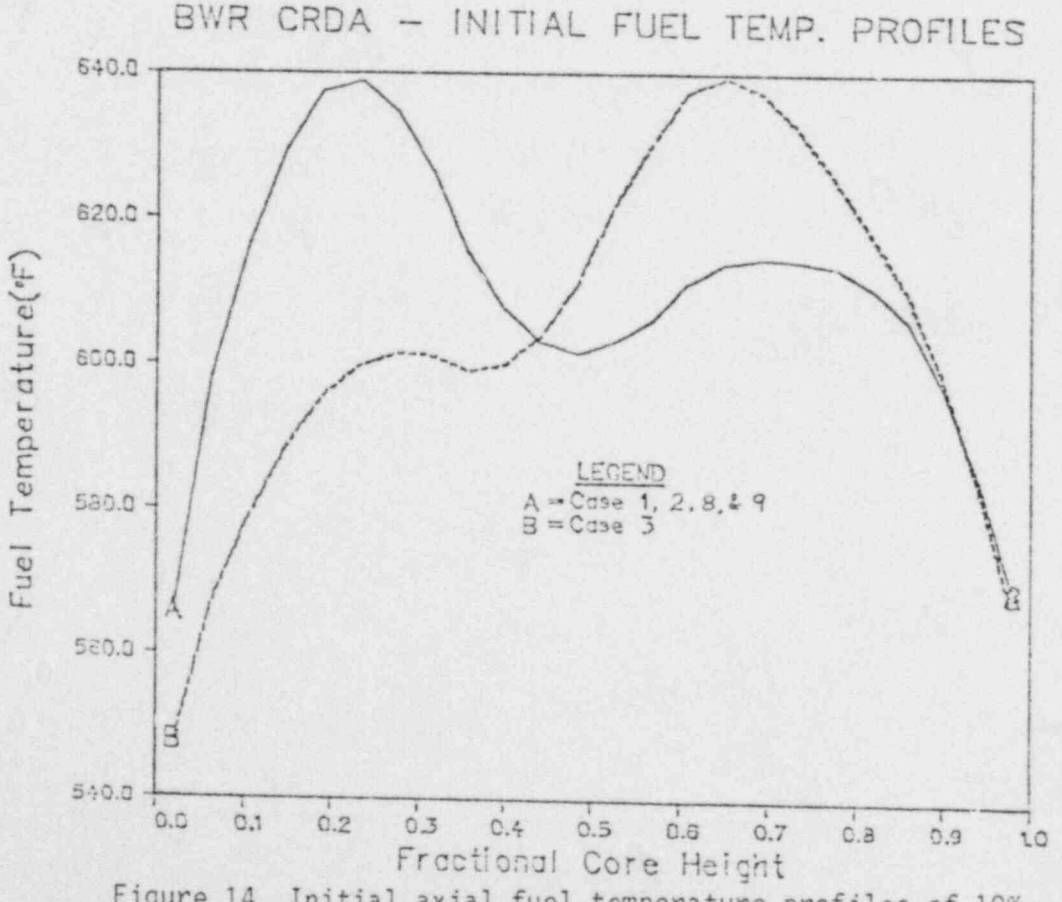

Figure 14 Initial axial fuel temperature profiles of 10% power cases

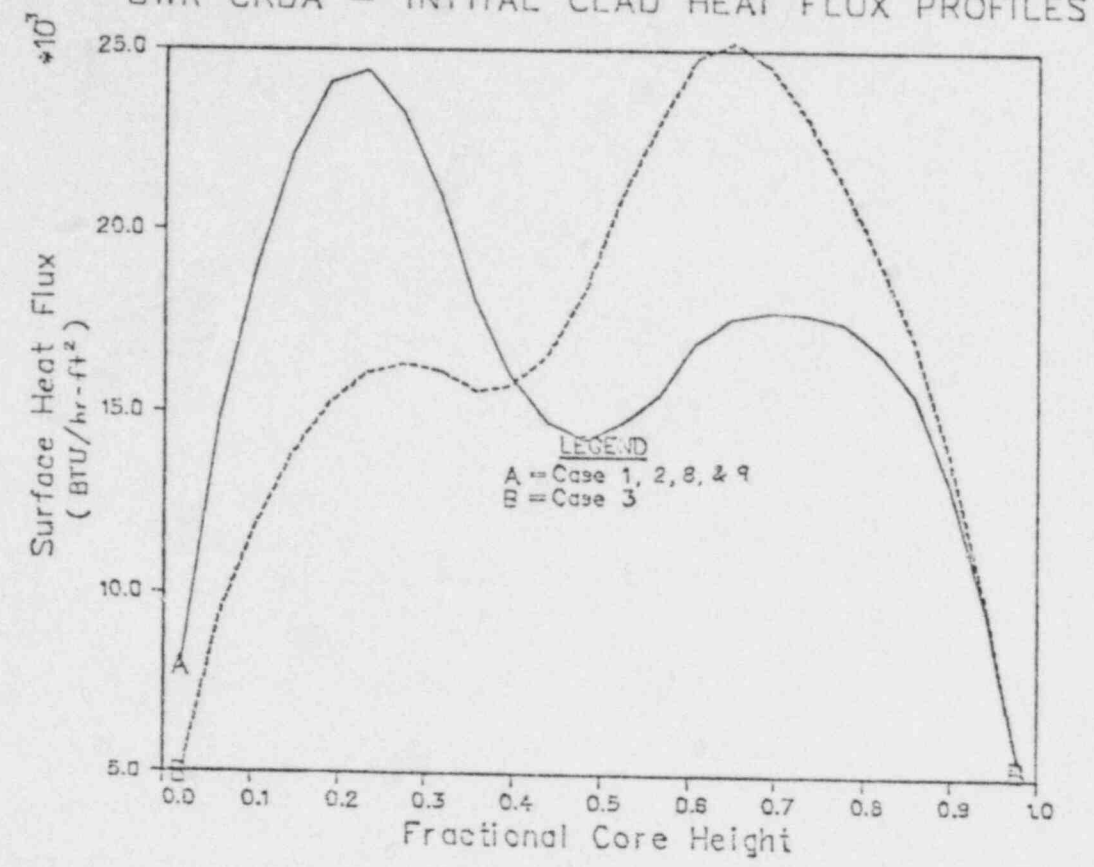

Figure 15 Initial heat flux distributions of 10% power cases

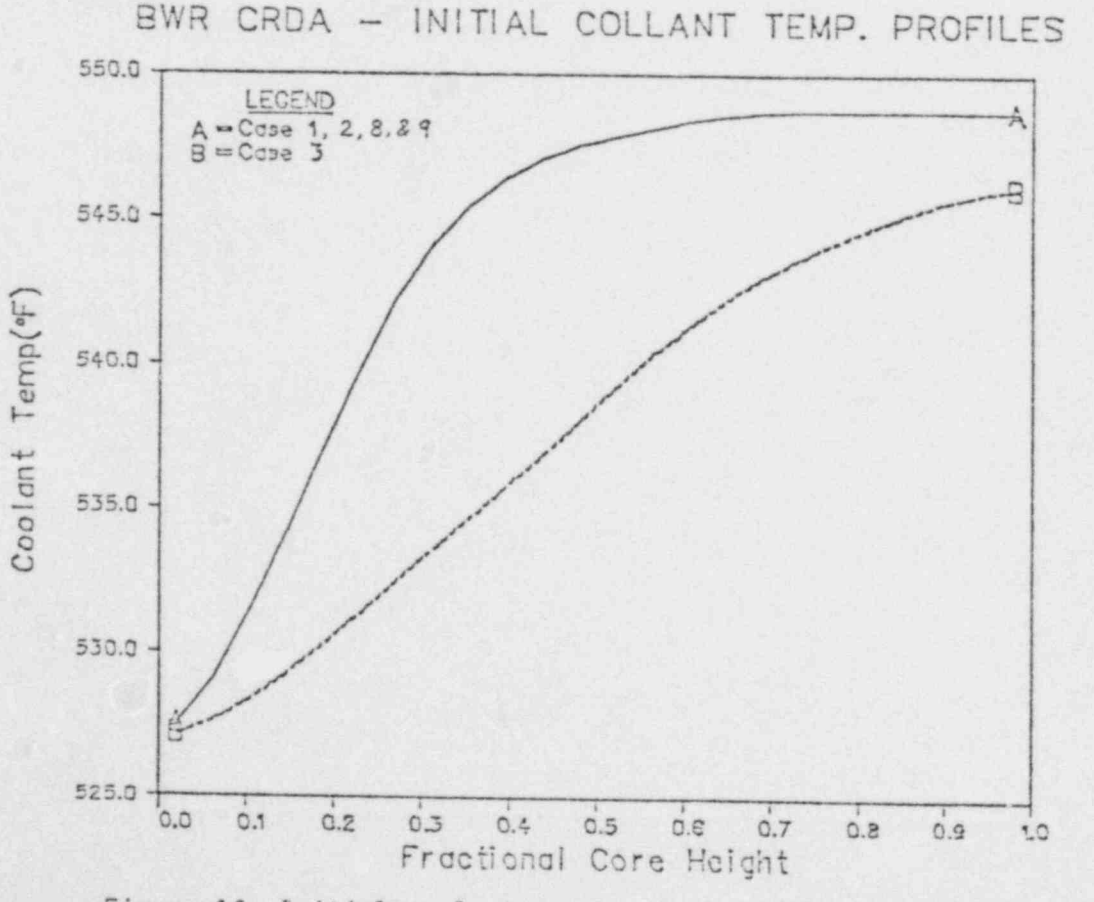

Figure 16 Initial coolant temperature profiles of 10% power cases

and coolant temperatures for the HZP cases are shown in Figures 17 and 18. For the 10% power cases the amount of voids in the core is relatively small because of the low power level. The fuel temperature and clad heat flux profiles resemble the axial power distribution (see Figure 9).

For the HZP cases, there are no voids in the core and the clad surface heat flux is also vanishingly small because of the zero power condition. For this reason, they are not presented in graphical form. The fuel temperature and coolant temperature profiles are both flat again because of the zero power condition. In fact, the temperature distribution across the fuel rod is also flat in this case.

3.3 Transient Characteristics

The transient neutronics is represented by the time behavior of the core thermal power (CTP), peak fuel enthalpy, and various feedback reactivities including the total reactivity. The transient thermal-hydraulics is represented by the time behavior of the average void fraction, average fuel temperature, and clad surface heat flux. Some global hot spot results will also be presented to highlight the local transient behavior.

We shall emphasize the effect of the moderator feedback on the accident. Here the moderator feedback is defined to be composed of the void feedback and the moderator temperature feedback. The moderator feedback has two primary sources of contribution: the heat transfer from fuel rods and the direct moderator heating due to gamma ray attenuation and neutron slowing down. The total moderator feedback will be first presented, the direct moderator heating effect will then be separately shown to identify its significance.

3.3.1 Moderator Feedback Effect

The moderator feedback effect during the accident is most visible in the time history of the core thermal power and peak fuel enthalpy. This is shown in Figures 19 and 20 for the reference 10% power case (Case 1). Here two curves are shown: one with and the other without the moderator feedback. The effect of the moderator feedback is clearly seen. It suppresses the power burst quite strongly and reduces the peak fuel enthalpy from 78 cal/gm to only 41 cal/gm.

For the HZP cases, the moderator feedback effect is quite a different story. The first HZP case (Case 4) assumes that the core is initially 20°F subcooled and the other HZP cases (e.g., Case 5) assume no inlet subcooling; that is, the core is initially at saturation. Figure 21 presents the time history of the core thermal power of the first HZP case (Case 4) with and without the moderator feedback. We see that the power excursion is hardly affected by the moderator feedback even though it is significantly affected afterward. This is because the HZP Case 4 starts out with a subcooled initial condition. In fact, the entire core is subcooled because there is 18.5% of rated flow in the core. The fuel rod temperature profile is initially flat. The thermal time constant in this case is, therefore, long enough not to affect the power excursion (see Appendix B.) However, the moderator feedback still helps reduce the peak fuel enthalpy by 28% over 2-second period as shown in Figure 22.

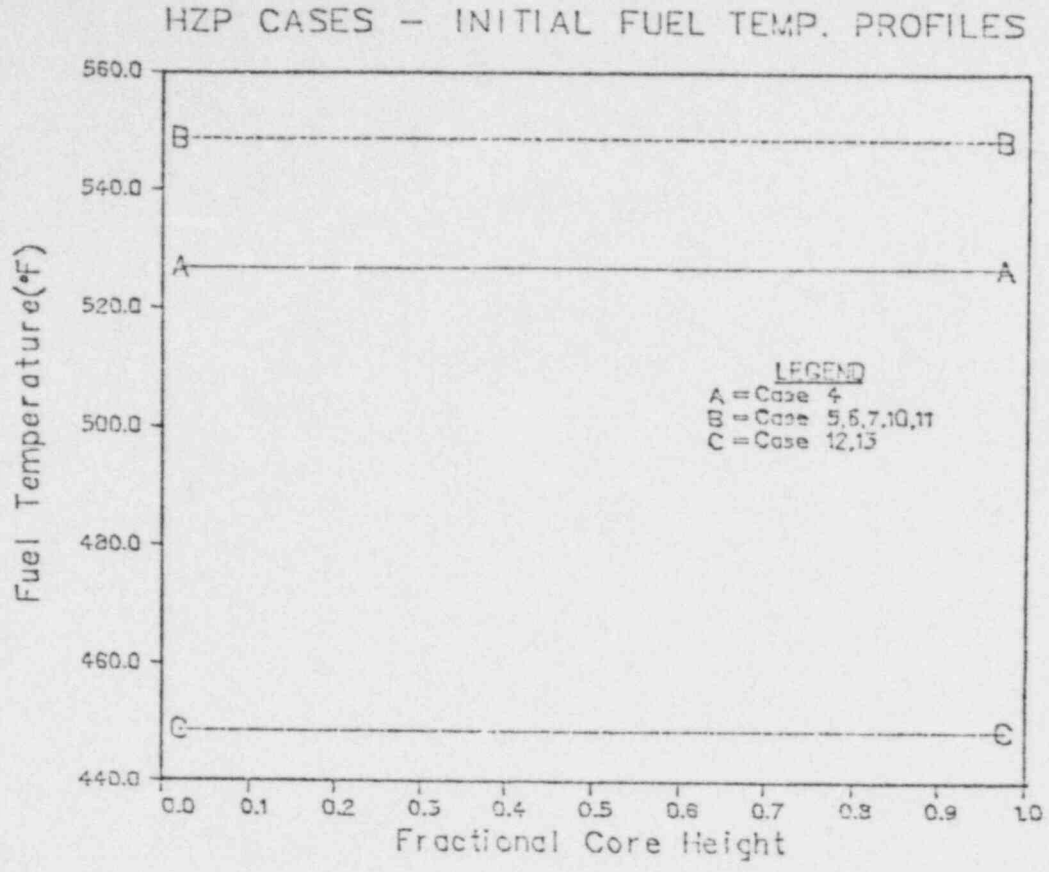

Figure 17 Initial average fuel temperature profiles of HZP cases

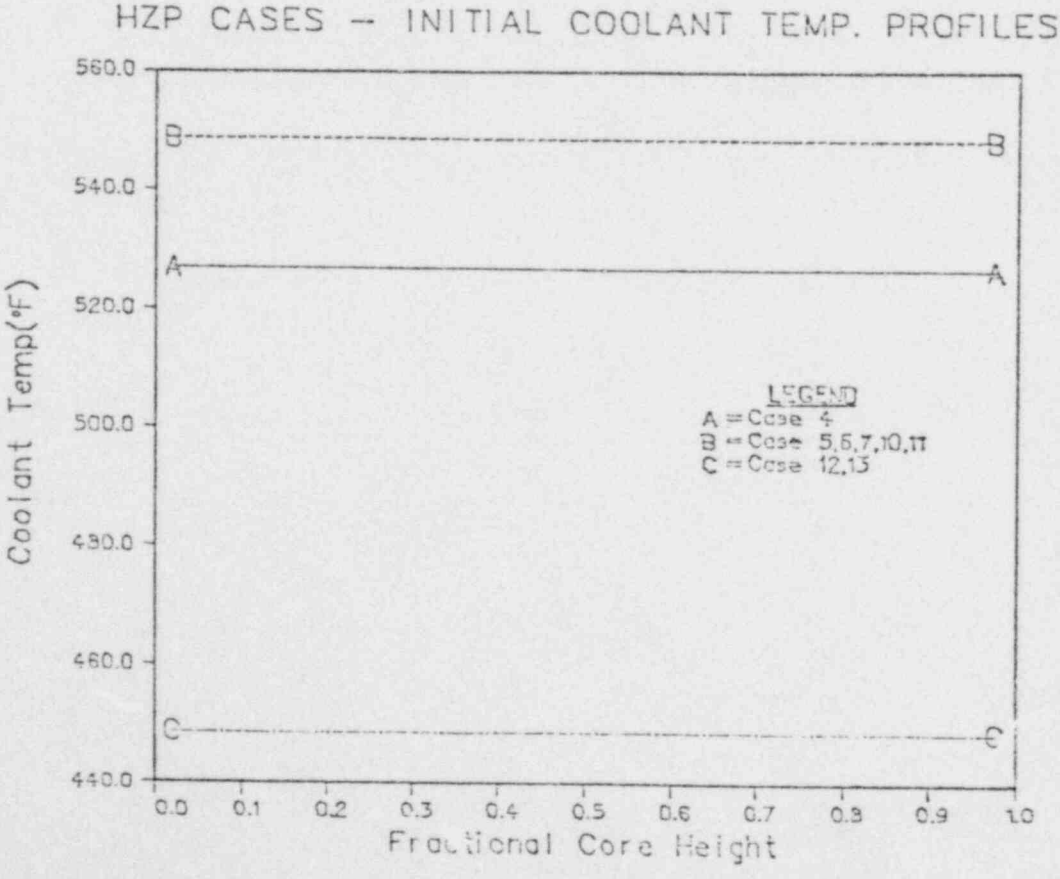

Figure 18 Initial coolant temperature profiles of HZP cases

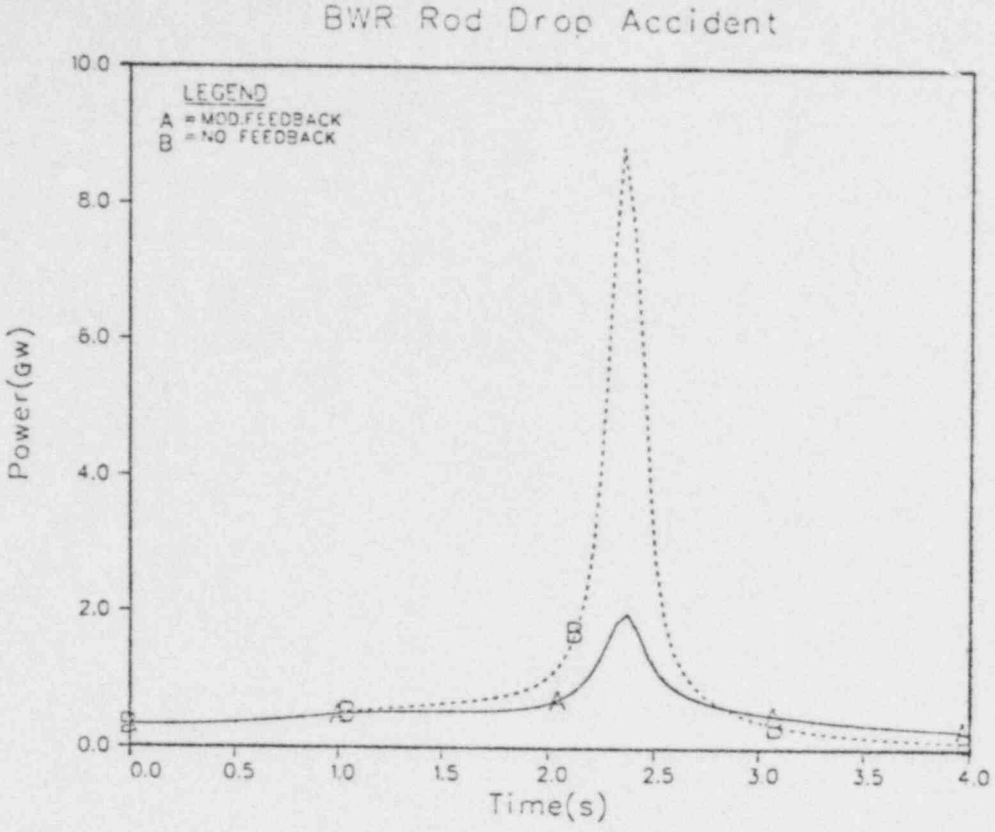

Figure 19 Transient behavior of core thermal power of reference 10% power case (Case 1)

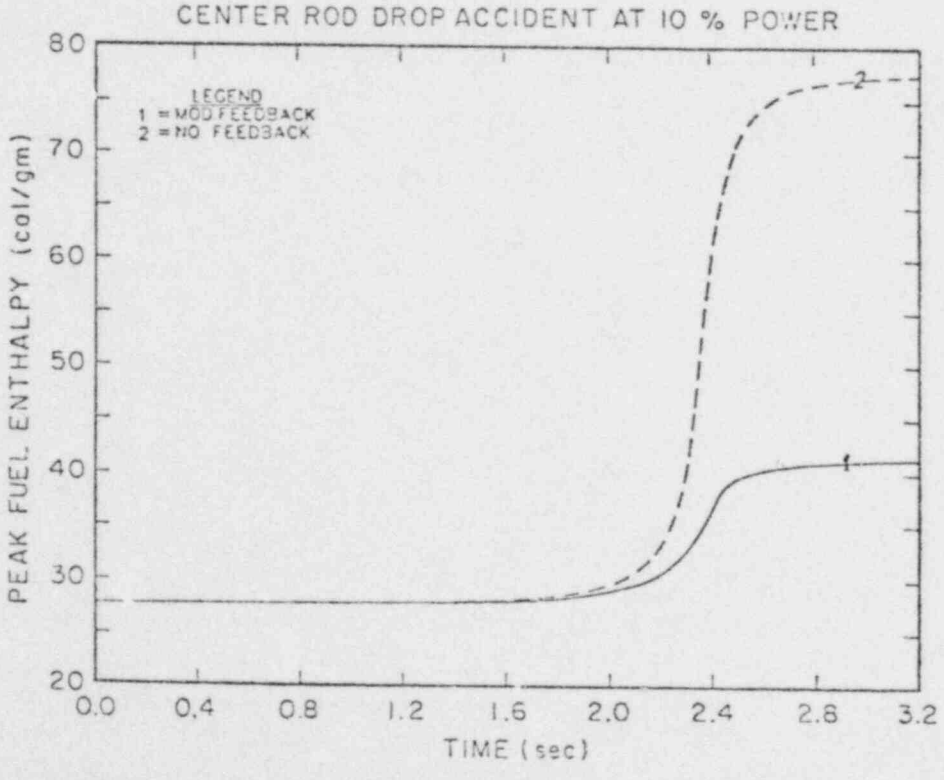

Figure 20 Transient behavior of peak fuel enthalpy of reference 10% power case (Case 1)

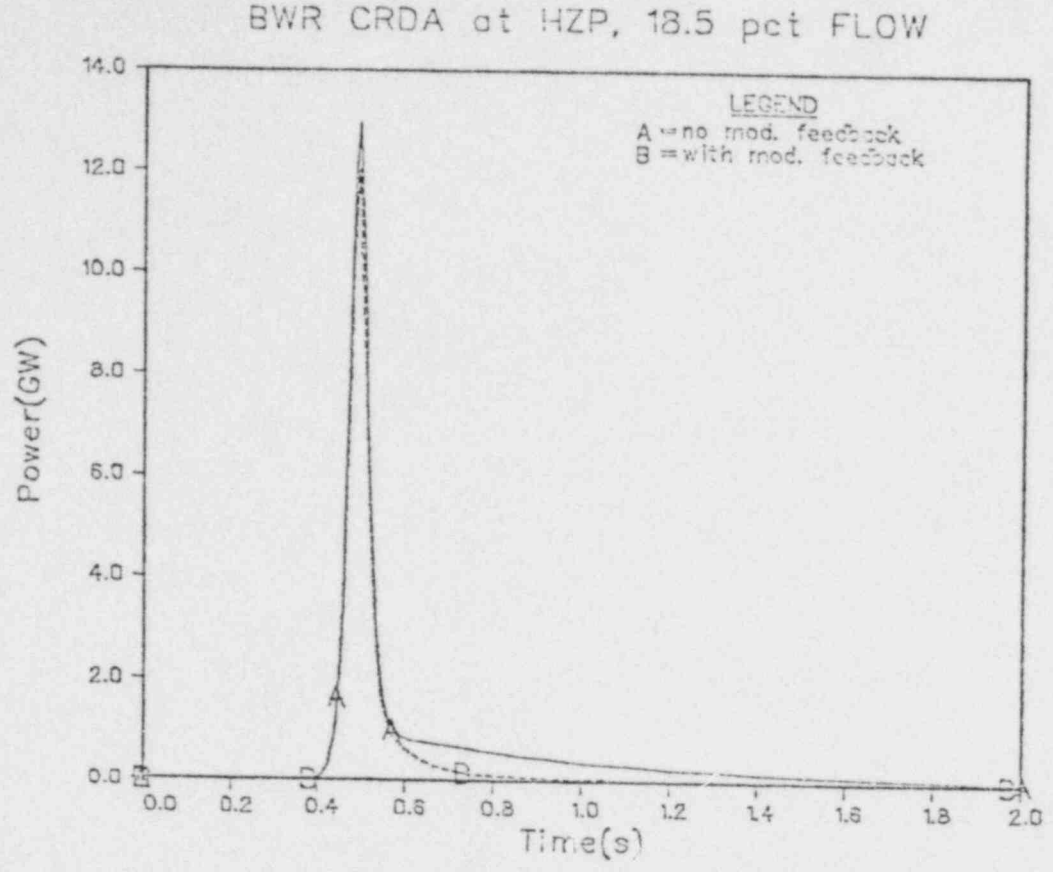

Figure 21 Transient behavior of core thermal power of sub-cooled HZP case (Case 4)

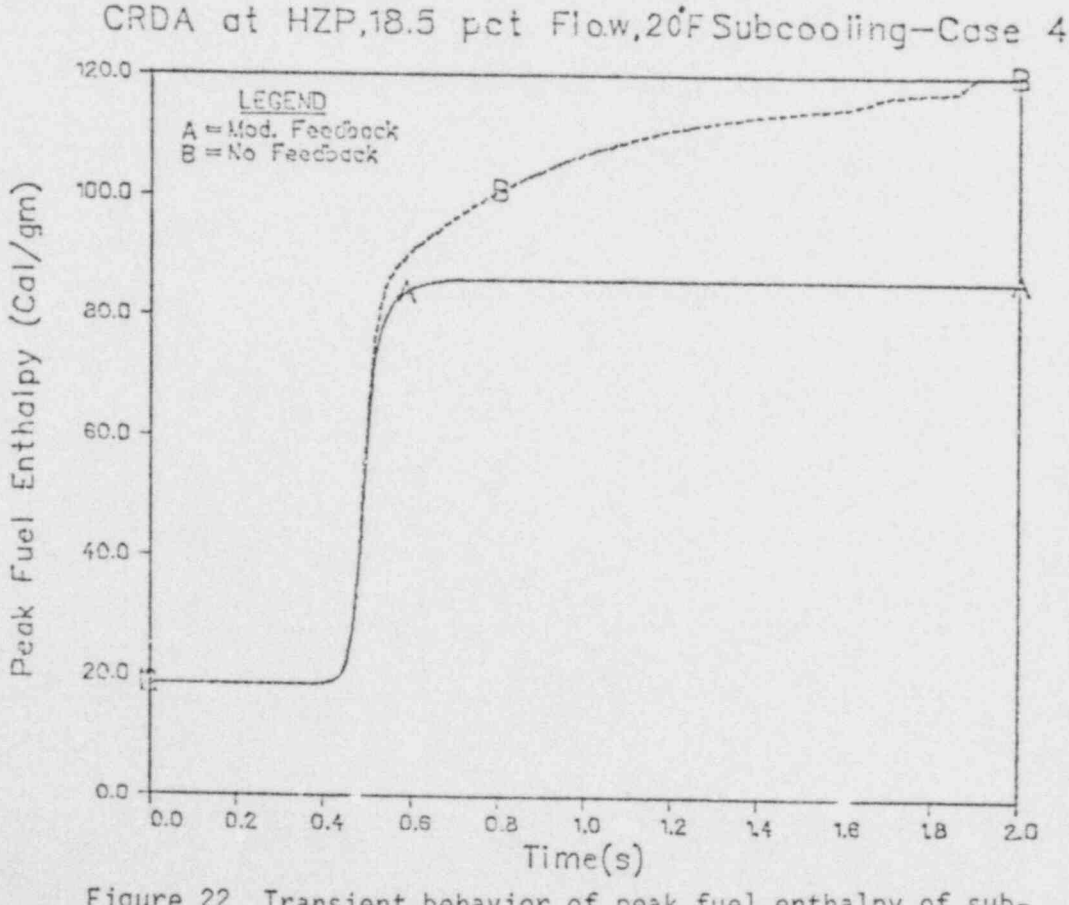

Figure 22 Transient behavior of peak fuel enthalpy of sub-cooled HZP case (Case 4)

Table VII summarizes the transient characteristics of all the accident cases considered in the present work. The 10% power cases are, in general, less severe than the HZP cases because the 10% power cases have a lower accident rod worth (see Table V) and more moderate initial power peaking factors (see Table VI). In summary, the moderator feedback effect is too important to be neglected in the rod drop accident analysis.

The typical transient behavior of various feedback reactivities is shown in Figure 23 for the reference 10% power case (Case 1) with the moderator feedback. (Note that scram reactivity in all graphs refers to control rod reactivity and includes both the accident rod worth and the scram rod worth.) We see that scram was never activated in this case because the core thermal power never exceeds 120% of rated throughout the transient. The dominant void feedback is also evident, actually stronger than Doppler feedback once steam voids start to increase in the core. Scram did occur in Case 1 without the moderator feedback as shown in Figure 24.

The transient reactivity behavior at HZP with inlet subcooling (Case 4) is shown in Figure 25 for the case with the moderator feedback and in Figure 26 for the case without the moderator feedback. (Note the difference in reactivity scales between the two figures.) The importance of the void feedback is evident after 0.6 sec. It is also apparent that most of the moderator feedback is attributable to the void feedback. The moderator temperature feedback plays a very minor role.

Figure 27 presents the transient behavior of the core-average void fraction for the reference 10% power case (Case 1). The rapid rise of the core-average void fraction after 1.5 sec indicates that the moderator feedback has come into play when the core power starts to rise. Figure 28 shows the transient behavior of the average fuel (pellet) temperature. The increase of the void fraction corresponds to the rise of the fuel temperature as the voids come primarily from heat transfer from fuel rods. Figure 29 presents the transient behavior of the radially averaged peak clad surface heat flux.

The transient thermal-hydraulic characteristics for the HZP case with inlet subcooling (Case 4) with the moderator feedback are presented in Figure 30 for the core-average void fraction, in Figure 31 for the average fuel temperature, and in Figure 32 for the average coolant temperature. We see that the fuel temperature starts to rise rapidly at around 0.4 s but the void fraction reaches only 1% at about 1.4 s into the transient even though very small amount of voids starts to form in the core at 0.6 sec. Such a time delay in heat transfer from fuel rods explains why the moderator feedback does not help suppress the power peak for the subcooled HZP case (Case 4) which occurs between 0.4 and 0.6 sec (see Figure 21). This phenomenon can be attributed to the effect of inlet subcooling which is present in this case. This will be discussed below.

3.3.2 Inlet Subcooling Effect

We have seen that the moderator feedback does not help suppress the power peak of the subcooled HZP case (Case 4) even though it does reduce the peak

TABLE VII

TRANSIENT CHARACTERISTICS OF THE ROD DROP ACCIDENTS

CRDA CASE	MODERATOR FEEDBACK	PEAK POWER (GW)	TIME OF PEAK (S)	PEAK FUEL ENTHALPY (CAL/GM)
1a	Yes	1.986	2.363	41
1b	No	8.851	2.363	78
2	Yes	2.455	2.378	44
3a	Yes	1.201	0.990	42
3b	No	4.738	1.002	86
4a	Yes	12.069	0.489	86
4b	No	12.964	0.489	120
5a	Yes	3.008	0.465	35
5b	No	13.570	0.483	136
6	No	8.961	0.666	125
7	Yes	13.236	0.483	85
8	No	5.274	3.766	76
9	No	14.095	2.258	89
10	No	21.112	0.374	141
11a	Yes	16.469	0.498	50
11b	No	80.540	0.509	326
12a	Yes	73.003	0.502	179
12b	No	79.314	0.503	312
13a	Yes	13.405	0.494	109
13b	No	14.481	0.494	147

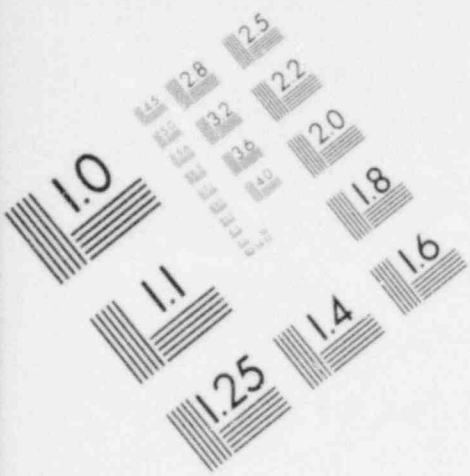

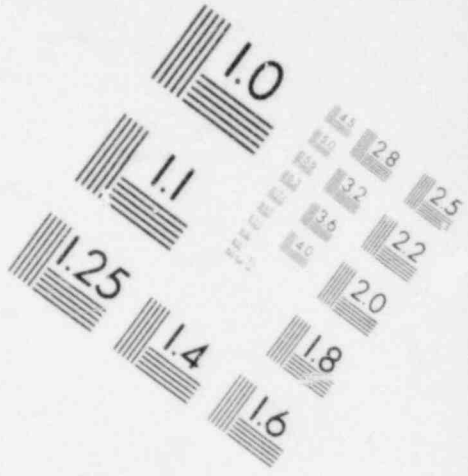

IMAGE EVALUATION
TEST TARGET (MT-3)

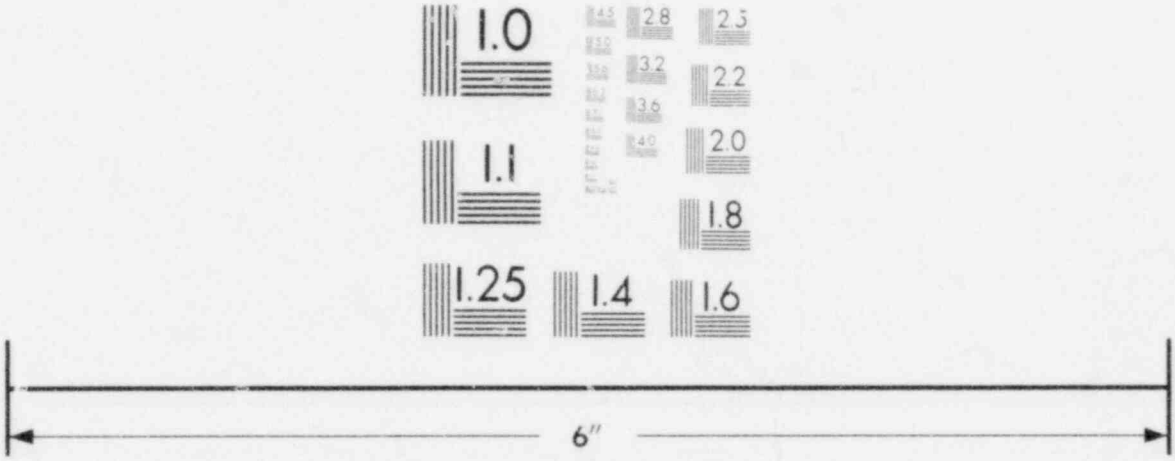

MICROCOPY RESOLUTION TEST CHART

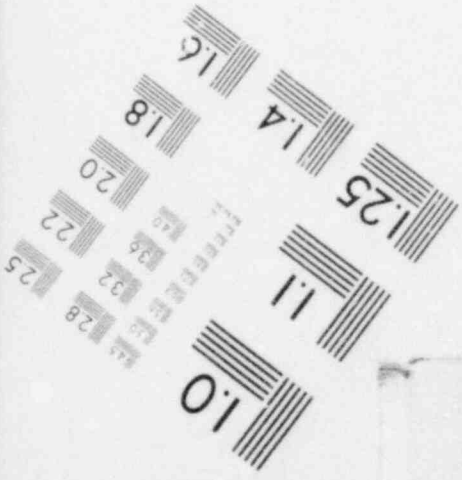

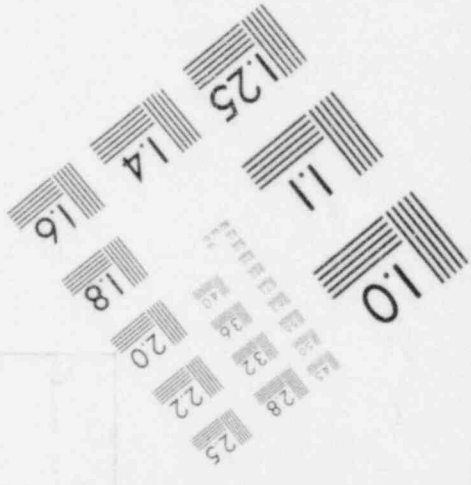

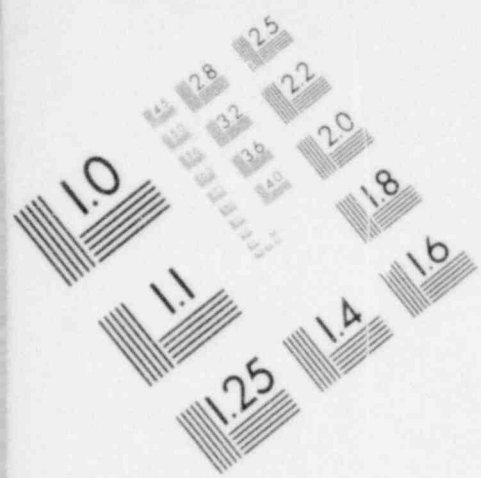

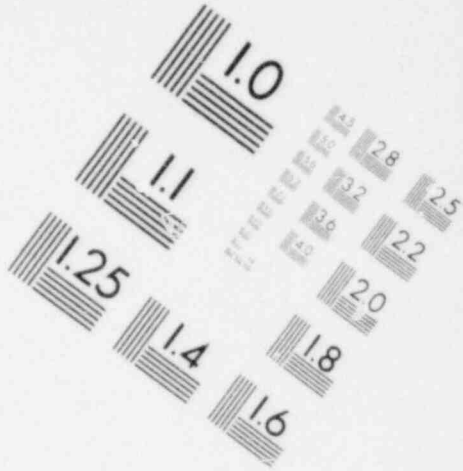

IMAGE EVALUATION
TEST TARGET (MT-3)

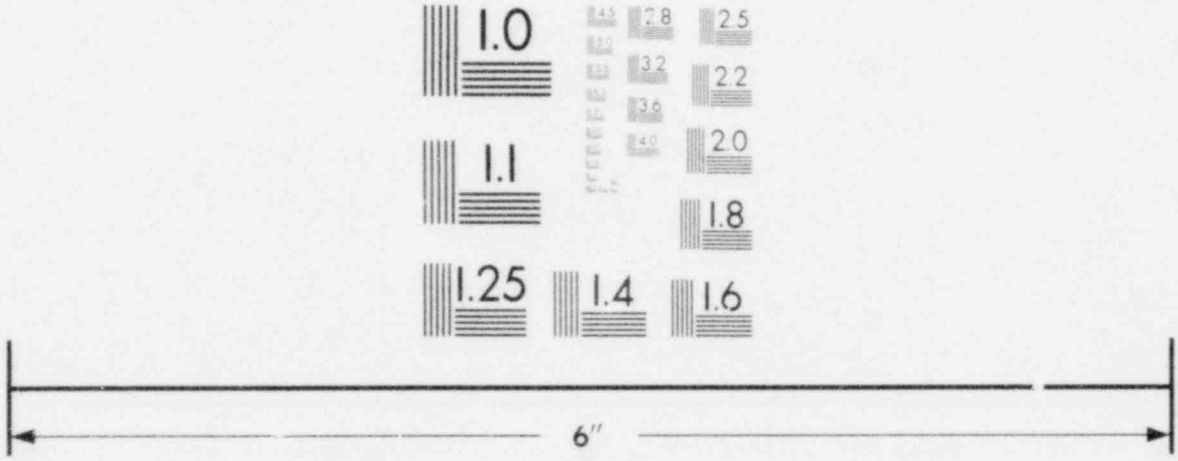

MICROCOPY RESOLUTION TEST CHART

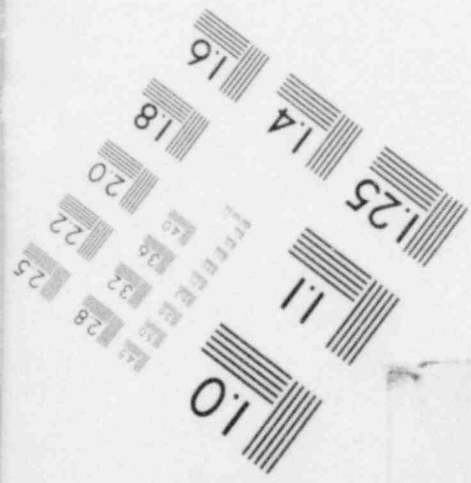

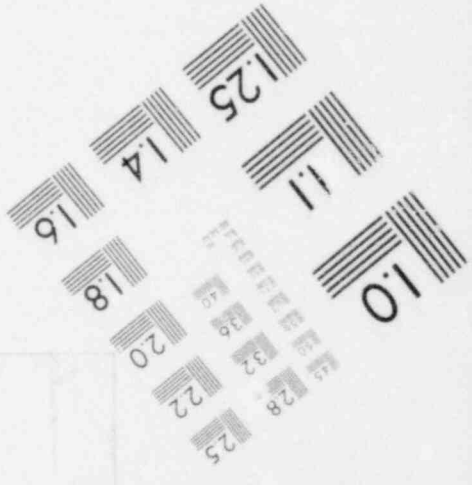

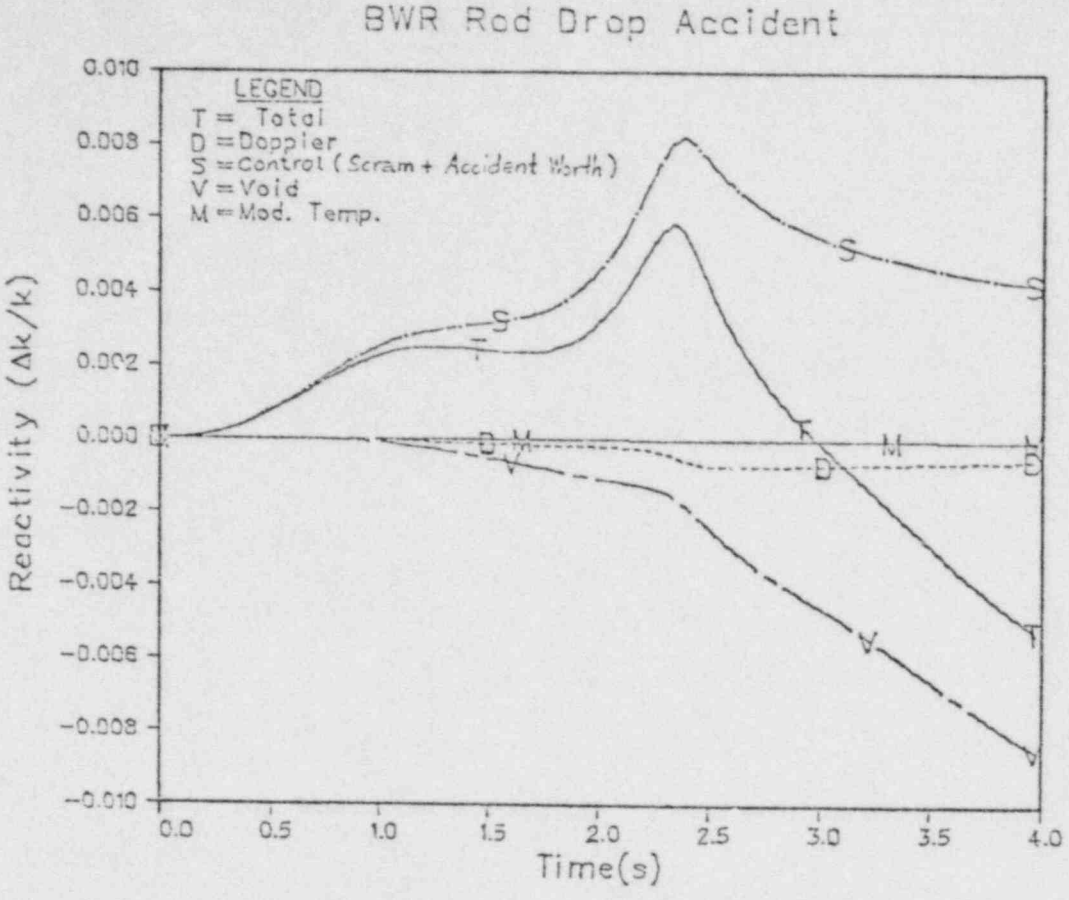

Figure 23 Various reactivity behavior of reference 10% power case (Case 1) with moderator feedback

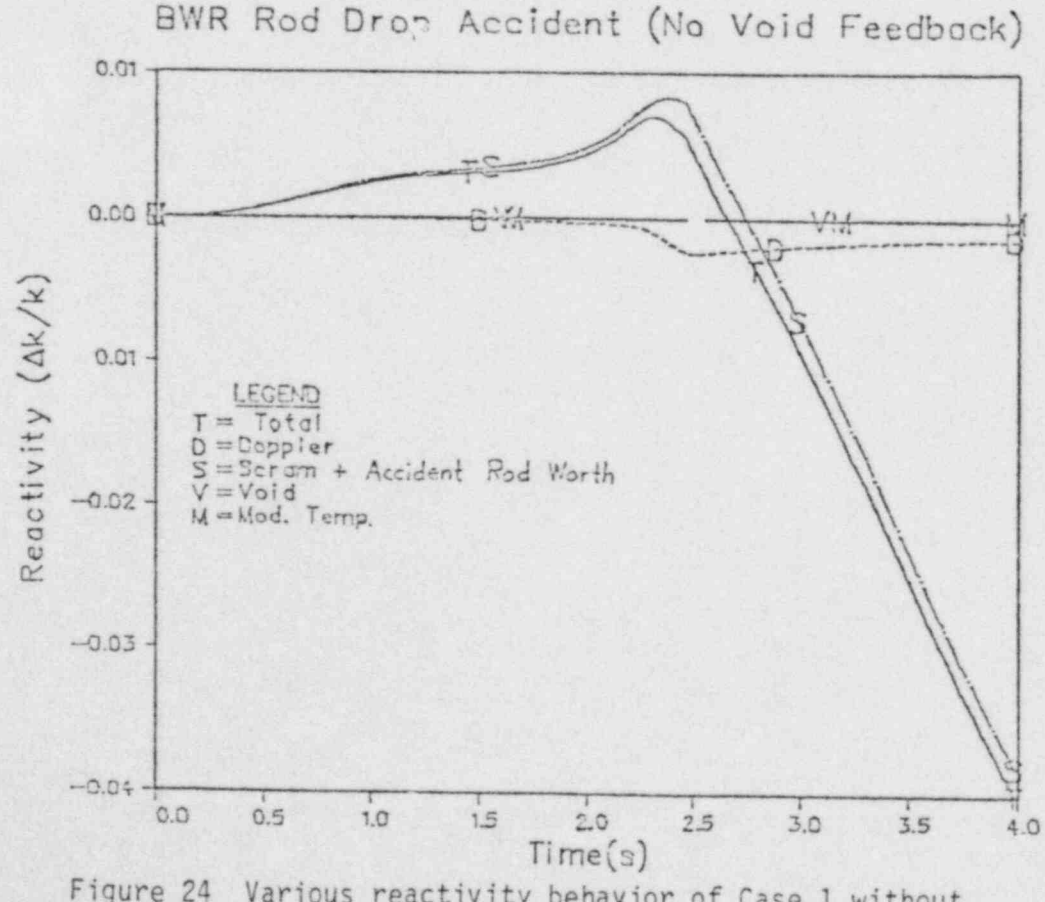

Figure 24 Various reactivity behavior of Case 1 without moderator feedback

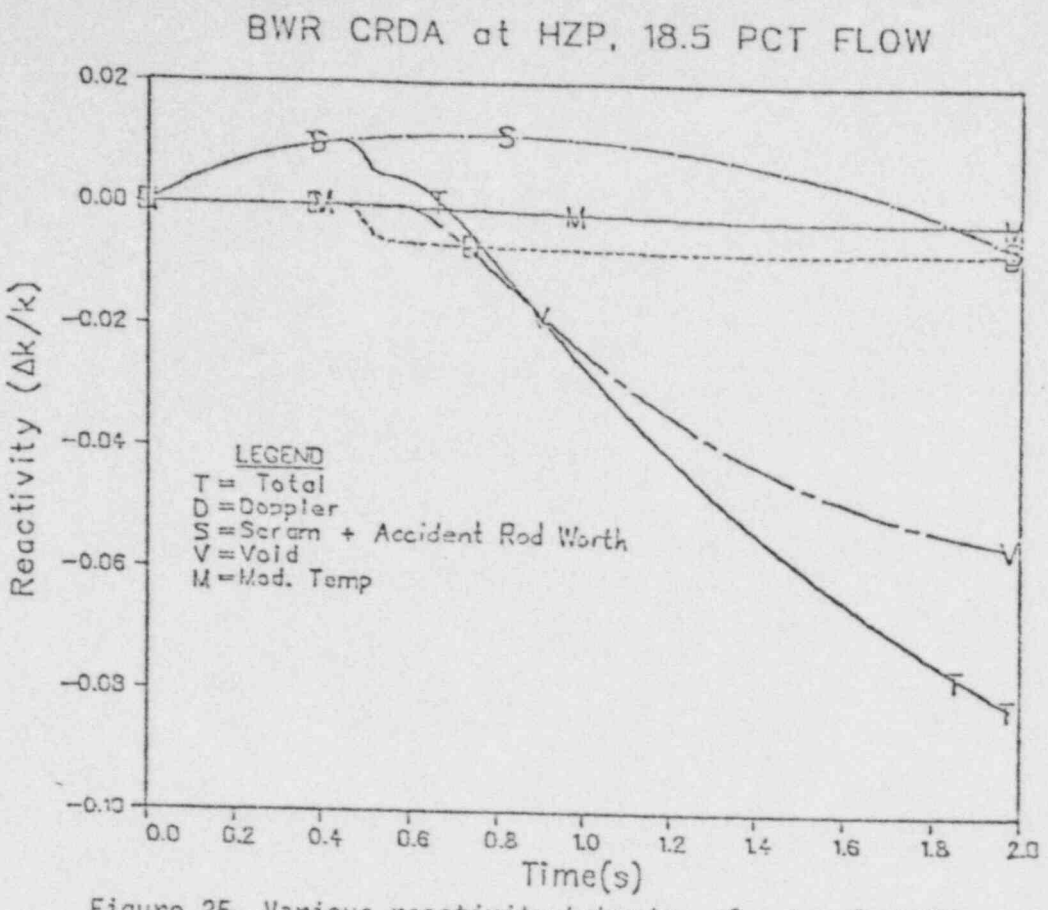

Figure 25 Various reactivity behavior of subcooled HZP case (Case 4) with moderator feedback

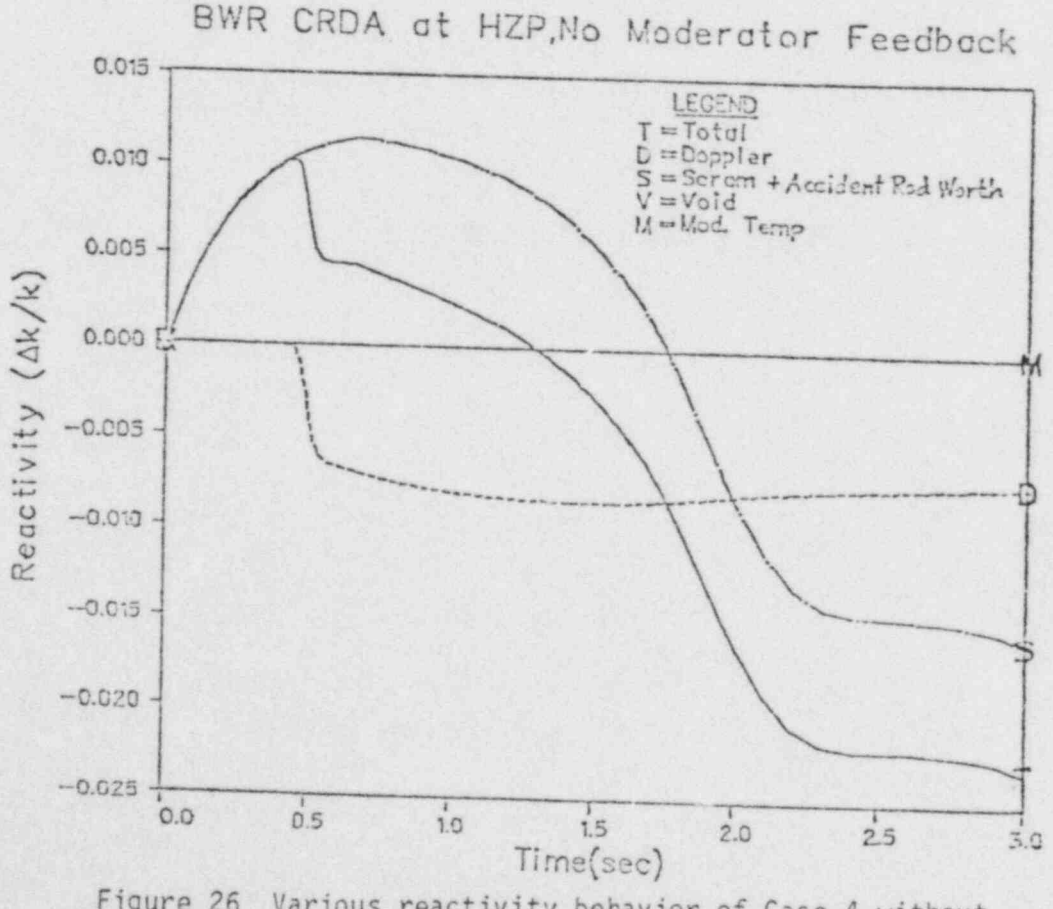

Figure 26 Various reactivity behavior of Case 4 without moderator feedback

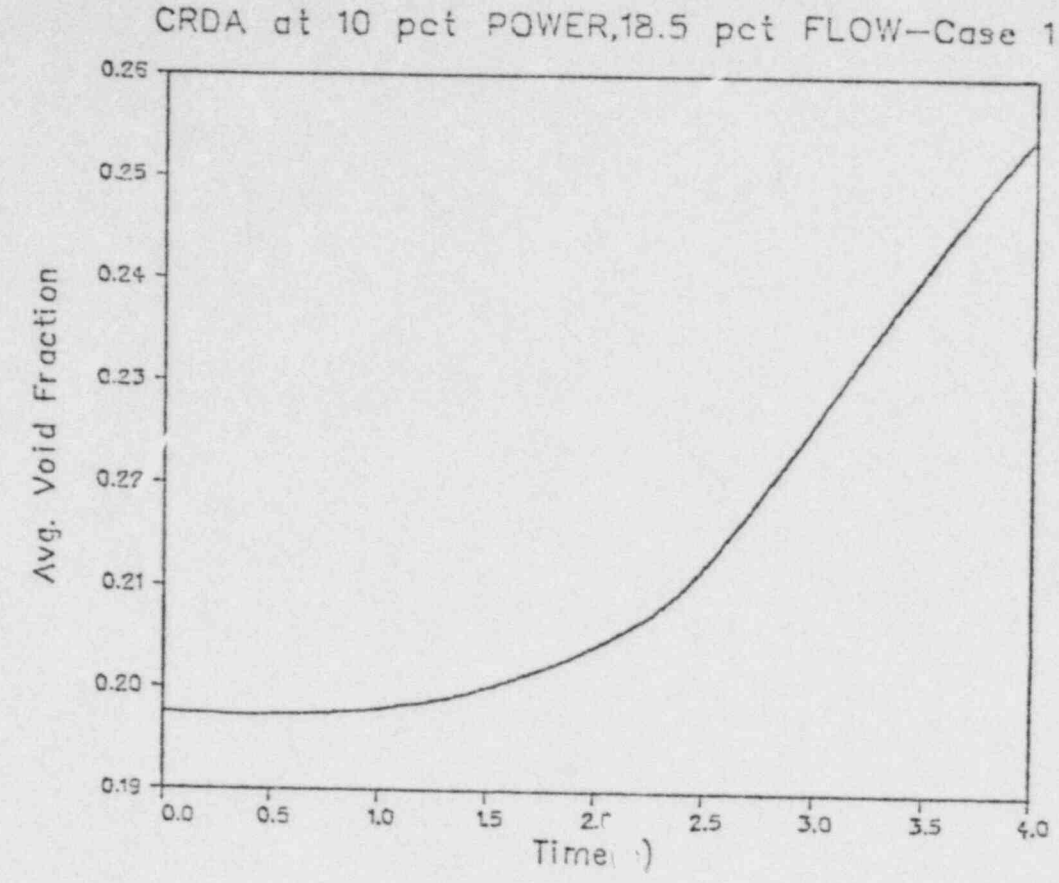

Figure 27 Transient void behavior of reference 10% power case (Case 1)

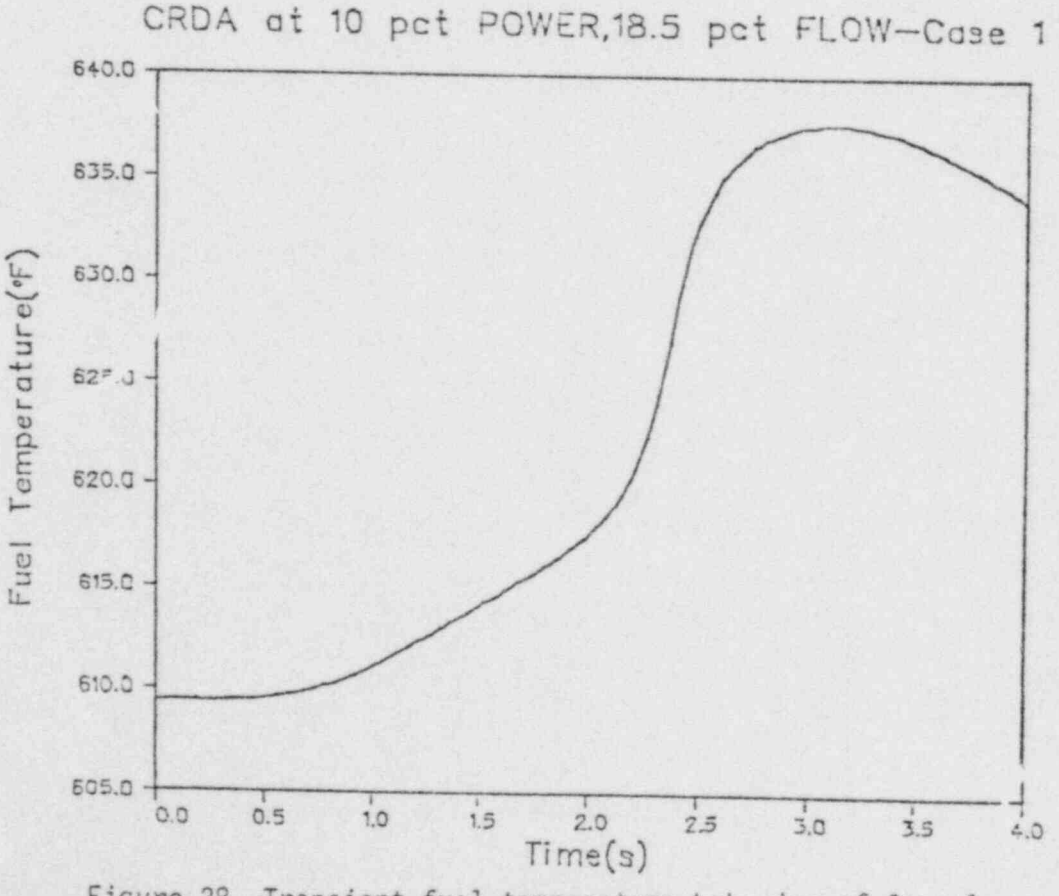

Figure 28 Transient fuel temperature behavior of Case 1

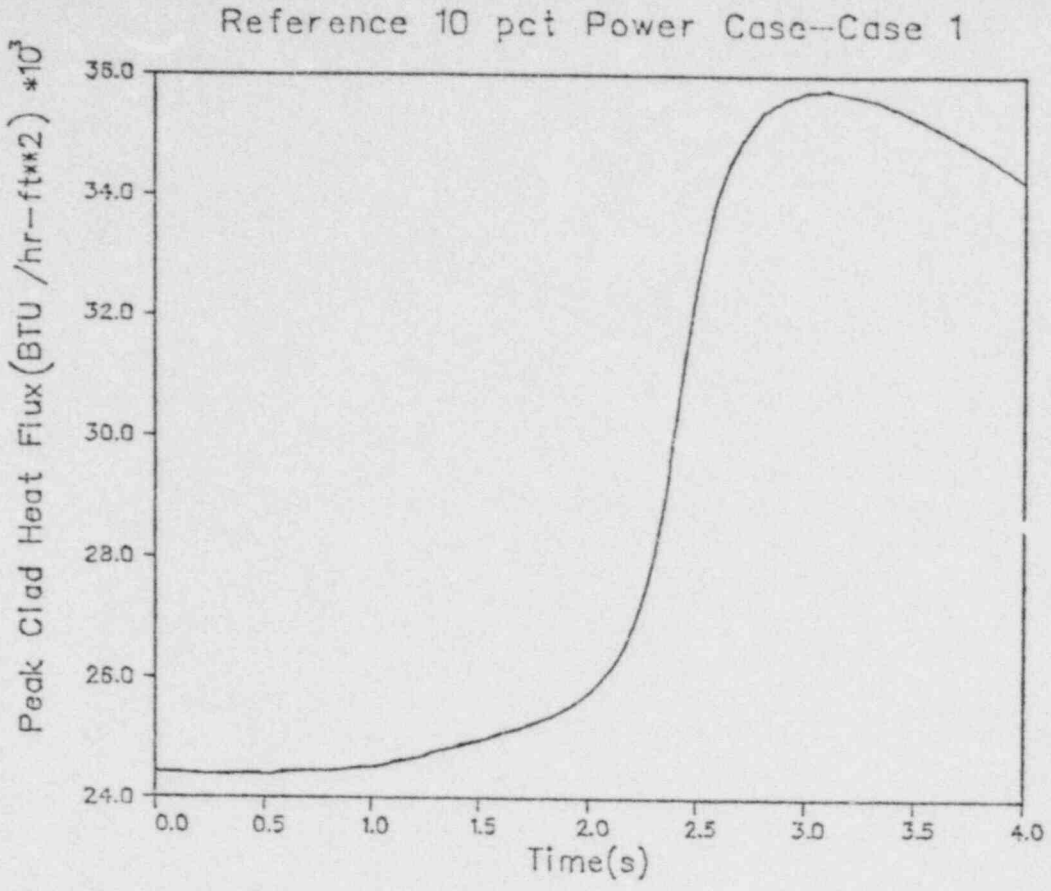

Figure 29 Transient behavior of radially averaged peak clad heat flux of reference 10% power case (Case 1)

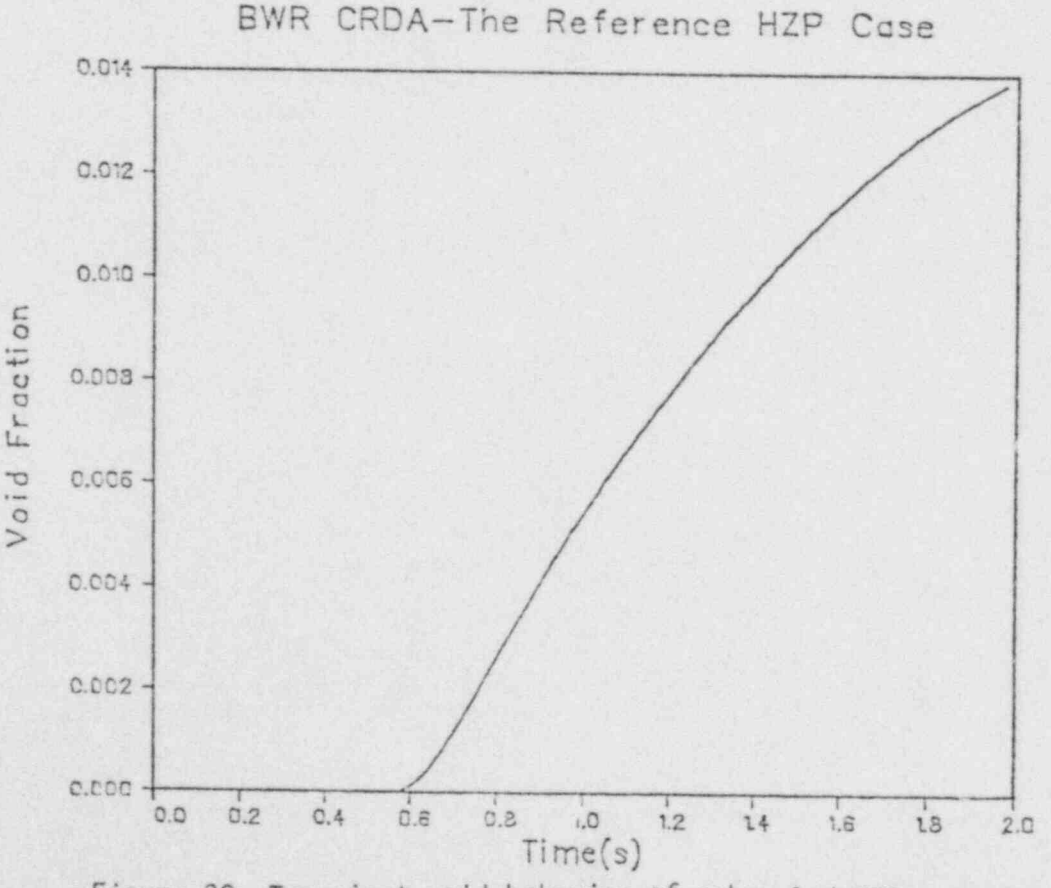

Figure 30 Transient void behavior of subcooled HZP case case (Case 4)

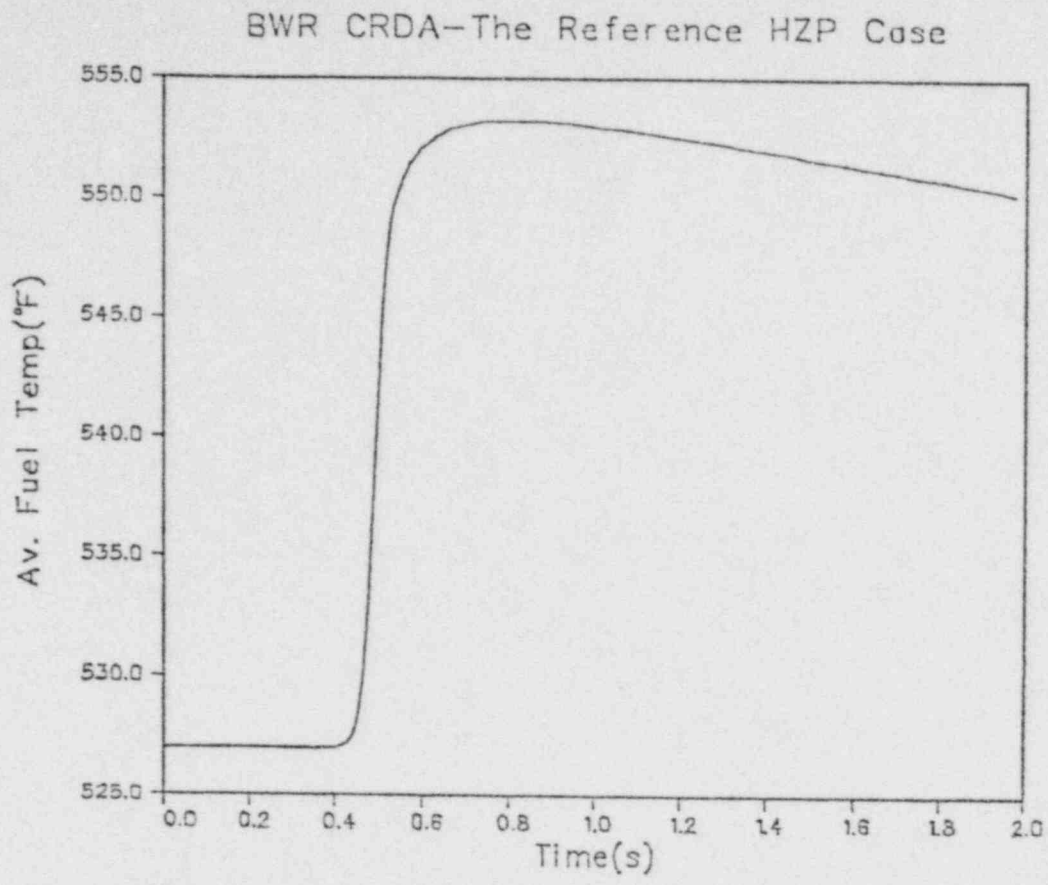

Figure 31 Transient fuel temperature behavior of subcooled HZP case (Case 4) with moderator feedback

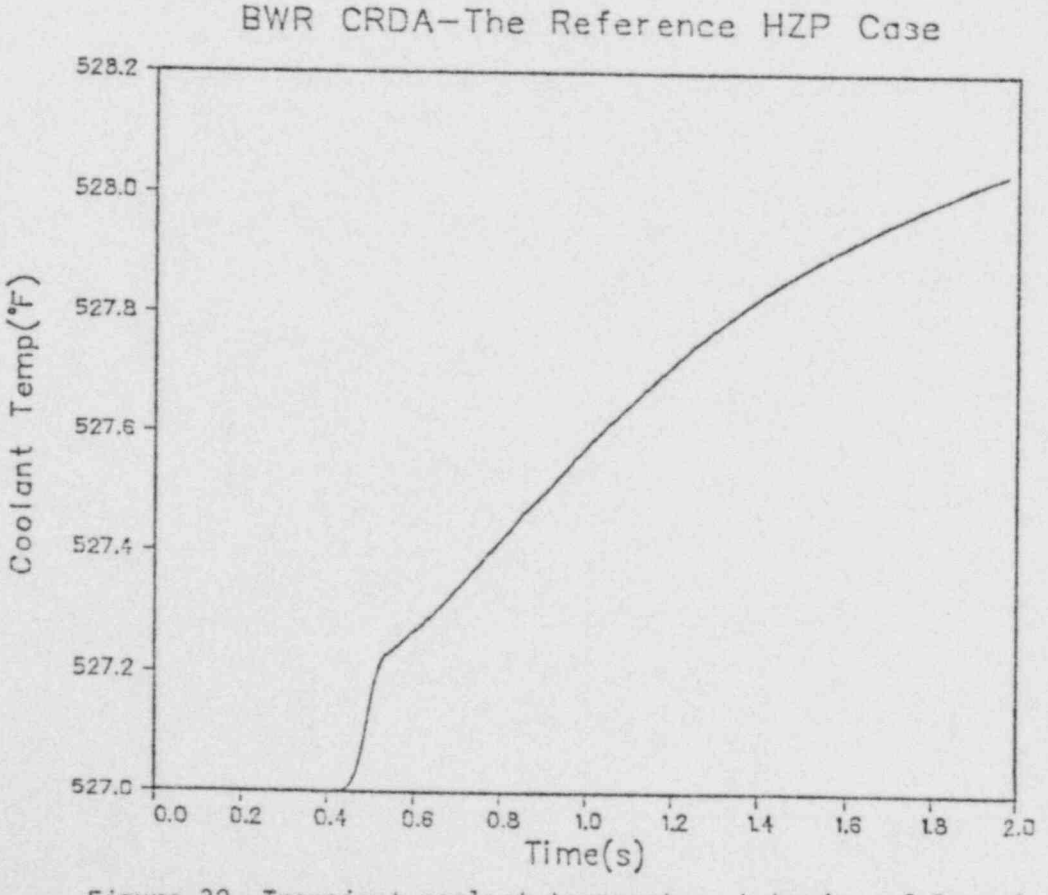

Figure 32 Transient coolant temperature behavior of Case 4 with moderator feedback

fuel enthalpy. This was due to the initial subcooled condition of the core. In practice, the BWR core is maintained at saturation condition at HZP.[1] To see the inlet subcooling effect on the accident, Case 5 was run with no inlet subcooling (i.e., the core is initially at saturation). This case is the same as the subcooled HZP case except for the inlet subcooling.

The initial steady-state conditions are shown in Figure 11 for the average power power profile, in Figure 12 for the average radial power profile, in Figure 17 for the average fuel temperature profile, and in Figure 18 for the average coolant temperature profile. The initial power profiles are nearly the same as the subcooled HZP case. Severe power peaking in both the axial and radial power distributions is still present. Both the fuel temperature and coolant temperature profiles are initially flat at a higher temperature than the subcooled case. As in the subcooled HZP case, there are no voids in the core at the start of the transient for Case 5.

The transient results are shown in Figure 33 for the core thermal power and in Figure 34 for various feedback reactivities for the case with moderator feedback. As expected, the moderator feedback effect is much more significant in this case than the subcooled case; helping suppress the power burst and reduce the peak fuel enthalpy by a factor of 3.5 (see Table VII). The void feedback comes into play much sooner in this case as shown in Figure 35.

In conclusion, the inlet subcooling effect for the HZP case plays a decisive role in the CRDA analysis and must be considered in defining the accident. Since the normal operational procedure is to maintain the core at saturation at zero power conditions, the CRDA at HZP should be defined to be initially at saturation. Calculations have also been done for two additional HZP cases having an abnormally large inlet subcooling (100°F). The results will be presented in Section 3.4.4. The conclusions on the inlet subcooling effect still apply for these cases except that the effect is enhanced.

3.3.3 Direct Moderator Heating Effect

Since the direct moderator heating (DMH) acts promptly on the moderator feedback, it may be important for the CRDA at power conditions. The reference 10% power case (Case 1) and the HZP case (Case 5) assume a 2% DMH. In order to quantify the DMH effect, these two cases were rerun with 0% DMH. They are designated as Case 2 and Case 7 in this report.

Figure 36 shows the DMH effect on the core thermal power of the 10% power case (Case 1). We see that most of the moderator feedback effect for the 10% power case comes from heat transfer from fuel rods. The DMH effect does help reduce the power peak by about 24%, but its overall effect on the transient is quite small as compared to the heat transfer effect. For instance, the 2% DMH only helps reduce the peak fuel enthalpy from 44 cal/gm to 41 cal/gm (see Table VII). The reason for the importance of heat conduction can be understood in terms of the thermal time constant. This will be discussed in Appendix B.

For the HZP case, it is quite a different story. The DMH effect accounts for most of the moderator feedback during the power excursion as demonstrated in Figure 37. Two primary reasons for this phenomenon are: (1) the initial

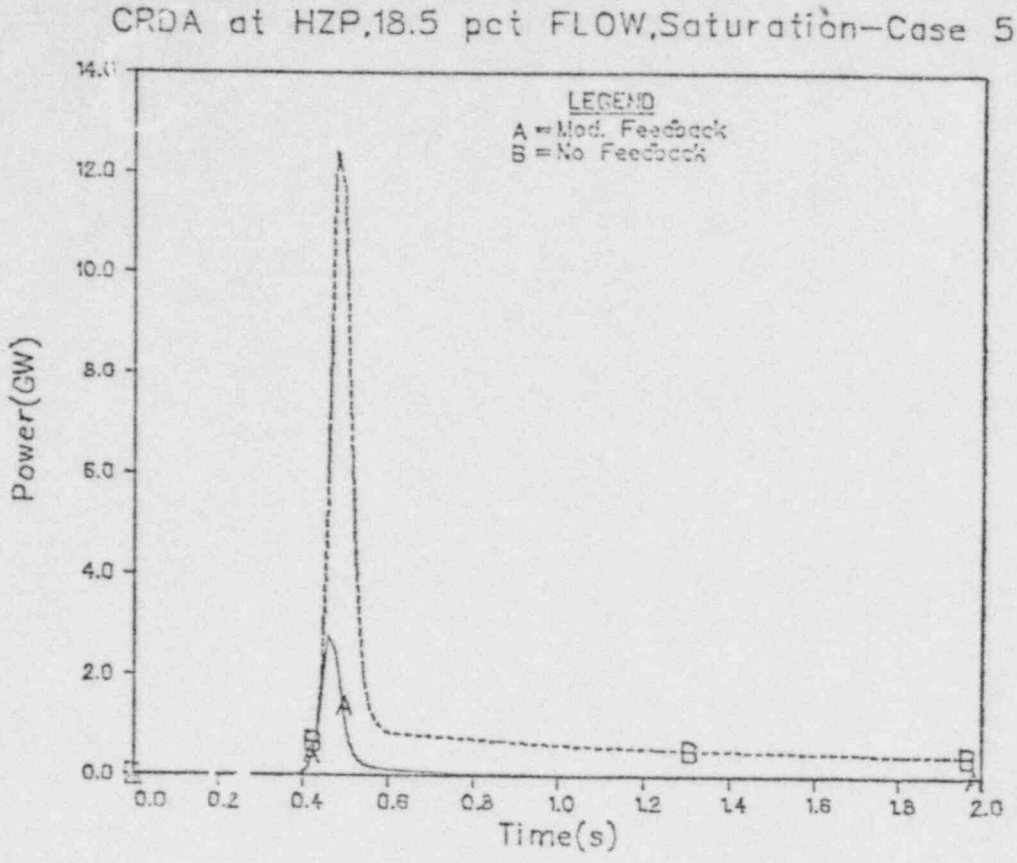

Figure 33 Transient power behavior of saturated HZP case (Case 5)

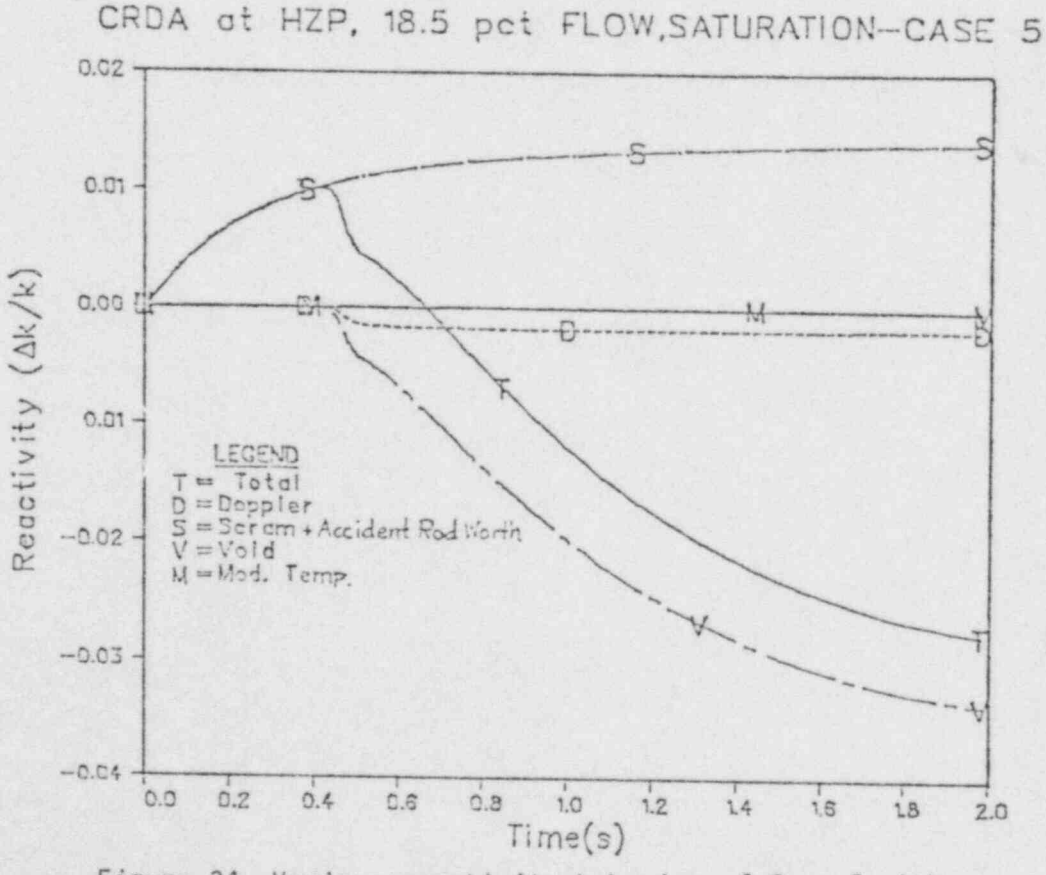

Figure 34 Various reactivity behavior of Case 5 with moderator feedback

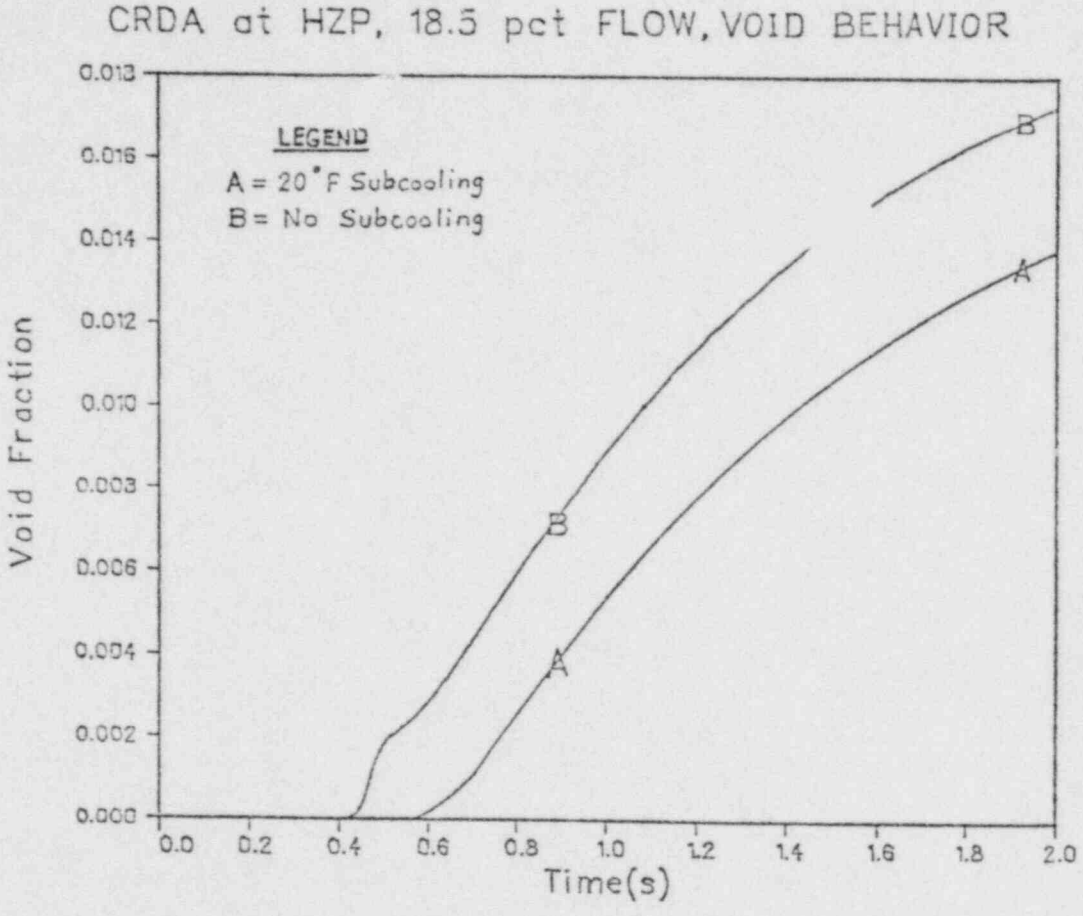

Figure 35 Effect of inlet subcooling on the HZP case

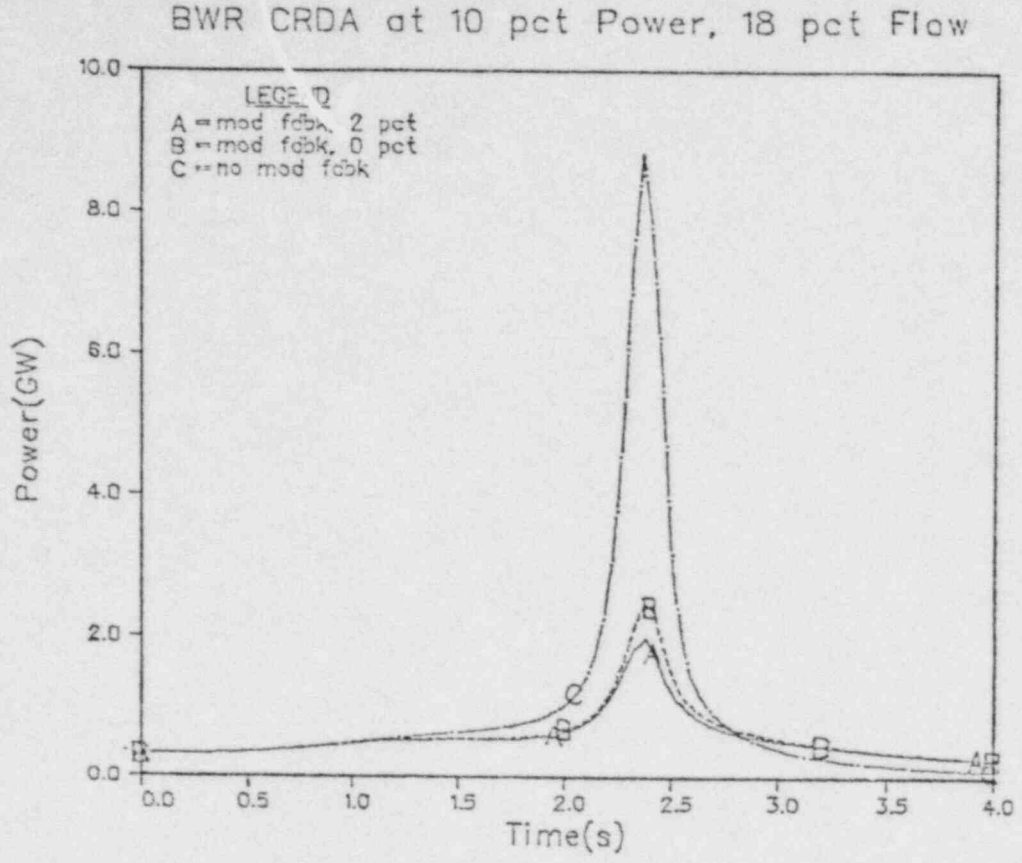

Figure 36 Direct moderator heating effect on the reference 10% power case (Case 1)

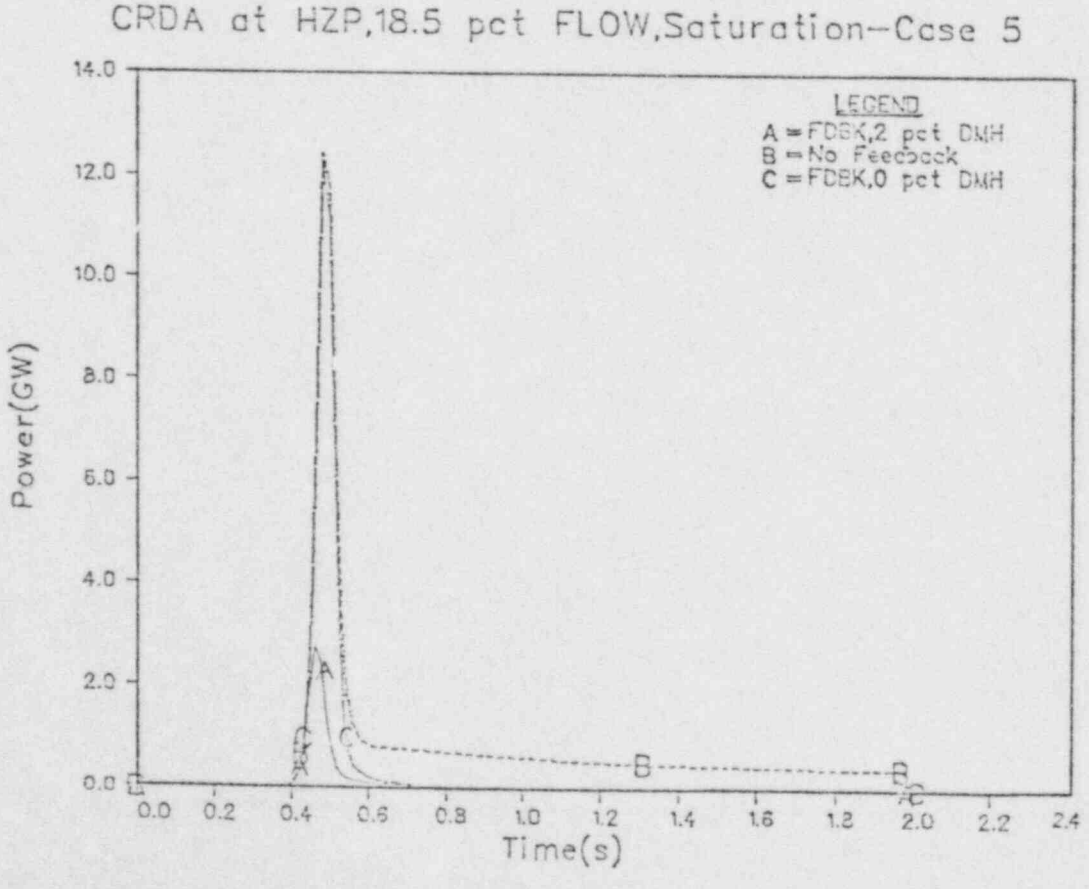

Figure 37 Direct moderator heating effect on saturated HZP case (Case 5)

saturation condition of the core which makes the core ready to produce steam voids once sufficient heat is deposited in the moderator by the DMH, and (2) the severe power excursion with a peak of 13 GW. The latter means that at the peak a 2% DMH corresponds to a direct heat generation rate of 260 MW.

We see that the overall effect of the moderator feedback depends on: (1) the thermal time constant associated with the heat transfer process, (2) the initial moderator condition (inlet subcooling), (3) the amount of DMH, and (4) the severity of the accident.

It is of interest to see what determines the thermal time constant. In Appendix B we derive the expression for thermal time constant from the transient heat conduction equation. We see that the thermal time constant depends on not only the material properties (thermal conductivity and heat capacity) but also the curvature (B^2) of the fuel rod temperature profile. The value of B^2 plays a particularly important role. In general, the curvature B^2 increases with the severity of the accident. For a highly localized accident such as a CRDA, a very steep fuel temperature gradient is expected during the power excursion. In this situation, B^2 is large and the thermal time constant is expected to be small. This explains why the heat transfer process comes into play so soon to account for most of the moderator feedback for the 10% power case. The relatively short thermal time constant for the 10% power case is also reflected in the time history of the core-average void fraction as shown in Figure 38.

The effect of DMH on the HZP case is quite evident in the time behavior of the core-average void fraction as shown in Figure 39. Note also that after about 0.6 s the case without DMH actually produces more voids than the case with the DMH. This is because the significantly reduced power excursion due to the DMH (see Figure 37) produces much less heat to be transferred from fuel rods to the coolant.

3.3.4 Core Flow Effect

In the normal operation of a BWR, core flow corresponds to core thermal power by following the power-flow control line. At low power operation it follows the natural circulation line. For the reference 10% power case, it was estimated to be about 18.5% of rated flow. Since the core flow must be specified in defining the rod drop accident in order to see the moderator feedback effect, it is of interest to study the effect of core flow on the CRDA.

For this purpose Case 3 was run with the inlet core flow rate doubled from the reference 10% power case (Case 1); other conditions being the same. The initial steady state conditions are shown in Figure 9 for the average axial power profile, in Figure 10 for the average radial power profile; in Figure 13 for the average axial void distribution, in Figure 14 for the axial fuel temperature profile, in Figure 15 for the clad heat flux distribution, and in Figure 16 for the axial coolant temperature profile.

Observation of the initial power profiles indicates that doubling the core flow shifts the axial peaking from the bottom toward the top (see Figure 9) and reduces the radial peaking in the central region and increases the radial

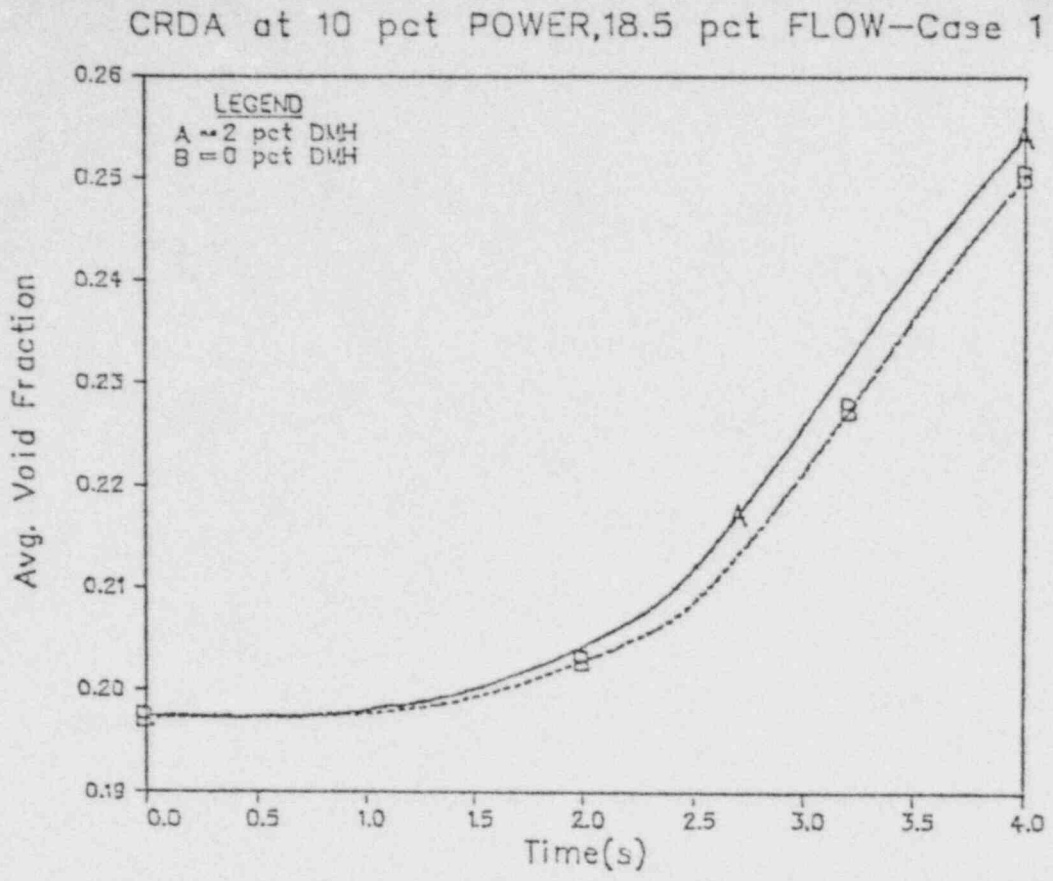

Figure 38 Direct moderator heating effect on void behavior of reference 10% power case (Case 1)

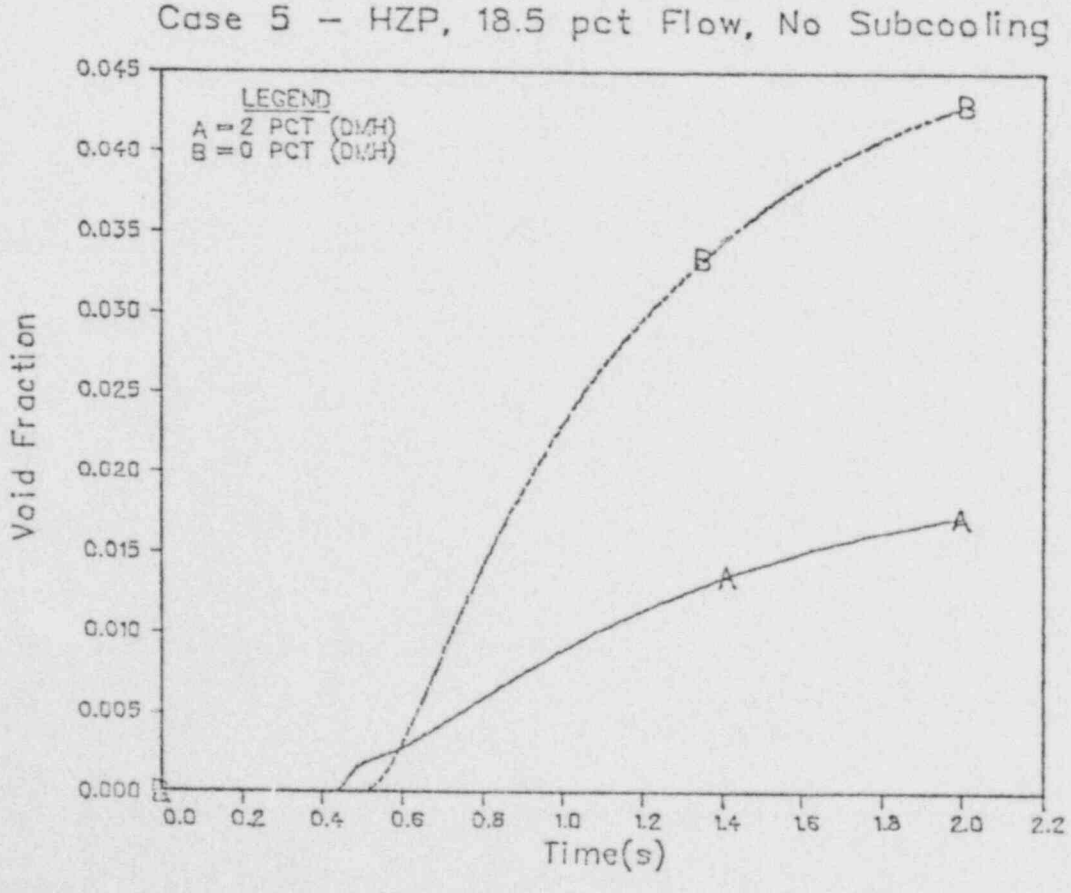

Figure 39 Direct moderator heating effect on void behavior of saturated HZP case (Case 5)

peaking in the peripheral region (see Figure 10). This is partly due to the reduced void content in the core because of the increased flow as shown in Figure 13. The consequence of this power distribution shift is to reduce the center rod worth from 0.826% $\Delta k/k$ to 0.467% $\Delta k/k$ and to increase the rate of positive reactivity insertion (owing to the top-peaked power shape).

Figure 40 shows the transient behavior of the core thermal power with and without the moderator feedback. The dramatic effect of the moderator feedback is still evident. Relative to the reference 10% power case (see Figure 19), the power excursion occurs earlier because of the increased accident reactivity insertion rate and the power peak is smaller due to the reduced accident rod worth. This demonstrates that the rod drop accident depends strongly on the initial power distributions which, in turn, depend on the core flow rate.

In summary, at the same power level, increasing the core flow tends to reduce the accident rod worth, but increases the rate of positive accident reactivity insertion. The net result, in this particular case, is to increase the peak fuel enthalpy as illustrated in Table VII (compare Case 1 and 3).

3.4 Sensitivity Studies

3.4.1 Effect of Rod Drop Velocity

The results presented up to now were all calculated with a rod drop velocity of 1.524 m/s (5.0 ft/s). A series of rod drop tests[5] indicated that the average rod drop velocity is about 0.945 m/s (3.1 ft/s). To see the effect of the rod drop velocity, Case 1 and 5 were rerun with a rod drop velocity of 3.1 ft/s. These cases are designated as Case 6 and 8 for the HZP and 10% power cases, respectively (see Table I). The moderator feedback was not included in these calculations.

The effect of the rod drop velocity is shown in Figure 41 for the 10% power case and in Figure 42 for the HZP case. The slower the rod drop velocity the less severe the accident is in terms of the power peak and the time to peak. The peak fuel enthalpy is also reduced (by 3% for the 10% power case and 8% for the HZP case) as shown in Table VII but not to the same extent as the core power peak.

3.4.2 Effect of Delayed Neutron Fraction

The present work was primarily aimed at the BOL conditions of the core. Consequently, all the calculations for the accident up to now were performed with BOL delayed neutron data listed in Table III with a total β of 0.00738. Sensitivity calculations were done with a typical EOC β of 0.00546 (as given in Table III) to see the effect of β on the accident for both the 10% power and HZP case. These cases are designated as Case 9 and Case 10 in Table I for the 10% power case and the HZP case, respectively. Except for the value of β, the calculations were done with the same BOL cross section data. As such, the results do not represent the true EOC condition. Rather, it should be regarded as the sensitivity of the accident to β alone. The rod drop velocity in these calculations is 1.524 m/s (5.0 ft/s).

The results are shown in Figure 43 for the 10% power case (Case 9) and in Figure 44 for the HZP case (Case 10). The smaller value of β produces a more

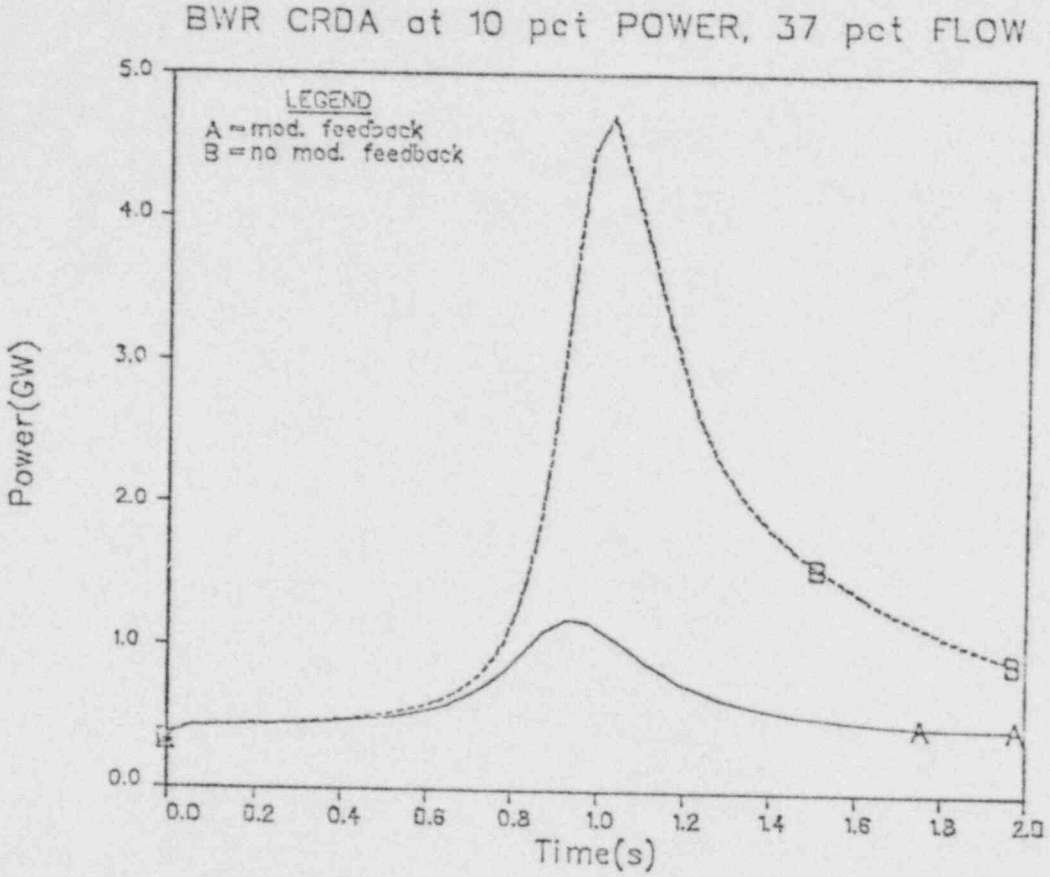

Figure 40 Transient power behavior of 10% power case with 37% flow (Case 3)

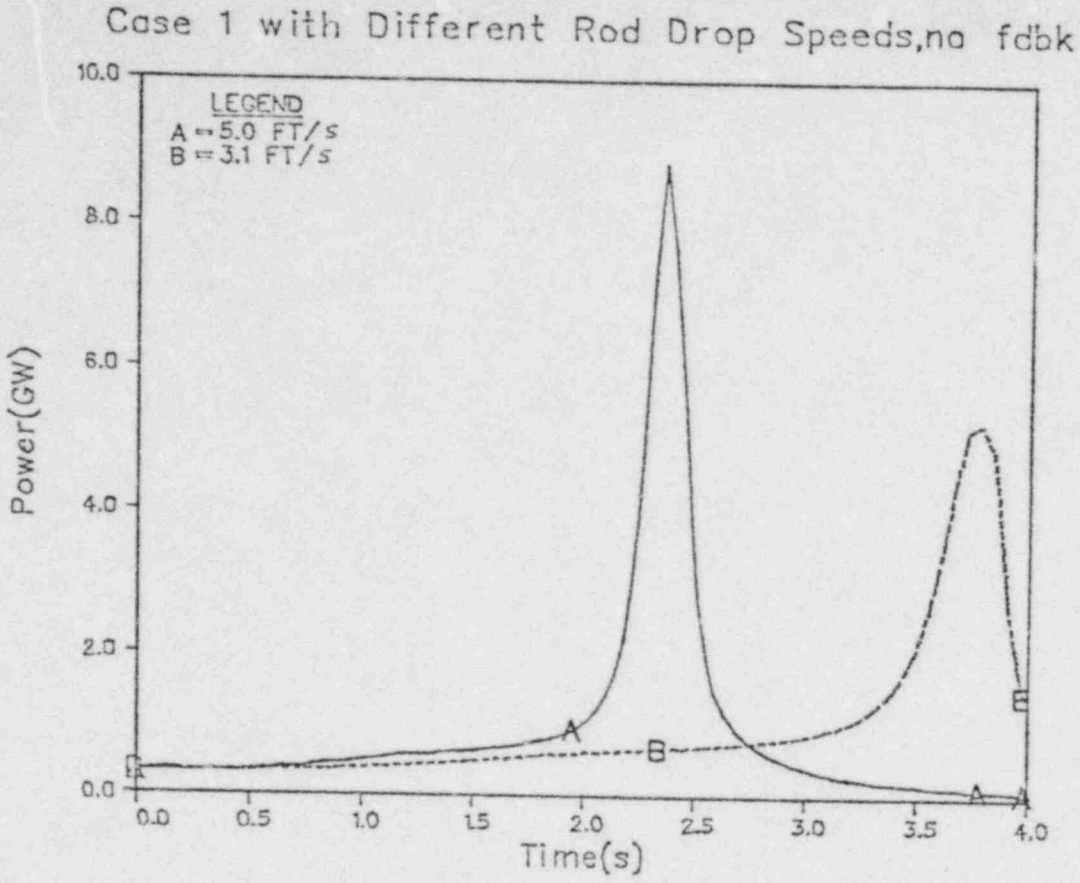

Figure 41 Effect of rod drop velocity on power behavior of 10% power case

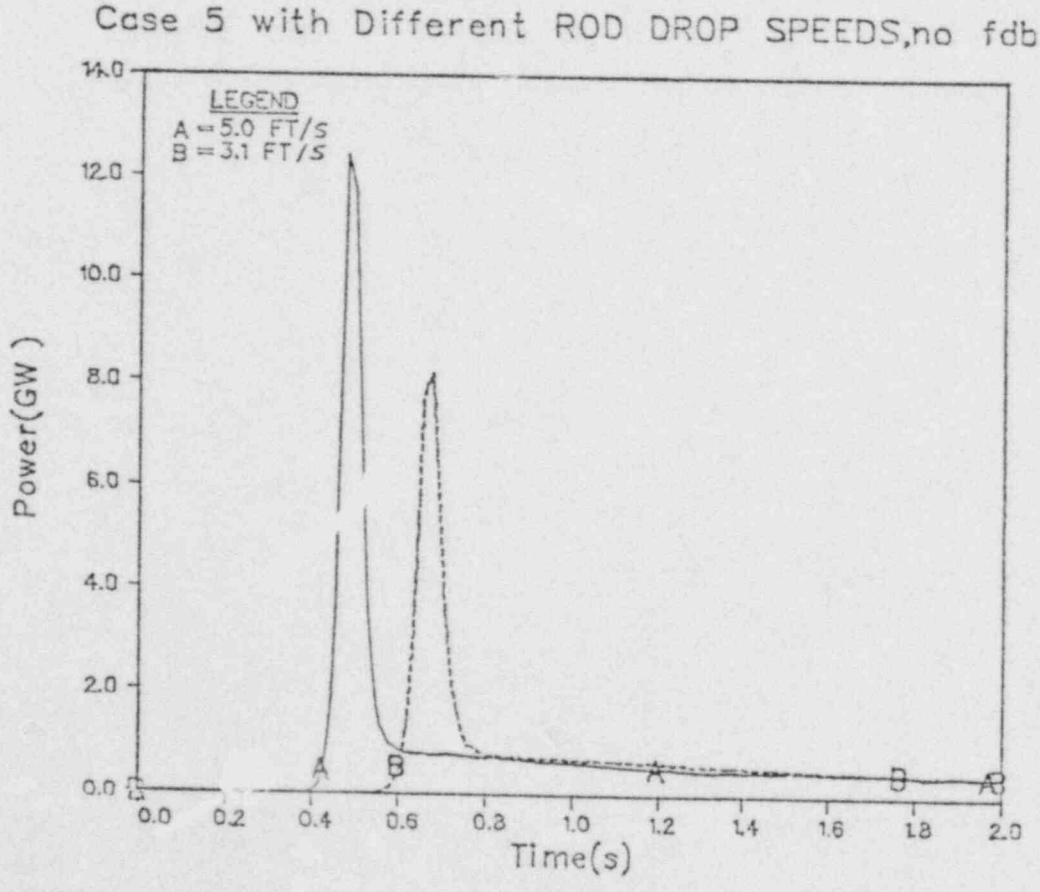

Figure 42 Effect of rod drop velocity on power behavior of saturated HZP case

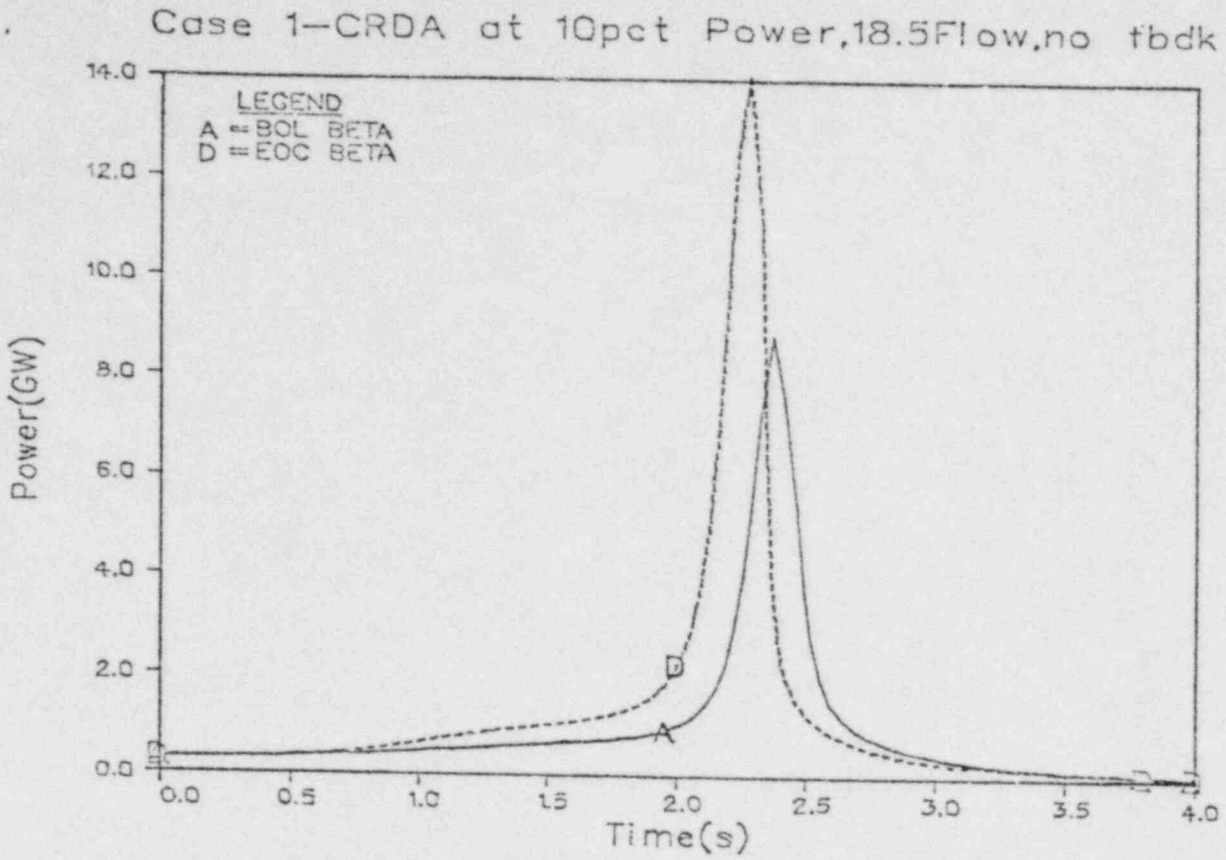

Figure 43 Effect of delayed neutron fraction on power behavior of 10% power case

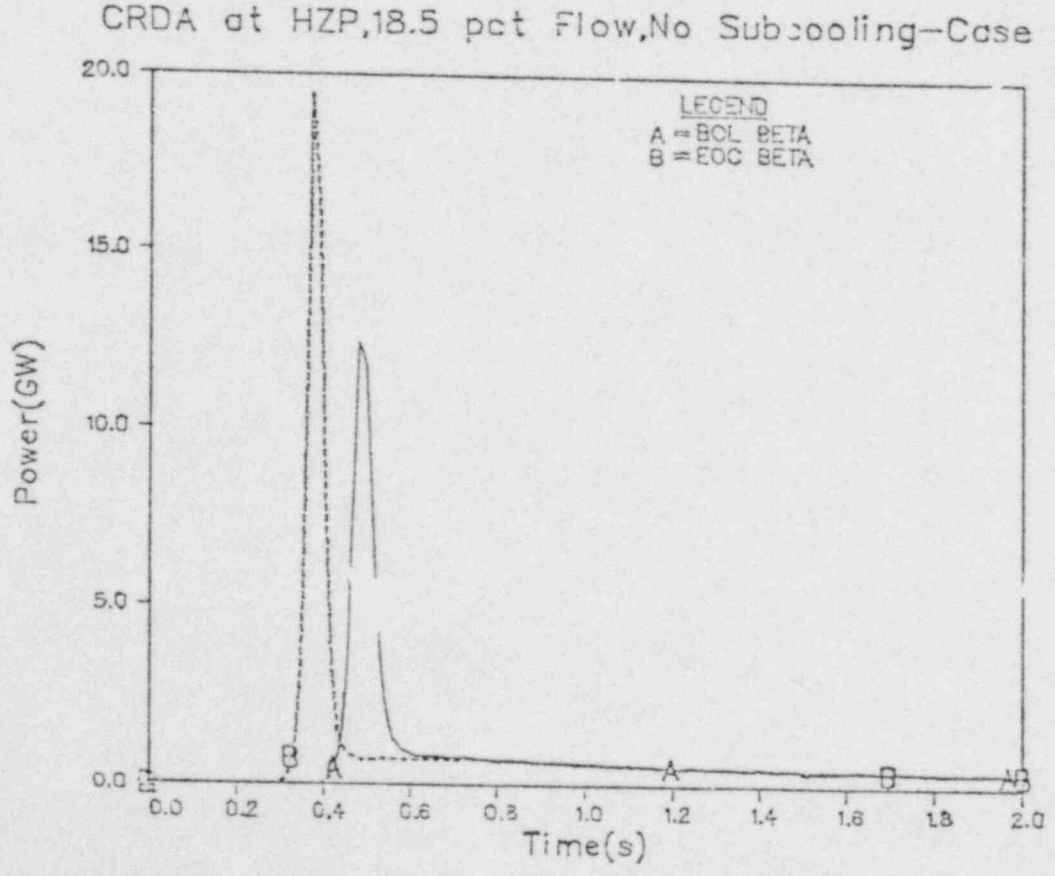

Figure 44 Effect of delayed neutron fraction for saturated HZP case

rapid and severe transient than the BOL β. The time to peak occurs earlier and the power peak also increases substantially (by 58% for the 10% power case and by 45% for the HZP case). This is also summarized in Table VII along with the peak fuel enthalpy. In both cases, the peak fuel enthalpy is increased by the smaller value of β.

3.4.3 Effect of Accident Rod Worth

Without moderator feedback the peak fuel enthalpy of the rod drop accident is sensitive to the accident rod worth[5]. It is, therefore, important to study the sensitivity of the accident to the accident rod worth.

We wish to redefine the initial conditions of the core such that the accident rod worth is approximately doubled. This was done by trying various combinations of the axial and radial power profiles achieved by different control rod patterns. The reference HZP case (Case 5) was redefined in this manner to increase substantially its accident rod worth. This is designated as Case 11. It should be pointed out that this case has the accident (center) rod initially fully inserted as opposed to the partially inserted accident rod of the reference HZP case. The initial conditions are shown in Figure 11 for the axial power profile, in Figure 12 for the radial power profile, in Figure 17 for the average fuel temperature profile, and in Figure 18 for the average coolant temperature distribution.

Examination of the initial power profiles indicates that, although the power peaking factors are significantly reduced (see Table VI), the power distribution is shifted such that the accident rod is withdrawn into higher neutron importance. This together with the fully inserted initial accident rod position nearly doubles the accident rod worth as shown in Table V (compare Case 11 to Case 5).

The transient results are presented in Figure 45 for the core thermal power, in Figure 46 for the peak fuel enthalpy, in Figure 47 for the core-average void fraction, and in Figure 48 for the average fuel temperature. The dramatic moderator feedback effect is still evident, reducing the peak fuel enthalpy from 326 cal/gm to only 50 cal/gm (see Table VII). Thus, some fuel rods will be assumed to fail without consideration of the moderator feedback because the peak fuel enthalpy exceeds the 280 cal/gm limit.

The rapid increase of the void fraction and fuel temperature at the start of the power excursion is also apparent. This is due mostly to the direct moderator heating effect. Since the core is initially at saturation, it is also expected that the extremely rapid power rise during the excursion will lead to a very steep temperature gradient, thus giving rise to a short thermal time constant. This is reflected in Figure 45 by the fact that the core thermal power is significantly suppressed after 0.5 s as compared to the case without moderator feedback.

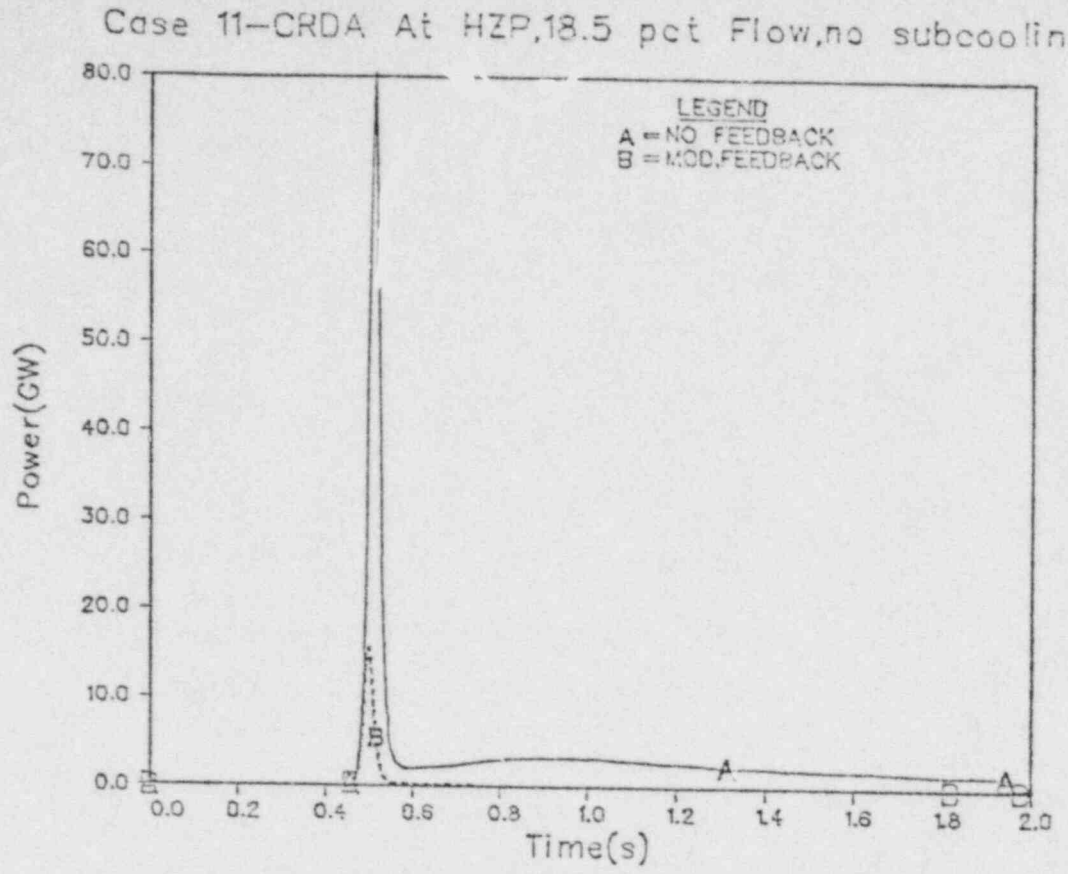

Figure 45 Transient power behavior of Case 11 with a doubled accident rod worth

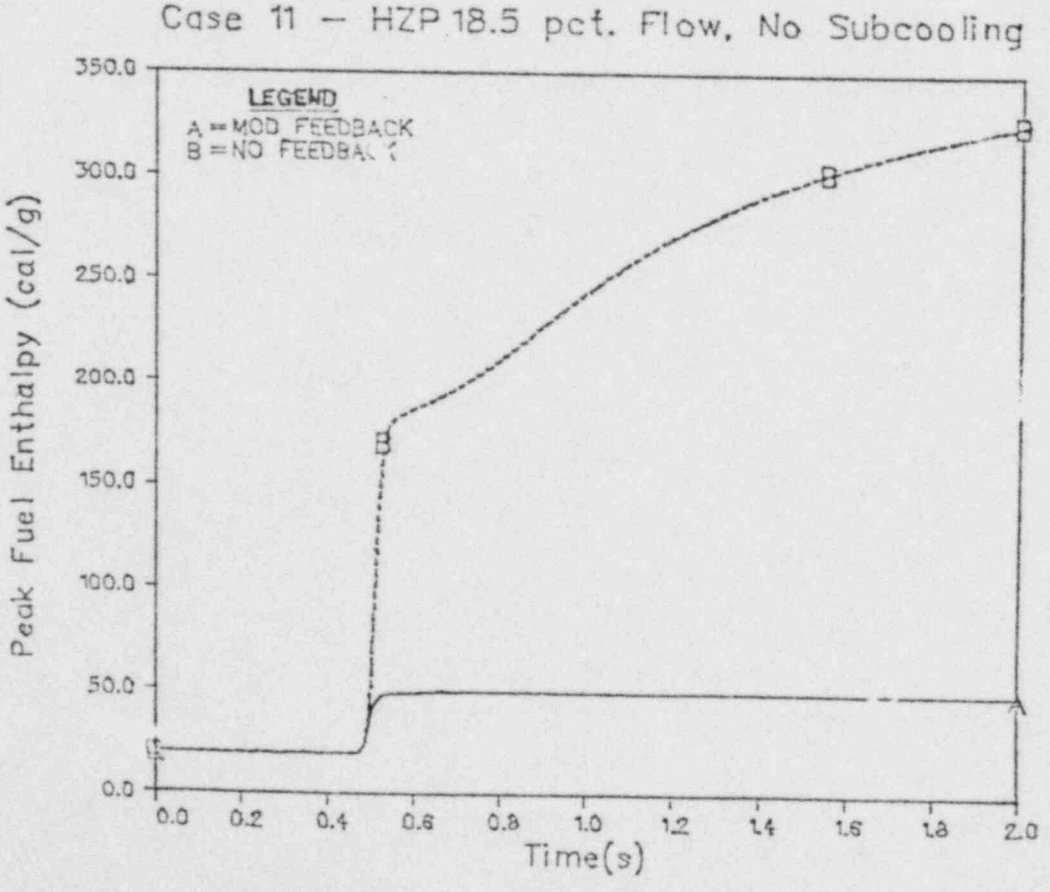

Figure 46 Transient behavior of peak fuel enthalpy of Case 11

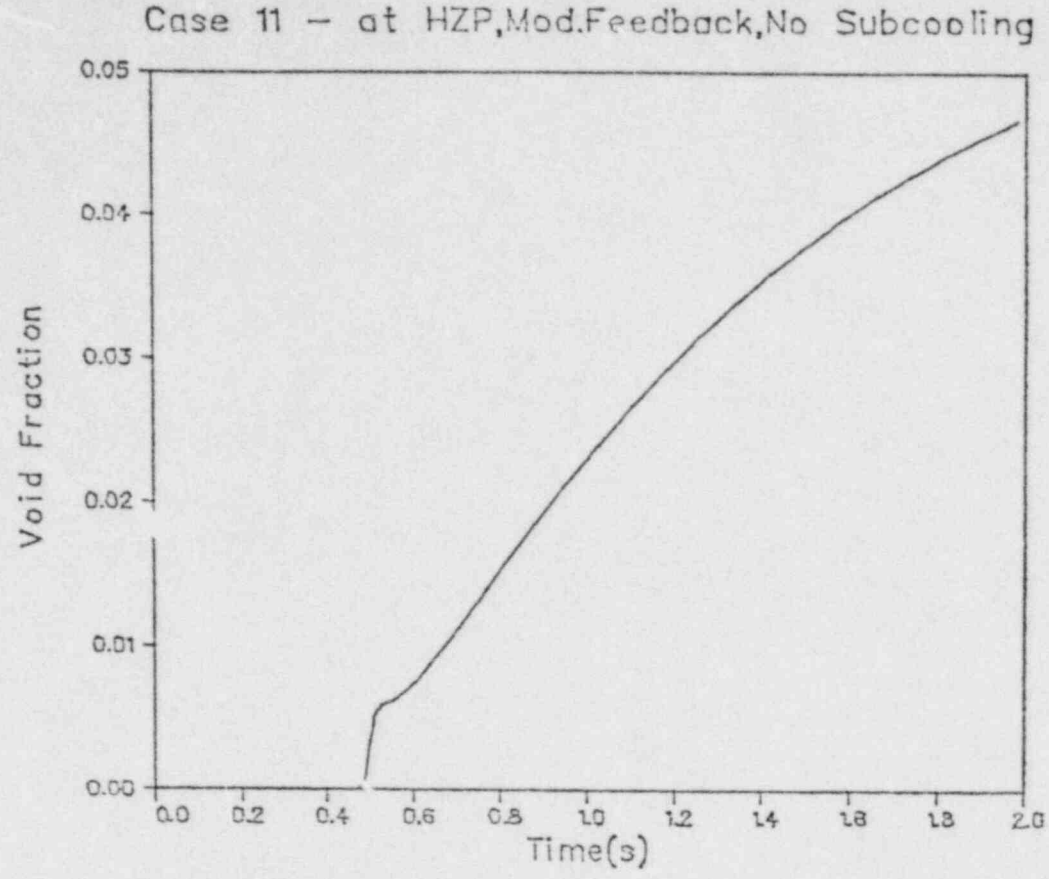

Figure 47 Transient void behavior of Case 11 with moderator feedback

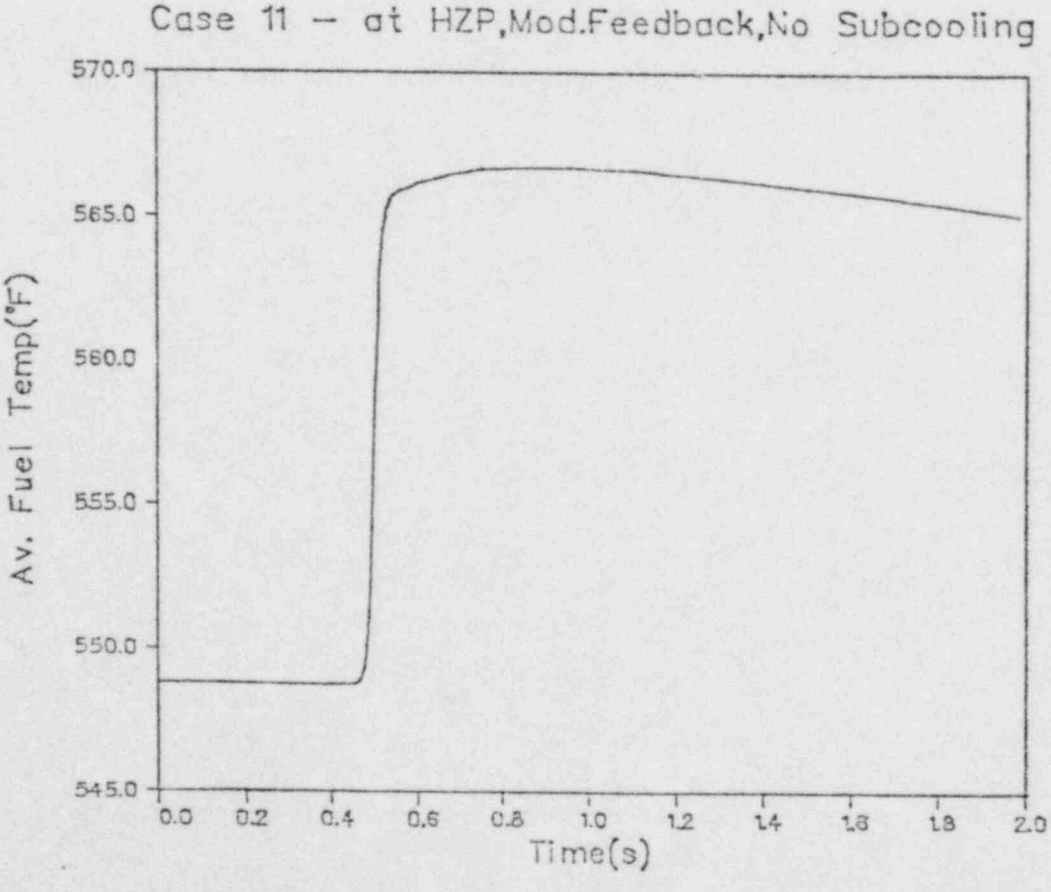

Figure 48 Transient fuel temperature behavior of Case 11 with moderator feedback

3.4.4 Effect of Extremely Large Inlet Subcooling

During the approach to the hot standby condition from the cold critical condition, a BWR may have large inlet subcooling (say, 100°F). Under such conditions, the reactor core is substantially subcooled and the moderator feedback would be considerably hampered during the rod drop accident. The effect of such a large inlet subcooling is of interest, even though we have calculated this effect for the case of 20°F inlet subcooling (cf. Section 3.3.2) because it is difficult to extrapolate from 20° to 100°F inlet subcooling.

We have, therefore, recalculated two HZP cases (Case 11 and Case 5) with 100°F inlet subcooling, everything else being the same. These two cases are designated as Case 12 and Case 13, respectively. Case 12 has an accident rod worth of 2.1% k/k and Case 13 has 1.2% k/k accident rod worth (see Table V).

The initial steady-state conditions are shown in Figures 11 and 12 for the axial and radial power profiles, and in Figures 17 and 18 for the average fuel and coolant temperature profiles. Note that the large inlet subcooling affects only slightly the initial power distributions. Thus the accident rod worth of these two cases remains more or less the same as the corresponding cases without inlet subcooling.

The transient results of Case 12 are presented in Figures 49 through 53. Figure 49 shows the core thermal power with and without moderator feedback. We see that the power excursion is hardly affected by the moderator feedback due to the large inlet subcooling. It does affect significantly the later part of the transient after about 0.7 sec when steam voids start to form in the core as shown in Figure 50. Relative to Case 11 (without inlet subcooling), the formation of voids for Case 12 is substantially delayed because of the large inlet subcooling (see Figures 47 and 50). Figure 51 shows the transient behavior of the peak fuel enthalpy of Case 12. It exceeds the 280 cal/gm limit if the moderator feedback is not taken into account. The moderator feedback does reduce it to 179 cal/gm well below the limit. Even without the moderator feedback the core on the average behaves normally as illustrated in Figure 52 by the core - average fuel temperature which is well below the melting point of about 5000°F. Figure 53 shows the transient behavior of various reactivity components of Case 12 with the moderator feedback. The strong void feedback after 0.7 s is clearly seen.

The transient results of Case 13 are presented in Figures 54 through 58. Figure 54 shows the transient power behavior of Case 13 with and without the moderator feedback. Once again the moderator feedback affects the power excursion little but helps reduce significantly the core thermal power after 1 s into the transient. This can be explained by the transient void behavior as shown in Figure 55. The void does not start to form until after 1 s into the transient. Thus, the moderator feedback will not affect the transient significantly prior to 1 s. Figure 56 shows the transient behavior of the peak fuel enthalpy of Case 13. Regardless of the moderator feedback, the peak fuel enthalpy is well below the 280 cal/gm limit. This is due to the relatively

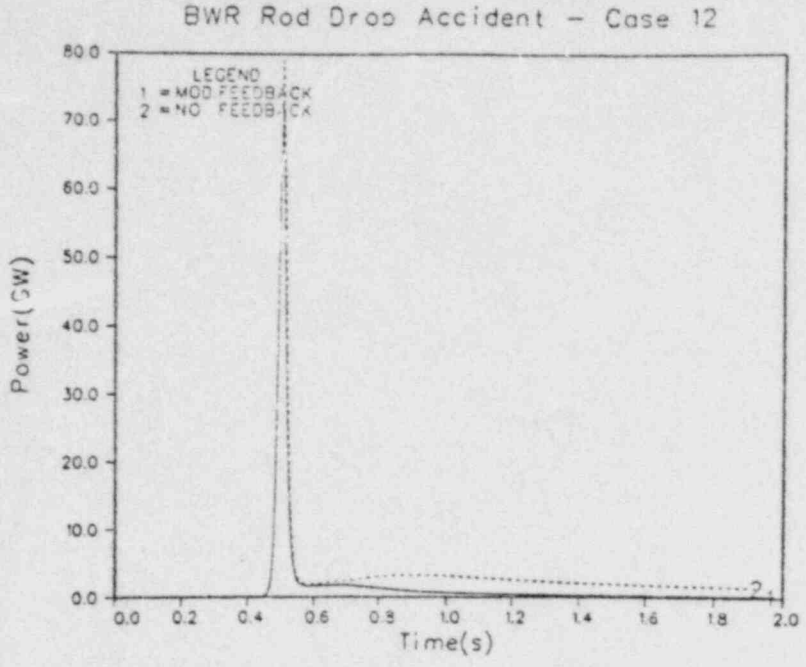

Figure 49 Transient power behavior of Case 12 with 100°F inlet subcooling

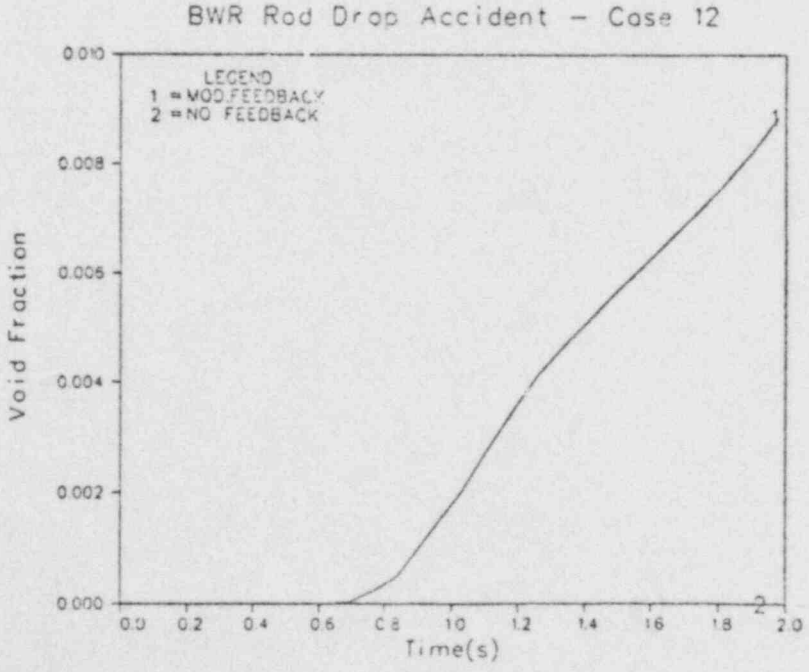

Figure 50 Transient void behavior of Case 12 with 100°F inlet subcooling

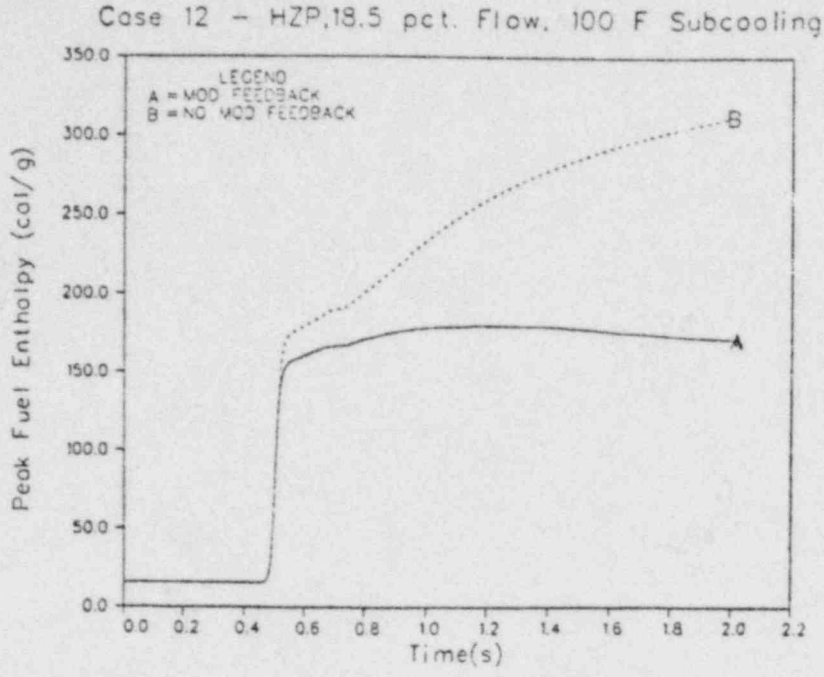

Figure 51 Transient behavior of peak fuel enthalpy of Case 12 with 100°F inlet subcooling

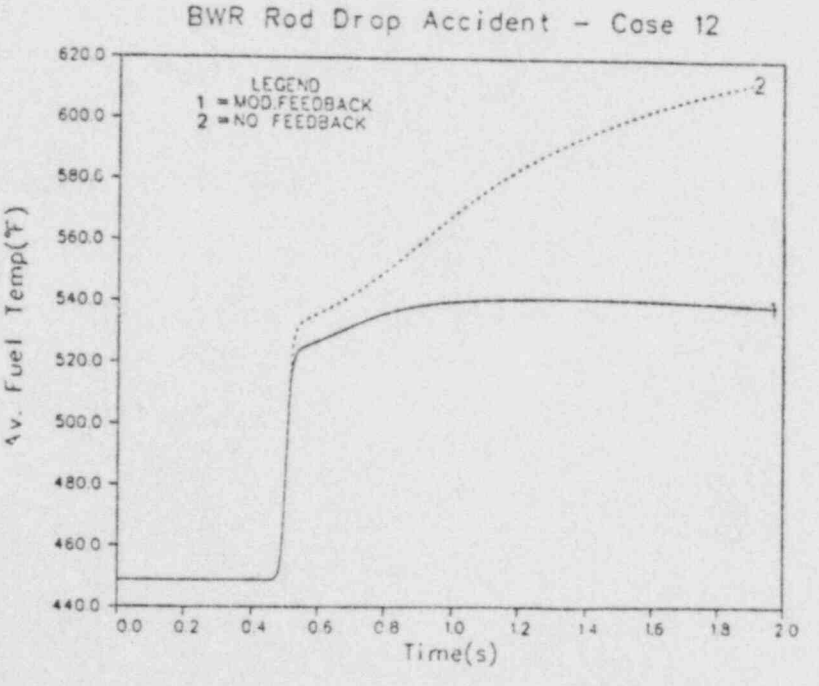

Figure 52 Transient fuel temperature behavior of Case 12 with 100°F inlet subcooling

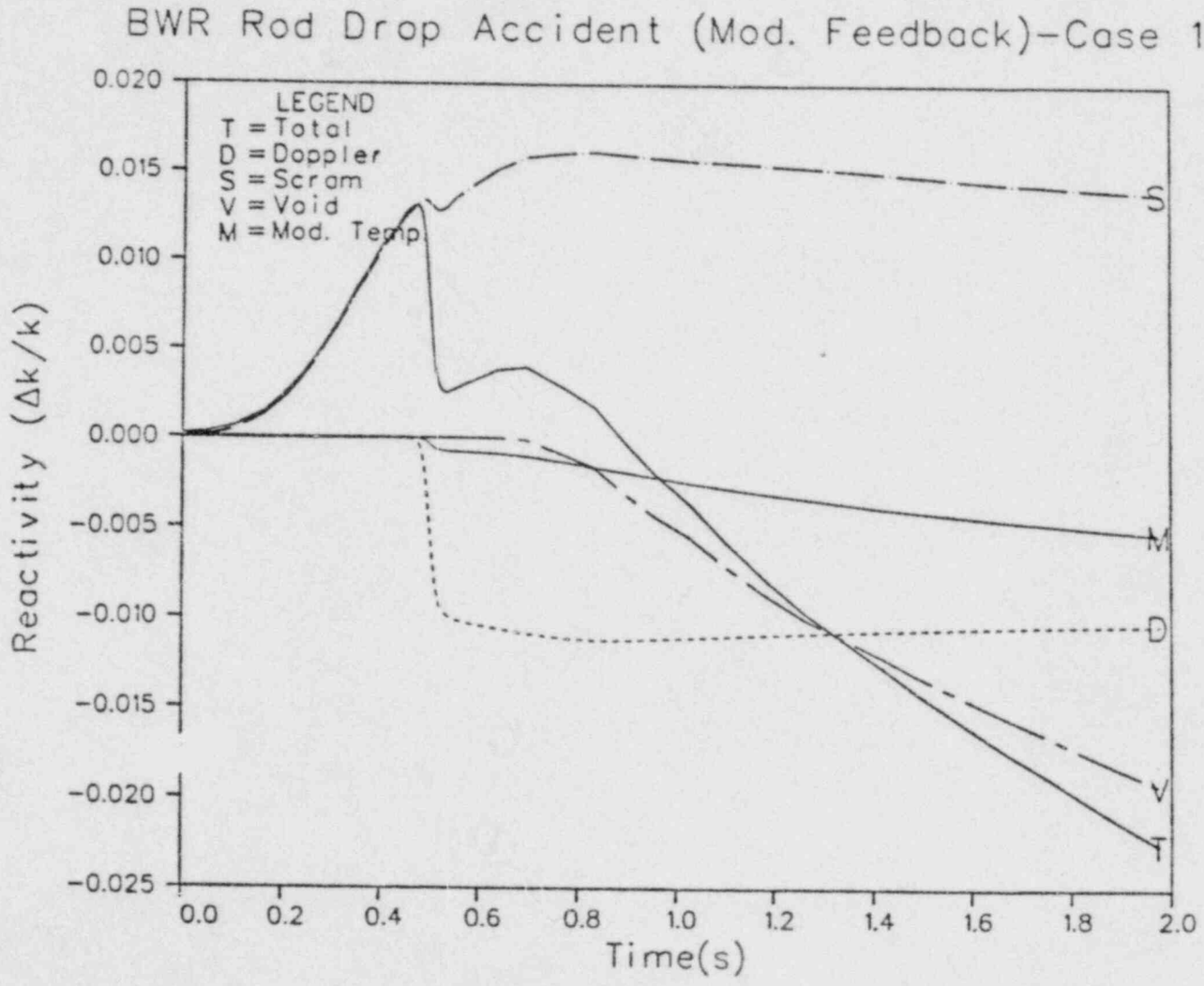

Figure 53 Various reactivity behavior of Case 12 with 100°F inlet subcooling

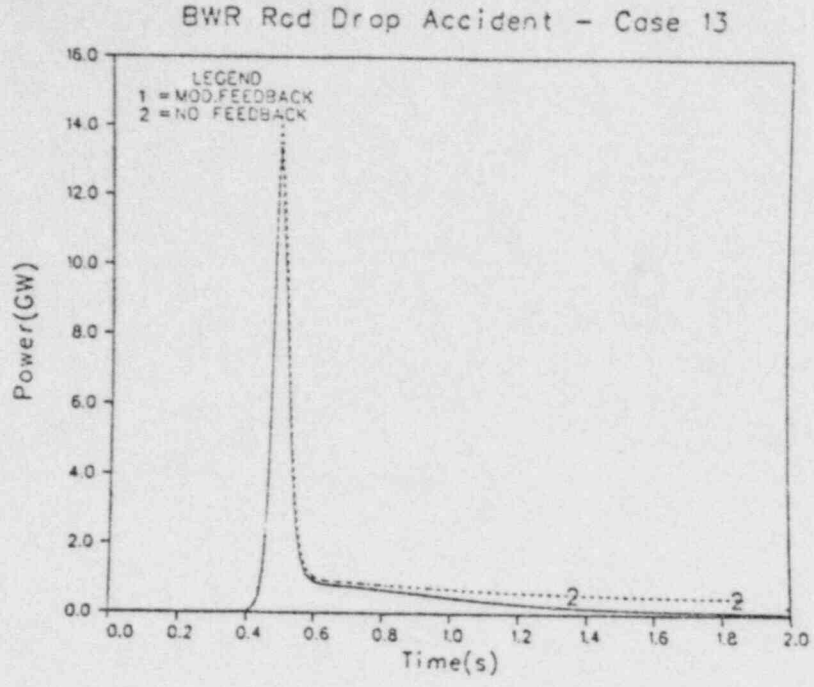

Figure 54 Transient power behavior of Case 13 with 100°F inlet subcooling

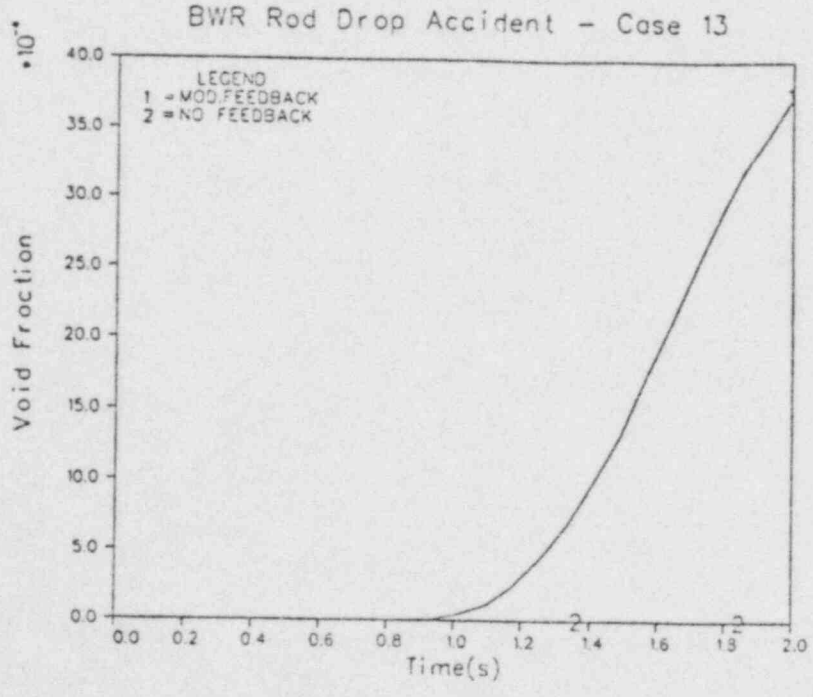

Figure 55 Transient void behavior of Case 13

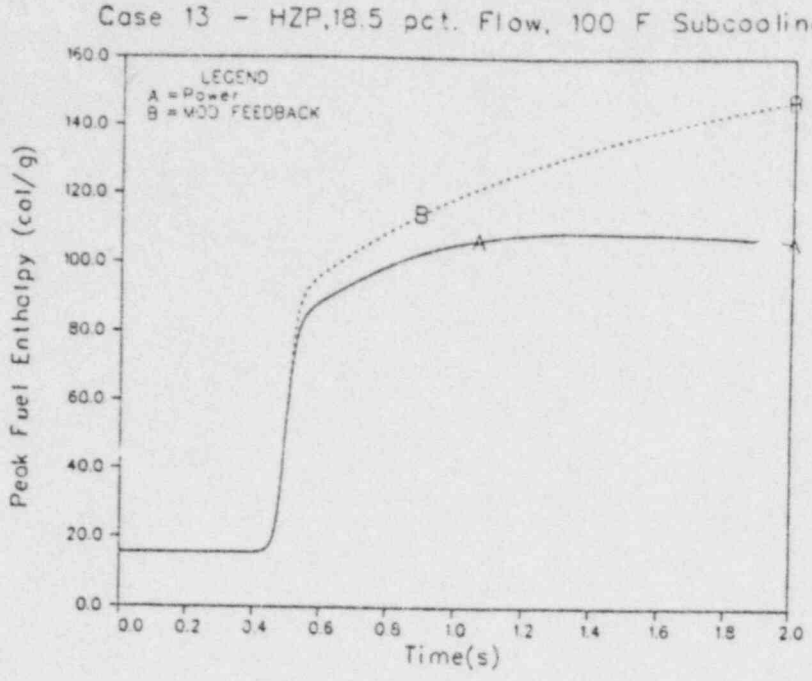

Figure 56 Transient behavior of peak fuel enthalpy of Case 13 with 100°F inlet subcooling

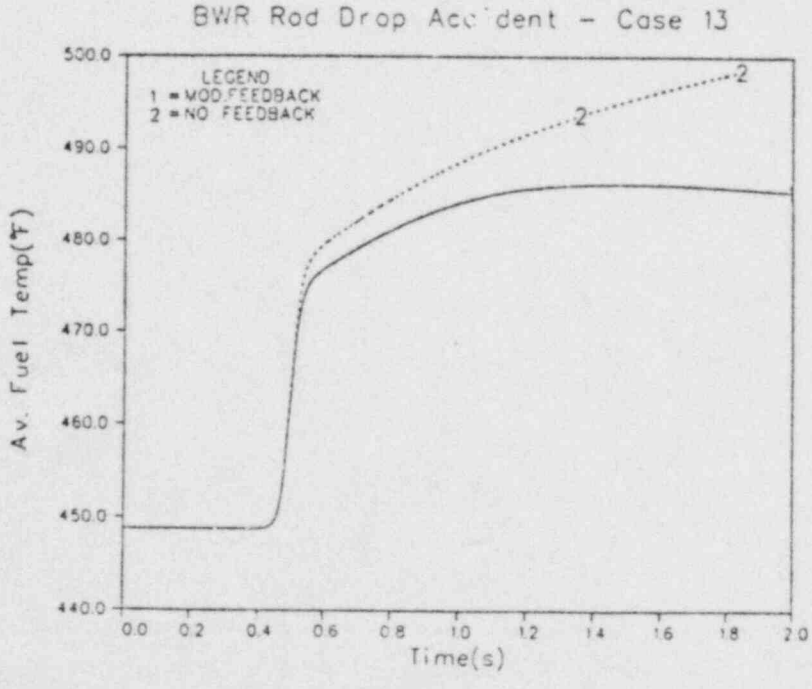

Figure 57 Transient fuel temperature behavior of Case 13

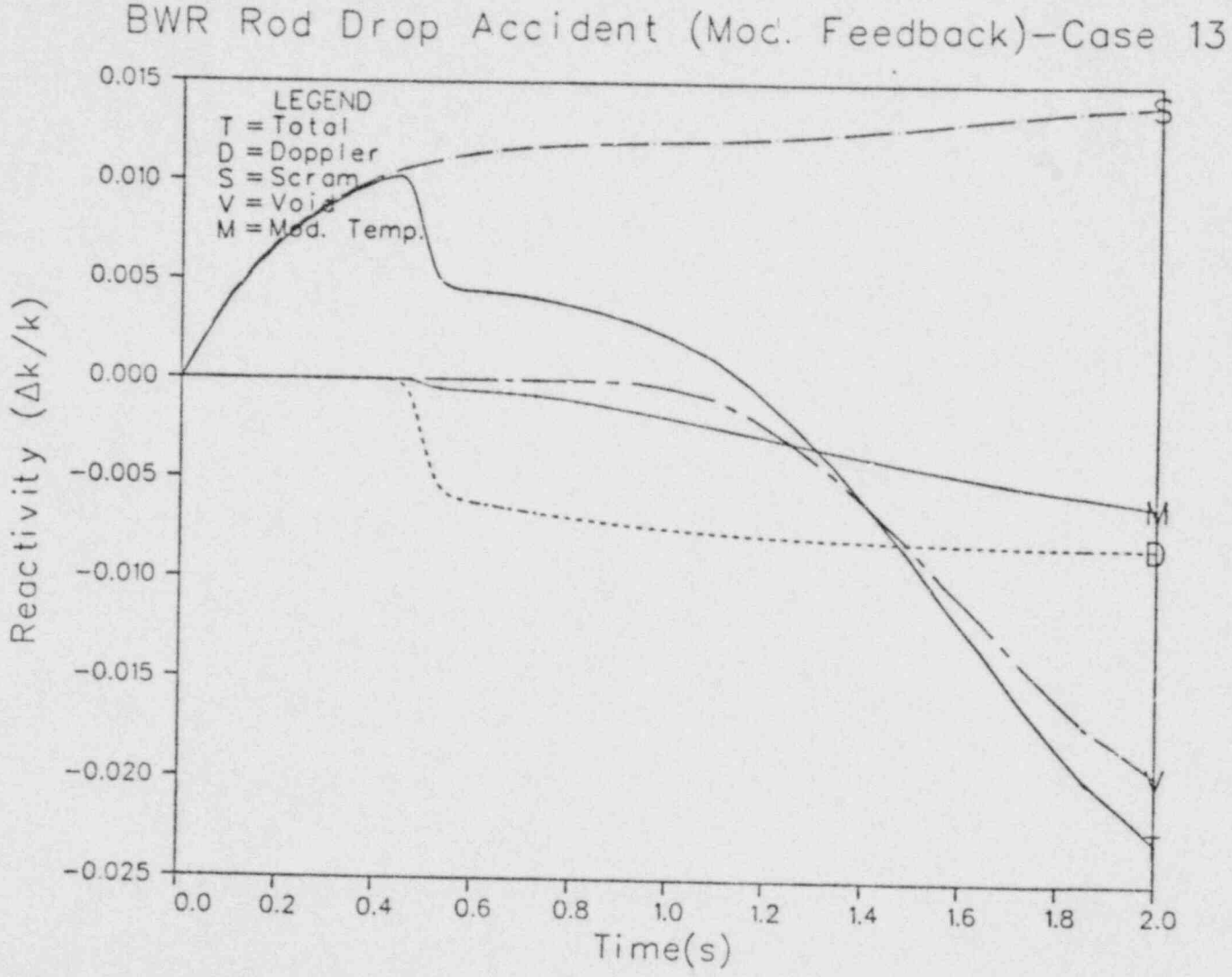

Figure 58 Various reactivity behavior of Case 13 with 100°F inlet subcooling

low accident rod worth (1.2% k/k) of Case 13. The core average fuel temperature is shown in Figure 57. It illustrates that the core on the average behaves normally and that the accident is a highly localized transient near the central control rod. Figure 58 shows the transient behavior of various reactivity components in Case 13. The strong void feedback is again evident after 1.2 s.

3.5 Hot Channel Results

Since the rod drop accident is a highly localized transient, hot channel results are of interest. Examples of important hot channel results are the peak fuel enthalpy which has been presented previously, the peak clad surface heat flux, peak fuel temperature, and peak clad wall temperature. The hot channel is defined as the hottest thermal-hydraulic region in the global sense. Thus, the local hot spot within this hottest region is not considered.

5.1 Reference 10% Power Case

The hot channel results of the reference 10% power case are presented in Figure 59 for the peak clad surface heat flux, in Figure 60 for the peak average fuel temperature, and in Figure 61 for the peak clad wall temperature. In Figures 59 and 60 we compare the case with the moderator feedback to the case without the moderator feedback. We see clearly the substantial effect of the moderator feedback on the hot spot results.

3.5.2 Hot Zero Power Cases

Since the HZP case is more severe, we present the hot channel results of both Case 5 and Case 11. Figure 62, 63, and 64 show the hot channel results of Case 5 while Figures 65 and 66 present those of Case 11. For each figure two curves are shown: one with the moderator feedback and the other without it so that we can clearly see the dramatic effect of the moderator feedback.

While Case 5 even without consideration of the moderator feedback does not seem to pose serious safety problems to fuel rods, Case 11 does if the moderator feedback is not taken into account. For example, the average fuel temperature approaches the melting point (5000°F) after 1.5 s into the accident (see Figure 66). Thus, Case 11 with a 2% accident rod worth serves to demonstrate the need to consider the moderator feedback in calculating the rod drop accident.

4.0 CONCLUSIONS

Detailed space-time dynamic calculations were performed with BNL-TWIGL for the center rod drop accident in a BWR. Only the core behavior was modeled in the present study. It would be necessary to model the hydraulics in the vessel outside the core as well, in order to obtain a complete picture of pressure and inlet flow variations. However, simple boundings calculations indicated that these variations were not large and hence the effect on moderator feedback would be of second order. The calculations were, therefore run with constant pressure and inlet flow. A study is underway to quantify these higher order effects.

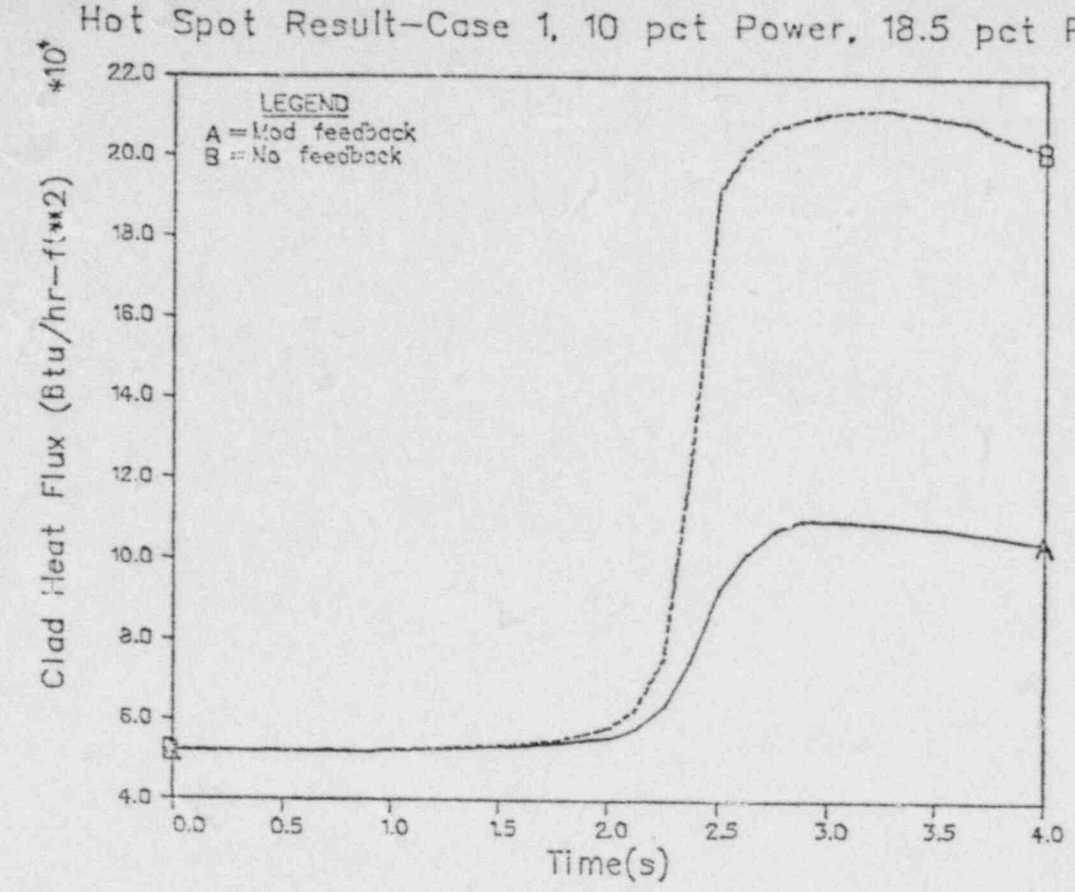

Figure 59 Transient behavior of peak clad heat flux of reference 10% power (Case 1)

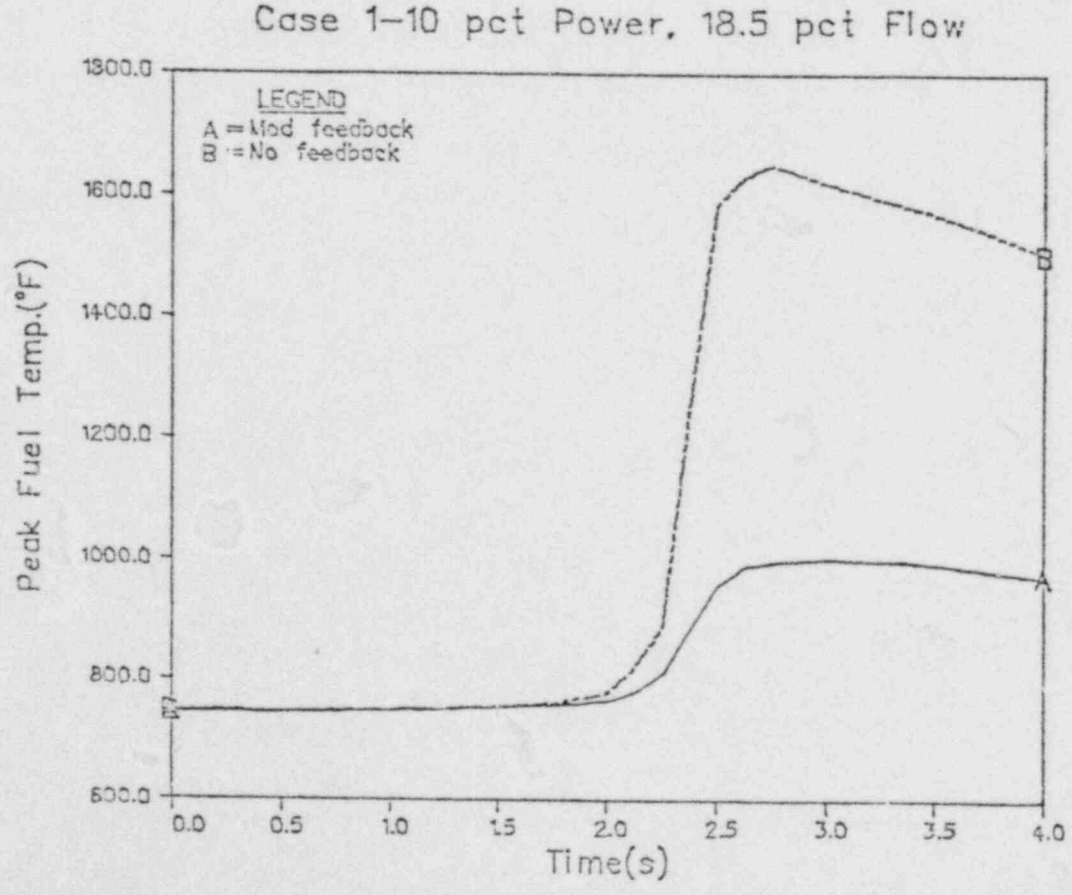

Figure 60 Transient behavior of peak fuel temperature of Case 1

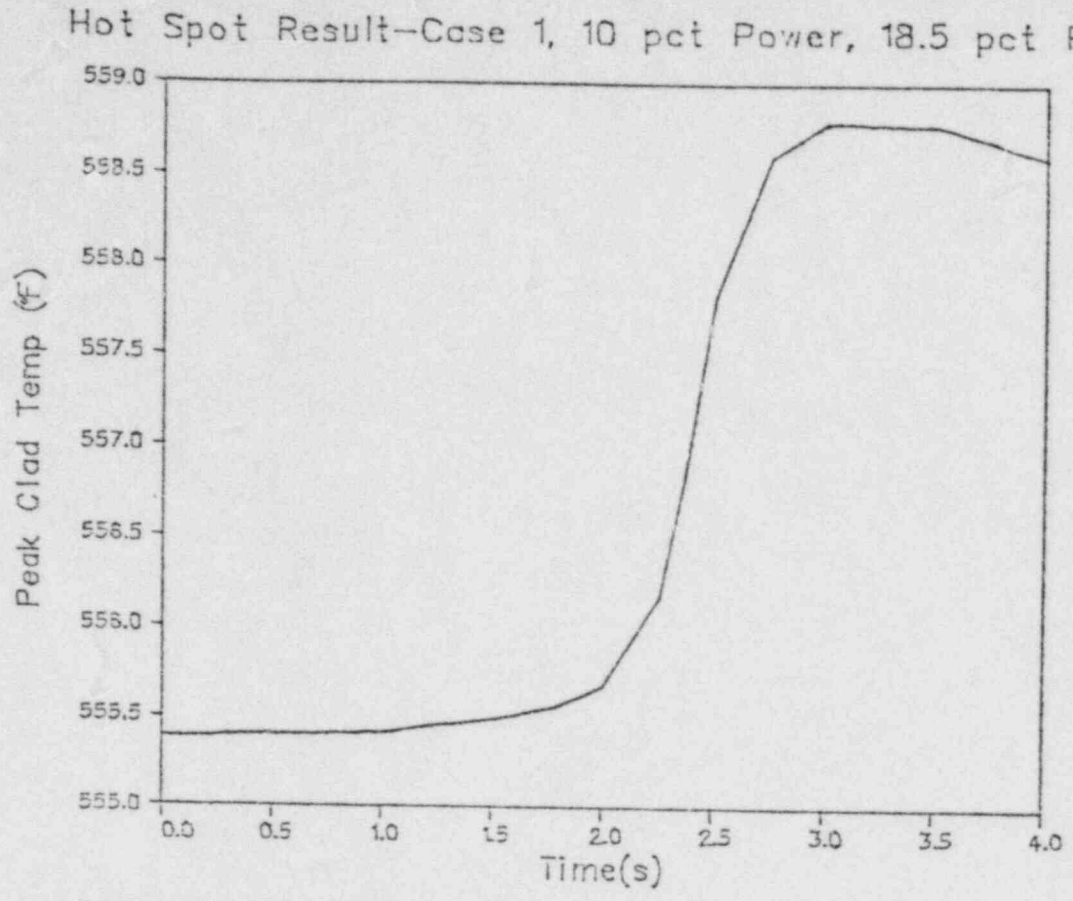

Figure 61 Transient behavior of peak clad temperature of Case 1

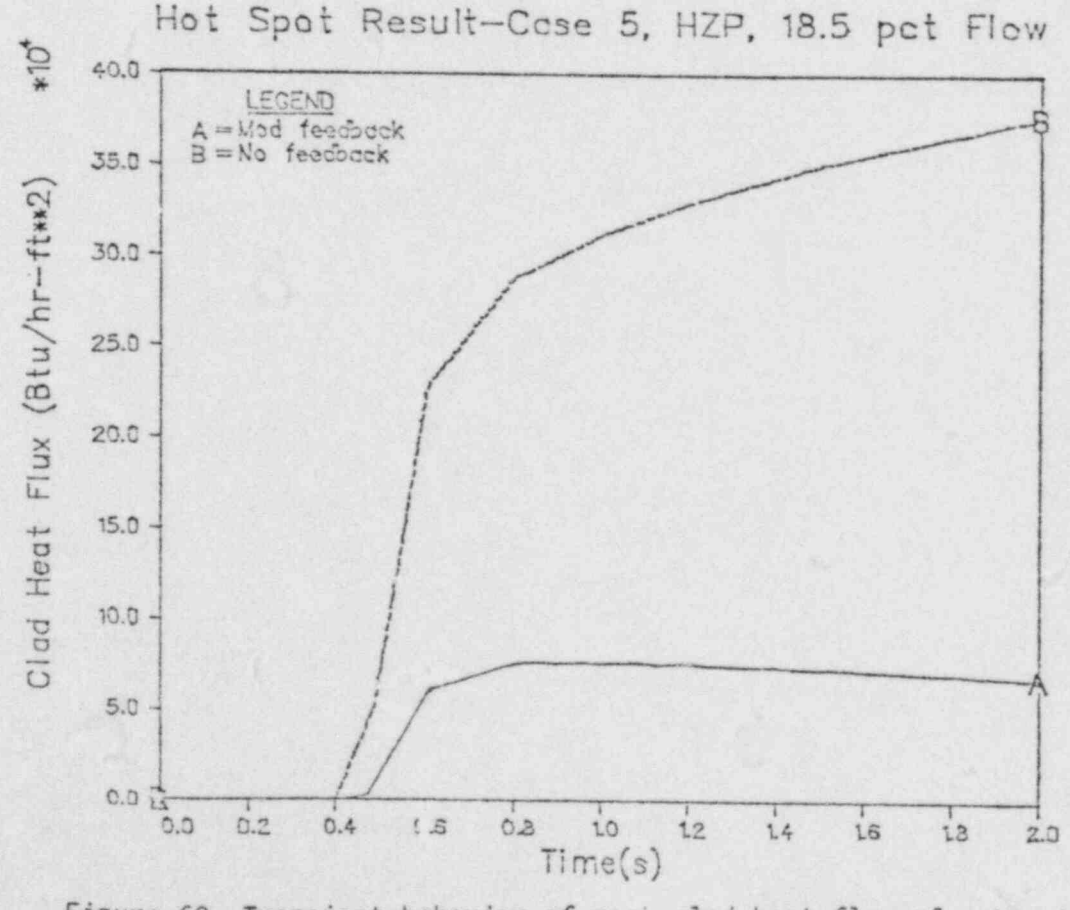

Figure 62 Transient behavior of pea clad heat flux of saturated HZP case (Case 5)

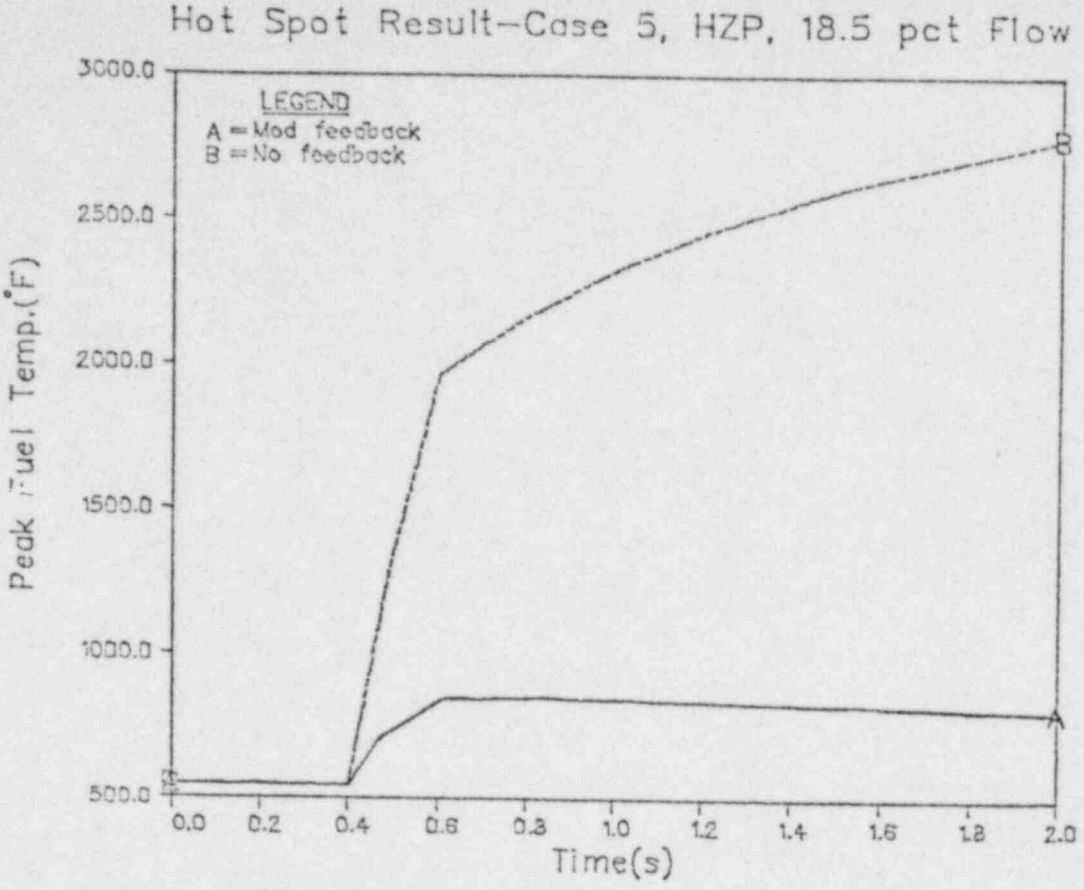

Figure 63 Transient behavior of peak fuel temperature of Case 5

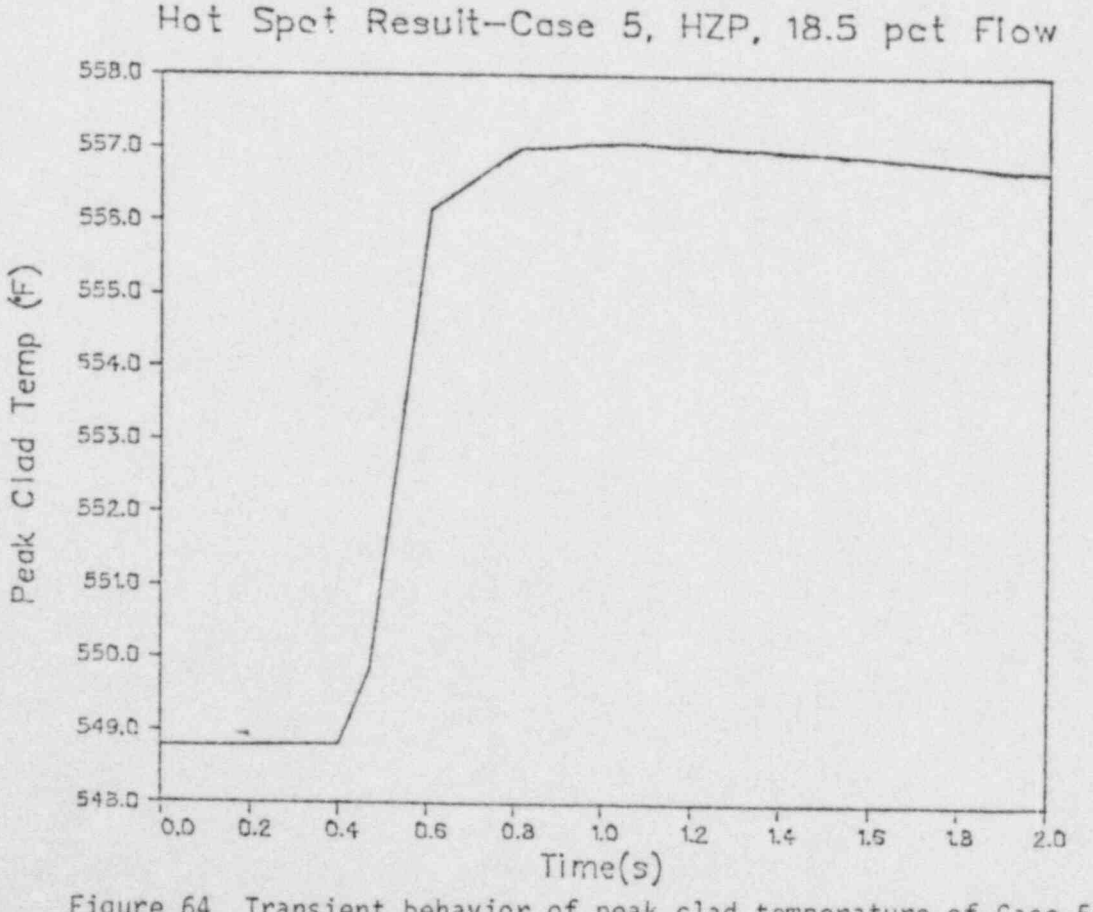

Figure 64 Transient behavior of peak clad temperature of Case 5

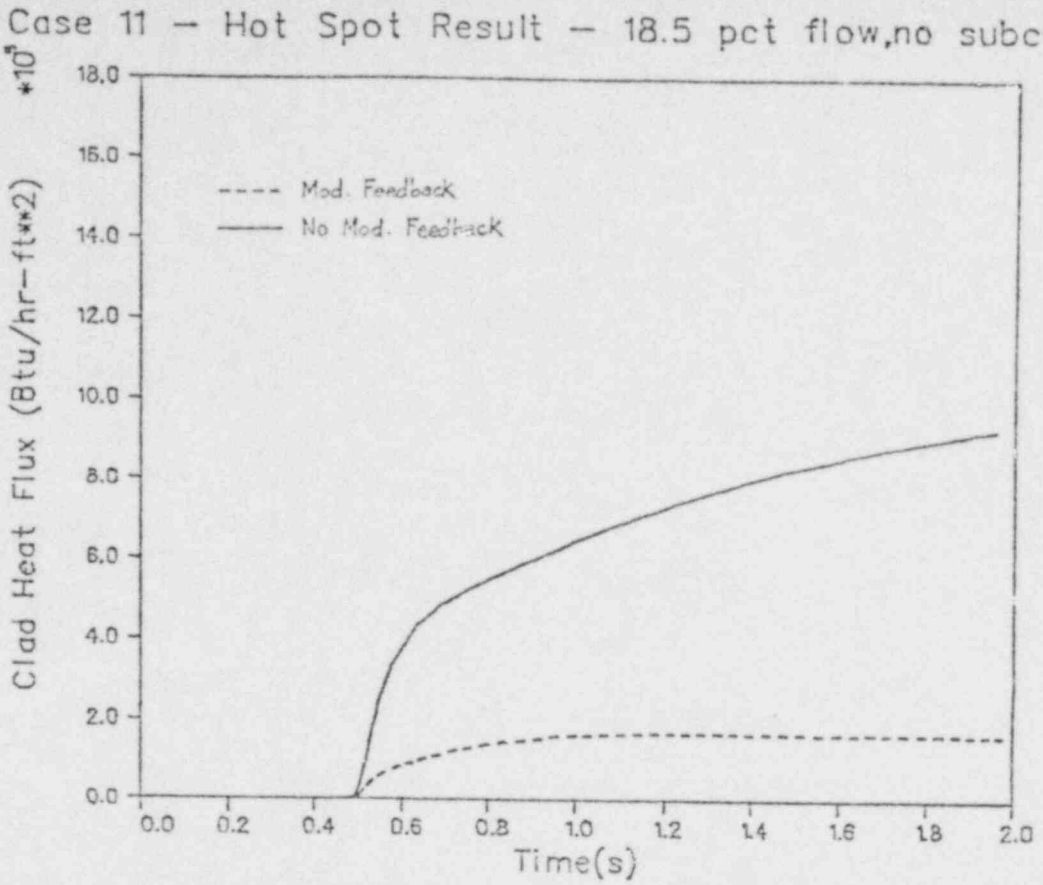

Figure 65 Transient behavior of peak clad heat flux of Case 11 with a double accident rod worth

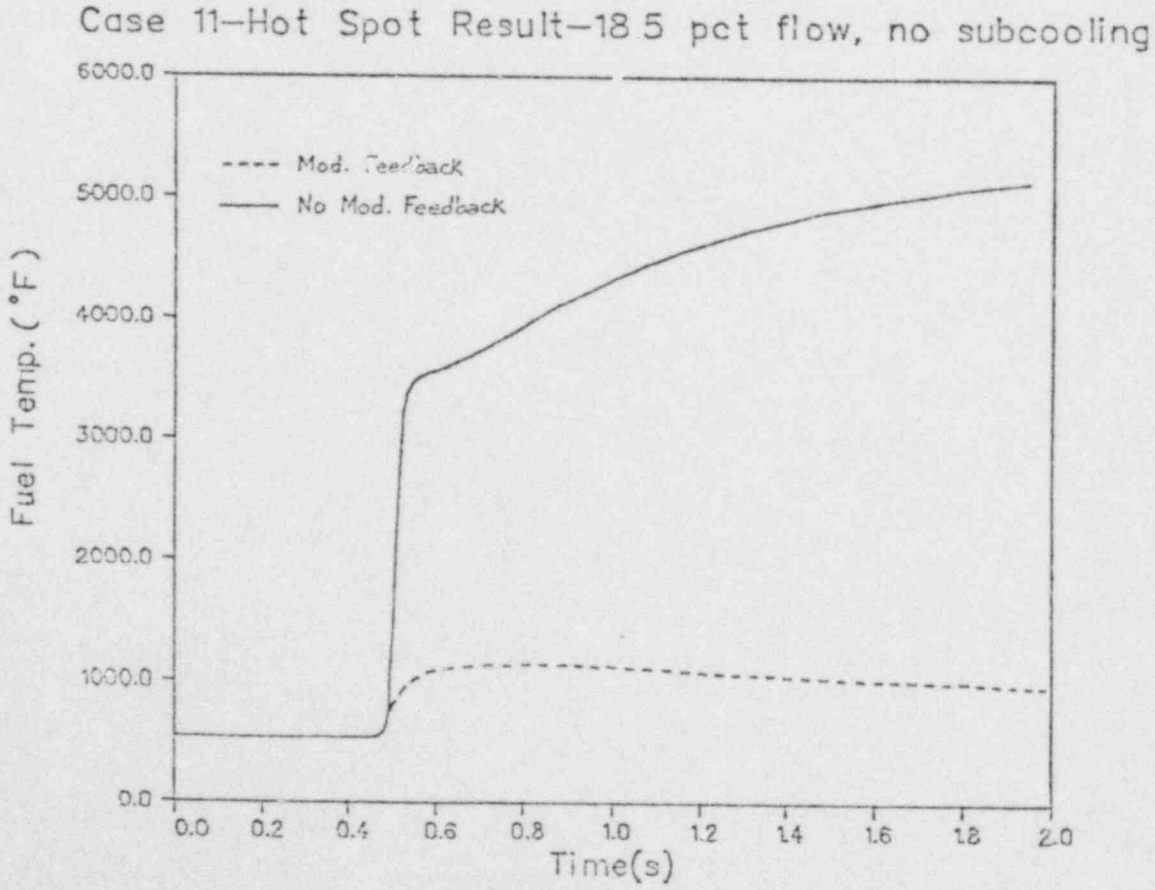

Figure 66 Transient peak fuel temperature behavior of Case 11

The accidents considered consist of a 10% power case and a hot zero power case, involving two core flow rates (18.5% and 37%), two direct moderator heating fractions (0 and 2%), three inlet subcoolings (0, 20 and 100°F), two accident rod drop velocities (3.1 ft/s and 5.0 ft/s), and two delayed neutron fractions (BOL and EOC). The importance of the inlet subcooling, direct moderator heating, and core flow effects is identified and evaluated. The effect of the accident rod worth, rod drop velocity, and delayed neutron fraction is also quantified. The overall beneficial effect of the moderator feedback on the rod drop accident is demonstrated.

The major conclusions derived from the present study are summarized as follows:

1. The moderator feedback effect is too important to be negelcted in the analysis of the rod drop accident in a BWR. It provides an inherent quenching mechanism in addition to Doppler feedback to help contain the accident considerably. The effect is most pronounced when there is voiding in the core and/or when the coolant temperature is close to saturation. In all cases considered (with moderator feedback) the resulting peak fuel enthalpy in below the limiting criterion of 280 cal/gm.

2. For 10% power cases, it is the heat transfer from fuel rods that contributes most to the moderator feedback. For HZP cases, it is the direct moderator heating that accounts for the majority of the moderator feedback.

3. For the accident at HZP, the initial inlet subcooling has a strong impact on the consequence of the accident. It should be correctly specified in defining the accident. It also suggests the importance of maintaining the core at saturation in the HZP condition.

4. Without moderator feedback results are sensitive to the accident rod worth. (However, the rod worth is a function of the initial power distribution which in turn depends on the control rod pattern and core flow rate. Increasing core flow reduces steam voids. This reduces the accident rod worth but increases the accident reactivity insertion rate due to the power shifting toward the top of the core.

5. The accident rod worth as determined from a dynamic calculation is different from that obtained by a static calculation based on the adiabatic approximation. In general, the dynamic rod worth is less than the static worth due to negative feedback effects.

REFERENCES

1. GESSAR: General Electric Standard Safety Analysis Report, Vol. 7, Chapter 15 (1975).

2. H. J. Richings, "RDA Statistical Analysis," a memo to D. Ross, Nuclear Regulatory Commission, (1975).

REFERENCES (Cont'd)

3. H. A. Brammer, J. E. Wood, and R. J. McWhorter, "Nuclear Excursion Technology," APED-5528, General Electric Co., (1965).

4. J. E. Wood, "Analysis Methods of Hypothetical Super-prompt Critical Reactivity Transients in Large Power Reactors," APED-5448, General Electric Co., (1968).

5. R. C. Stirn, et. al., "Rod Drop Accident Analysis for Large Boiling Water Reactors," NEDO-10527, General Electric Co., (1972), also Supplement 1 (1972) and Supplement 2 (1973).

6. G. S. Lellouche, "NØAH," BNL-50157 (T-523), Brookhaven National Laboratory, (1969).

7. D. J. Diamond, G. S. Lellouche, and M. M. Levine, "Rod Drop and Scram in Boiling Water Reactors," Part I, BNL-16717, Brookhaven National Laboratory, (1972).

8. G. S. Lellouche, and D. J. Diamond, "Rod Drop and Scram in Boiling Water Reactors," Part II, BNL-18106, Brookhaven National Laboratory, (1973).

9. G. Lellouche, D. J. Diamond, and M. M. Levine, "Application of Reactivity Weight Factors to Reactor Transients," BNL-16650, Brookhaven National Laboratory, (1972).

10. A. Birkhofer, A. Schmidt, and W. Werner, "Comparison of Two- and Three-Dimensional Calculations for Super Prompt Critical Excursions," Nucl. Tech., 24, 7, (1974).

11. D. J. Diamond, Ed., "BNL-TWIGL, A Program for Calculating Rapid LWR Core Transients," BNL-NUREG-21925, Brookhaven National Laboratory, (1976).

12. H. S. Cheng, D. J. Diamond, and M. S. Lu, "Boiling Water Reactor Scram Reactivity Characteristics," Nucl. Tech., 37, 246, (1978).

13. H. S. Cheng, M. S. Lu, and D. J. Diamond, "A Space-Time Analysis of Void Reactivity Feedback in Boiling Water Reactors," Nucl. Tech., 41, 229, (1978).

14. H. S. Cheng, M. S. Lu, and D. J. Diamond, "A Space-Time Analysis of Void Reactivity Feedback in Boiling Water Reactors," BNL-NUREG-23501, Brookhaven National Laboratory, (1977).

15. K. D. Lathrop, and F. W. Brinkley, "TWØTRAN-II: An Interfaced, Exportable Version of TWØTRAN Program for Two-Dimensional Transport," LA-4848-MS, Los Alamos Scientific Laboratory, (1973).

16. W. Rothenstein, Y. Barhen, E. Taviv, "The Revised HAMMER Code," EPRI-NP-565, Electric Power Research Institute, (1977).

ACKNOWLEDGEMENTS

The authors would like to thank D. Fieno, and H. Richings of the U. S. Nuclear Regulatory Commission for their many helpful discussions in the course of this work. The work of J. Penoyar in making the modifications to BNL-TWIGL and of J. Zahra in providing graphical output is also greatly appreciated.

The work was sponsored by the United States Nuclear Regulatory Commission.

DISTRIBUTION LIST

U. S. Nuclear Regulatory Commission

Director, Office of Nuclear Regulatory Branch
H. Denton
W. Dircks
M. Dunenfeld (2)
S. Fabic
D. Fieno (7)
Public Document Room
Bethesda Technical Library
Advisory Committee Reactor Safeguards (16)
W. Johnston
R. Minogue
T. Murley
D. Ross
L. Rubenstein
T. Speis

Brookhaven National Laboratory

W. Y. Kato
Reactor Safety Analysis Group
Core Performance Group
DNE Associate Chairmen
Nuclear Safety Group Leaders

External

T. Anderson, W
J. Askew, AEEW
F. del Pozo, NUCLENOR
Z. Martinson, INEL
R. Mills, C-E
C. Owsley, ENC
T. Sauar, ScP
B. Sehgal, EPRI,
G. Sherwood, GE
H. Stewart, TVA
R. Stirn, GE
J. Taylor, B&W
B. Zolotar, EPRI

Appendix A

Mathematical Definitions of Accident Rod Worth

Let ρ_A^D denote the dynamic rod worth and ρ_A^S the static rod worth. If we define the perturbed flux $\phi = \phi_o + \delta\phi$ and the perturbed operator $M = M_o + \delta M$ such that $M_o\phi_o = o$ (i.e., the reactor is initially critical), we can define the accident rod worth as follows:

$$\rho_A^D = \frac{1}{\mathcal{F}_D} \langle \phi_o^*, \delta M \phi_D \rangle \tag{A-1}$$

$$\rho_A^S = \frac{1}{\mathcal{F}_S} \langle \phi_o^*, \delta M \phi_S \rangle \tag{A-2}$$

where ϕ_D is the perturbed neutron flux obtained from a transient calculation with the thermal-hydraulic feedback, ϕ_S is that from steady state calculation without the thermal-hydraulic feedback (i.e., the thermal-hydraulic conditions of the perturbed state are held the same as those of the initial unperturbed state), ϕ_o^* is the initial unperturbed adjoint flux chosen as the weighting function to minimize the residual reactivity, δM is the change in the diffusion theory operator M due to the accident rod withdrawal:

$$\delta M = \delta A + (1-\beta)\chi_p \delta F^T + \sum_i \beta_i \chi_i \delta F^T \tag{A-3}$$

The normalization constants $\mathcal{F}_D$ and $\mathcal{F}_S$ are given by

$$\mathcal{F}_D = \langle \phi_o^*, (1-\beta)\chi_p F^T \phi_D + \sum_i \beta_i \chi_i F^T \phi_D \rangle, \tag{A-4}$$

$$\mathcal{F}_S = \langle \phi_o^*, (1-\beta)\chi_p F^T \phi_S + \sum_i \beta_i \chi_i F^T \phi_S \rangle, \tag{A-5}$$

where, in a two-group approximation, we have

$$F^T = [\nu\Sigma_{f1} \ \nu\Sigma_{f2}], \tag{A-6}$$

$$\delta F^T = [\delta \nu\Sigma_{f1} \quad \delta\nu\Sigma_{f2}], \tag{A-7}$$

$$A = \begin{bmatrix} \nabla\cdot D_1\nabla-\Sigma_1 & 0 \\ \Sigma_{s\ell_1} & \nabla\cdot D_2\nabla-\Sigma_2 \end{bmatrix}, \tag{A-8}$$

$$\delta A = \begin{bmatrix} \nabla\cdot\delta D_1\nabla-\delta\Sigma_1 & 0 \\ \delta\Sigma_{s\ell_1} & \nabla\cdot\delta D_2\nabla-\delta\Sigma_2 \end{bmatrix}, \tag{A-9}$$

$$X_p = \begin{bmatrix} 1 \\ 0 \end{bmatrix}, \qquad X_i = \begin{bmatrix} 1 \\ 0 \end{bmatrix}, \tag{A-10}$$

$$\phi = \begin{bmatrix} \phi_1 \\ \phi_2 \end{bmatrix}, \qquad \phi^*_o = \begin{bmatrix} \phi^*_{1_0} \\ \phi^*_{2_0} \end{bmatrix}. \tag{A-11}$$

We have calculated the dynamic and static rod worths using BNL-TWIGL. The dynamic rod worth is obtained from the transient dynamic calculations whereas, the static rod worth is the result of the adiabatic steady-state calculation. In BNL-TWIGL, the steady-state solution is obtained by solving a pseudo-transient problem with a vanishingly small time derivative. The same solution technique is used to obtain the spatial solution at each pseudo-time step so that the steady-state solution will be numerically consistent with the transient solution at the start of the transient.

The steady-state solution obtained by the above technique is equivalent to the solution obtained with the more common technique that treats the steady-state problem as an eigenvalue problem. The eigenvalue (or k_{eff}) of the perturbed steady-state problem with the unperturbed thermal-hydraulic condition is then

related to the static rod worth as follows:

$$\rho_A^S = \frac{k_{eff} - 1}{k_{eff}}$$

Here we have assumed that the reactor is initially critical.

Appendix B

Thermal Time Constant Associated with Heat Conduction

Let us consider the time-dependent heat conduction equation with a heat source $\dot{q}'''$ for a fuel rod:

$$\rho c_p \frac{\partial T}{\partial t} = \frac{1}{r} \frac{\partial}{\partial r} \left(rk \frac{\partial T}{\partial r} \right) + \dot{q}''' \tag{B-1}$$

The first term on the RHS is a measure of the fuel rod temperature gradient. Define a constant B^2 such that

$$- \frac{1}{r} \frac{\partial}{\partial r} \left(rk \frac{\partial T}{\partial r} \right) = k B^2 T. \tag{B-2}$$

Equation (B-1) then becomes

$$\rho c_p \frac{\partial T}{\partial t} = -k B^2 T + \dot{q}''' \tag{B-3}$$

The time constant associated with the heat conduction process is defined by the homogeneous solution of Eq. (B-3). For the case of constant material properties, the homogeneous solution is given by

$$T = T_o e^{-t/\tau}, \tag{B-4}$$

where T_o is the initial temperature of interest and τ is the thermal time constant given by

$$\tau = \frac{\rho c_p}{k B^2} . \tag{B-5}$$

We see that the thermal time constant depends on not only the material properties (ρ, c_p, and k) but also the curvature (B^2) of the fuel rod temperature profile. A fine-mesh calculation of the fuel temperature profile by, say a finite-difference approximation would enable us to calculate the curvature B^2 by

Eq. (B-2). In the following we shall estimate the curvature B^2 for a homogenized fuel rod by means of a quadratic approximation. This is considered sufficient for realizing the impact that B^2 can have on the thermal time constant.

Consider a fuel rod composed of the pellet, gap, and clad. To be compatible with the constant property assumption, we shall treat the fuel rod as a homogenized solid cylinder with composite material properties. We further assume that the fuel temperature profile can be approximated by a quadratic representation:

$$T(r) = T_{\ell}\left[1 - \alpha\left(\frac{r}{R}\right)^2\right], \quad 0 \leq \alpha \leq 1 \tag{B-6}$$

where T_{ℓ} is the centerline fuel temperature and R is the radius of the homogenized fuel rod. Note that the linear term is not there because it must vanish due to the boundary condition $\partial T/\partial r = 0$ at $r = 0$.

The curvature B^2 at the outer boundary of the fuel rod for the case of constant k reduces to

$$B^2 = -\frac{1}{T}\frac{1}{r}\frac{\partial}{\partial r}\left(r\frac{\partial T}{\partial r}\right)\Bigg|_{r=R} \tag{B-7}$$

Substituting Eq. (B-6) into(B-7), we obtain

$$B^2 = \frac{4\alpha}{(1-\alpha)R^2} \tag{B-8}$$

where $0 \leq \alpha \leq 1$.

If the fuel temperature profile is flat, $\alpha = 0$ and $B^2 = 0$. This leads to an infinitely long thermal time constant. On the other extreme, if $\alpha = 1$, $B^2 = \infty$ and the thermal time constant is zero. Figure B-1 illustrates the trend of curvature B^2 as a function of the parameter α. We see that B^2 increases very sharply as the parameter α approaches unity. For those transients where the

quadratic approximation applies, it is expected that the parameter α will increase toward unity as the transient becomes more severe. In this situation ($\alpha \rightarrow 1$) the thermal time constant can be very short.

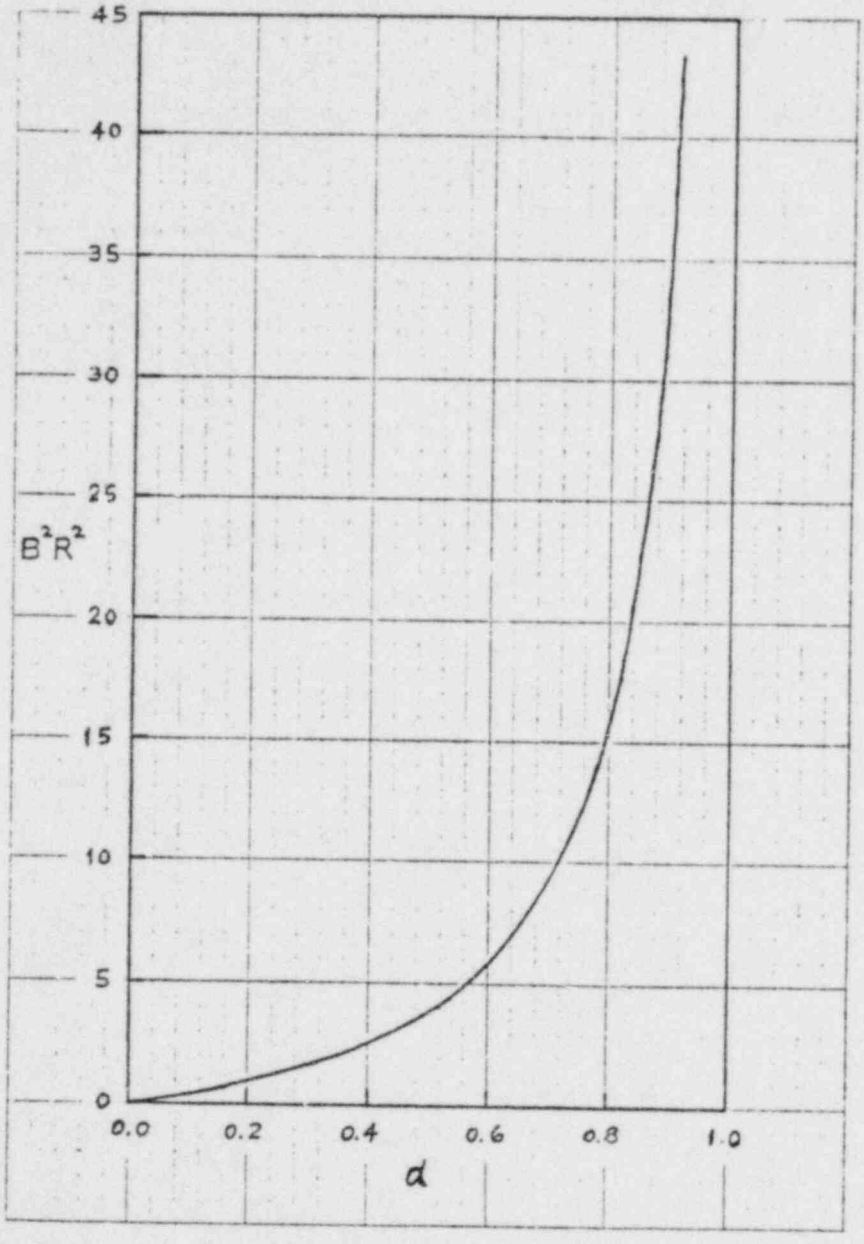

Figure B-1 Dependence of temperature curvature B^2 on the parameter α